Calhoun: The NPS Institutional Archive

DSpace Repository

Theses and Dissertations 1. Thesis and Dissertation Collection, all items

1978

Advanced cooling methods for marine gas turbines.

Strawbridge, Carl Neilson

Massachusetts Institute of Technology

http://hdl.handle.net/10945/18334

Downloaded from NPS Archive: Calhoun

Calhoun is the Naval Postgraduate School's public access digital repository for research materials and institutional publications created by the NPS community. Calhoun is named for Professor of Mathematics Guy K. Calhoun, NPS's first appointed -- and published -- scholarly author.

Dudley Knox Library / Naval Postgraduate School
411 Dyer Road / 1 University Circle
Monterey, California USA 93943

http://www.nps.edu/library

ADVANCED COOLING METHODS FOR MARINE GAS TURBINES.

Carl Neilson Strawbridge

Thesis
S7895

REPORT DOCUMENTATION PAGE

READ INSTRUCTIONS
BEFORE COMPLETING FORM

1. REPORT NUMBER

2. GOVT ACCESSION NO.

3. RECIPIENT'S CATALOG NUMBER

4. TITLE (and Subtitle)
ADVANCED COOLING METHODS FOR MARINE GAS TURBINE

5. TYPE OF REPORT & PERIOD COVERED
THESIS

6. PERFORMING ORG. REPORT NUMBER

7. AUTHOR(s)
STRAWBRIDGE, CARL NEILSON

8. CONTRACT OR GRANT NUMBER(s)

9. PERFORMING ORGANIZATION NAME AND ADDRESS
MASS. INST. OF TECHNOLOGY

10. PROGRAM ELEMENT, PROJECT, TASK AREA & WORK UNIT NUMBERS

11. CONTROLLING OFFICE NAME AND ADDRESS
CODE 031
NAVAL POSTGRADUATE SCHOOL
MONTEREY, CALIFORNIA, 93940

12. REPORT DATE
MAY 78

13. NUMBER OF PAGES
176

14. MONITORING AGENCY NAME & ADDRESS (if different from Controlling Office)

15. SECURITY CLASS. (of this report)
UNCLASS

15a. DECLASSIFICATION/DOWNGRADING SCHEDULE

16. DISTRIBUTION STATEMENT (of this Report)
APPROVED FOR PUBLIC RELEASE; DISTRIBUTION UNLIMITED

17. DISTRIBUTION STATEMENT (of the abstract entered in Block 20, if different from Report)

18. SUPPLEMENTARY NOTES

19. KEY WORDS (Continue on reverse side if necessary and identify by block number)
COOLING METHODS, MARINE GAS TURBINES

20. ABSTRACT (Continue on reverse side if necessary and identify by block number)
SEE REVERSE

DD FORM 1 JAN 73 1473 EDITION OF 1 NOV 65 IS OBSOLETE
(Page 1) S/N 0102-014-6601 |

ABSTRACT

The development of sophisticated gas turbine hot section cooling methods appears to enhance the usefulness of the gas turbine as a marine propulsion plant. The state-of-the-art in cooling systems is reviewed and a qualitative assessment of selected methods is made. A computer model was employed to quantitatively compare the impact of film, transpiration and water cooling on gas turbine performance.

The performance gains as predicted by this method for film and transpiration air cooling methods are minor compared to standard impingement-convection methods in simple cycle applications. Transpiration and water cooling techniques in combined cycles permit the attainment of efficiencies exceeding fifty percent. However, the cooling water flow rates predicted in this study indicate a probable over-simplification of coolant side heat transfer modelling.

Thesis Supervisor: A. Douglas Carmichael

Title: Professor of Power Engineering

Thesis Reader: David Gordon Wilson

Title: Professor of Mechanical Engineering

Approved for public release;
distribution unlimited.

DUDLEY KNOX LIBRARY
NAVAL POSTGRADUATE SCHOOL
MONTEREY, CALIFORNIA 93943-5002

ADVANCED COOLING METHODS FOR MARINE GAS TURBINES

by

Carl Neilson Strawbridge

Lieutenant, United States Navy
B.S., U.S. Naval Academy
(1972)

Submitted in partial fulfillment
of the requirements for the
Degree of Master of Science
in Naval Architecture and Marine Engineering
and the
Degree of Master of Science
in Mechanical Engineering

at the

Massachusetts Institute of Technology
May, 1978

© Carl Neilson Strawbridge
1978

Thesis
S7595
c. 2

ADVANCED COOLING METHODS FOR MARINE GAS TURBINES

by

Carl Neilson Strawbridge

Submitted to the Department of Ocean Engineering on 12 May 1978, in partial fulfillment of the requirements for the degrees of Master of Science in Naval Architecture and Marine Engineering and Master of Science in Mechanical Engineering.

ABSTRACT

The development of sophisticated gas turbine hot section cooling methods appears to enhance the usefulness of the gas turbine as a marine propulsion plant. The state-of-the-art in cooling systems is reviewed and a qualitative assessment of selected methods is made. A computer model was employed to quantitatively compare the impact of film, transpiration and water cooling on gas turbine performance.

The performance gains as predicted by this method for film and transpiration air cooling methods are minor compared to standard impingement-convection methods in simple cycle applications. Transpiration and water cooling techniques in combined cycles permit the attainment of efficiencies exceeding fifty percent. However, the cooling water flow rates predicted in this study indicate a probable over-simplification of coolant side heat transfer modelling.

Thesis Supervisor: A. Douglas Carmichael

Title: Professor of Power Engineering

Thesis Reader: David Gordon Wilson

Title: Professor of Mechanical Engineering

ACKNOWLEDGEMENTS

The author extends his appreciation to Professors A. Douglas Carmichael and David Gordon Wilson for their assistance and guidance, to Miss Cheryl Gibson for her careful and thorough work in the typing of this manuscript, and to his wife, Linda, for her patience, assistance and understanding.

TABLE OF CONTENTS

Page

Abstract 2

Acknowledgements 3

Table of Contents 4

List of Figures 6

List of Tables 9

1. Introduction 10

    1.1 Background 10

    1.2 Cooling System Goals and Design Criteria 13

    1.3 Future Requirements 16

    1.4 Marine Applications 19

    1.5 Purpose of the Study 23

2. Description of Turbine Cooling Methods 25

    2.1 Background and Methods of Classification. 25

    2.2 Blade Cooling Methods 27

3. Thermodynamics of Cooling 44

    3.1 Review of Thermodynamics 44

    3.2 Heat Transfer in Turbine Blades 63

    3.3 Cooled Turbine Losses 71

    3.4 Cooling Loss Parameters 73

4. Cooling System Effectiveness 82

    4.1 Measuring Effectiveness 82

Page

4.2 Factors Affecting Cooling Effectiveness by Method 87

4.3 Development of Effectiveness Correlations 95

4.4 Comments on Correlations 97

5. Comparison of Air Cooling Methods ....

5.1 Computer Model Utilization 101

5.2 Comparison of Air Cooling Methods 104

6. Water Cooled Gas Turbine 123

6.1 Background 123

6.2 Method of Model Development 124

6.3 Cooling Water Requirements 130

6.4 Performance Results 132

7. Implications for Marine Utilization 144

7.1 Method of Comparison 144

7.2 Comparison Results 145

8. Conclusions 155

References 160

Appendix I-A - Computer Model Vector Diagram 163

Appendix I-B - Water Cooled Model (GTTR) Variable and Subroutine Listing 165

Appendix I-C - Continuity Across Rotor 170

Appendix I-D - Preliminary Heat Exchanger Sizing .. 172

Appendix II - Sample Calculations for Table 7.1 ... 174

LIST OF FIGURES

Page

1.1 Cooled Gas Turbine Development Trends 12

1.2 Open Cycle Power vs. Pressure Ratio 14

1.3 Effect of Maximum Cooling Air Temperature and Pressure Ratio on Cooling Air Thermal Capacity 18

2.1 Hot Section Components Requiring Cooling 26

2.2 Blade Cooling Methods 29

2.3 Hypothetical Blade Profiles Illustrating Blade Cooling Methods 32

2.4 Convection Cooled Designs 33

2.5 Transpiration Air Cooled Turbine Blade Concept 37

2.6 Free Convection Open Thermosyphon 40

2.7 Closed-Loop Thermosyphon Cooling System .. 42

3.1 Isobars on T-s Diagram 47

3.2 Brayton Cycle Representation 47

3.3 Simple Cycle Efficiency Variation with Pressure Ratio (Loss-Less) 51

3.4 Simple Cycle Specific Work Output 51

3.5 Temperature Relations in High Speed Flow Over Insulated Plate 54

3.6 Turbine Isentropic Efficiency 56

3.7 Reheat Effect in Turbine (Expansion) 58

3.8 Typical Cascade Blade Temperature Distribution 64

Page

3.9 Typical Turbine Blade Heat Transfer Coefficient Distribution 64

3.10 Chordwise Thermal Gradients with Transpiration Cooling 66

3.11 Gas Side Heat Transfer Correlations for Turbines and Cascades 68

3.12 Effect of Cooling Losses on Turbine Efficiency 75

3.13 Estimated Cooling Loss Per Stage at Various Pressures 78

3.14 Cooling at Constant Stagnation Pressure .. 79

4.1 Heat Balance on Air-Cooled Blade 84

4.2 Normal and Angled Injection of Cooling Air 90

4.3 Effect of Film Blowing Rate on Surface Heat Flux 91

4.4 Air Cooling Effectiveness Versus Coolant Mass Fraction For Various Methods 98

5.1 Cooling Air Requirements for Various Cooling Methods 106

5.2 Comparison of Effects of Cooling Method on Efficiency and Specific Fuel Consumption (Simple Cycle) 107

5.3 Variation of Exhaust Temperature and Specific Power with Cooling Method 110

5.4 Transpiration Versus Composite Cooling Efficiencies (Simple Cycle) 112

5.5 Combined Cycle Performance Variations with Cooling Method 119

5.6 Steam Cycle Work vs. Gas Turbine Exhaust Temperature 121

Page

6.1 Computer Model Heat Transfer Diagram 129

6.2 Simple Cycle Water Cooled Turbine Efficiency and Specific Fuel Consumption.. 134

6.3 Water-Cooled Turbine Heat Loss and Coolant Flow Rate 135

6.4 Combined Cycle Efficiency for Water Cooled Turbine 137

6.5 Effect of Cooling Method on Performance for Moderate Temperature Increases 139

6.6 Mean Heat Transfer Predictions 141

6.7 Combined Cycle Coolant Distribution Map .. 143

7.1 Typical Part Load Specific Fuel Consumption for Simple Cycle Gas Turbine . 146

7.2 Schematic of Single State Flash Evaporator for Water-Cooled Gas Turbine .. 150

I-1 Velocity Triangles 164

I-2 Continuity Through a Pair of Rotor Blades 171

I-3 Heat Exchanger Schematic 173

LIST OF TABLES

Page

1.1 Comparison of Industrial and Aero-Derivative Type Gas Turbines in Marine Use 22

2.1 Air Cooling Development Chain 30

2.2 Experimental Cooled Gas Turbine Test Summary 36

5.1 Simple Cycle Parameters 104

5.2 Comparison of Performance with Cooling Method (Open Cycle) 108

5.3 Comparison of Effects of Precooling and Increasing Allowable Metal Temperature with Cooling Method 114

5.4 Combined Cycle Parameters 116

5.5 Comparison of Performance with Cooling Method (Combined Cycle) 118

5.6 Effect of Boiler Pressure on Transpiration Cooled Gas Turbine Performance (Combined Cycle 122

6.1 Water Cooled Gas Turbine Simple Cycle Performance 133

6.2 Water Cooled Gas Turbine Combined Cycle Performance 138

7.1 Improvements in Performance of Projected Shipboard Gas Turbine Propulsion Plants Relative to a Standard Cooled Simple Cycle 148

7.2 Comparison of actual to Proposed Water-Cooled Gas Turbine Design 153

1. INTRODUCTION

The gas turbine has developed within the last twenty years into a competitive, adaptable prime mover for use as a gas generator in aircraft and for the generation of shaft power for stationary and marine use. The competitive characteristics responsible for this development include simplicity, reliability, flexibility of design, high power-to-weight ratio, and relatively low maintenance costs of the open cycle gas turbine. Supporting this development has been the rapid expansion of the field of gas turbine cooling systems, essential to the improvement of thermal efficiency in the modern gas turbine while maintaining simplicity, reliability and adequate component life for commercial and marine service.

1.1 BACKGROUND

The apparent simplicity of engine cooling as perceived during the initial engineering attempts at design has yielded to a cautious appreciation of the complex issues and phenomena that arise in the cooled turbine.

Figure 1.1 indicates the past development of the cooled turbine [1]. The impetus behind the development of cooled turbines originated from the aircraft industry following World War II; supported by military budgets and

the dramatic potential impact that the jet engine was having on aircraft design, engine researchers recognized the need for increased turbine inlet temperatures for performance gains. The slow pace of materials development plus the high cost and relative scarcity of critical metals forced the designers to consider cooling methods to keep blade temperatures below creep-failure and thermal fatigue limits while maintaining the highest practicable inlet temperature. Figure 1.1(a) illustrates that although materials improvements resulted in engine temperature increases of only about 18 degrees (F) per year from 1952 through 1966 the introduction of cooling around 1965 enabled turbine inlet temperatures to increase from a rate of about 17 degrees (F) per year to over 40 degrees (F) per year from 1955 to 1967.

One of the tremendous benefits of blade cooling is the increase in blade life resulting from a reduction in blade temperatures; on a creep-life basis a 35 degree (F) reduction of blade temperature can double a typical aero-engine blade life [1]. This is roughly equivalent to a reduction in the average blade stress level of 3000 psi. Thus the increase in blade cooling of 40 degrees (F) per year has resulted in much greater time between overhauls for a constant inlet temperature, or, for a constant maintenance interval, higher operating

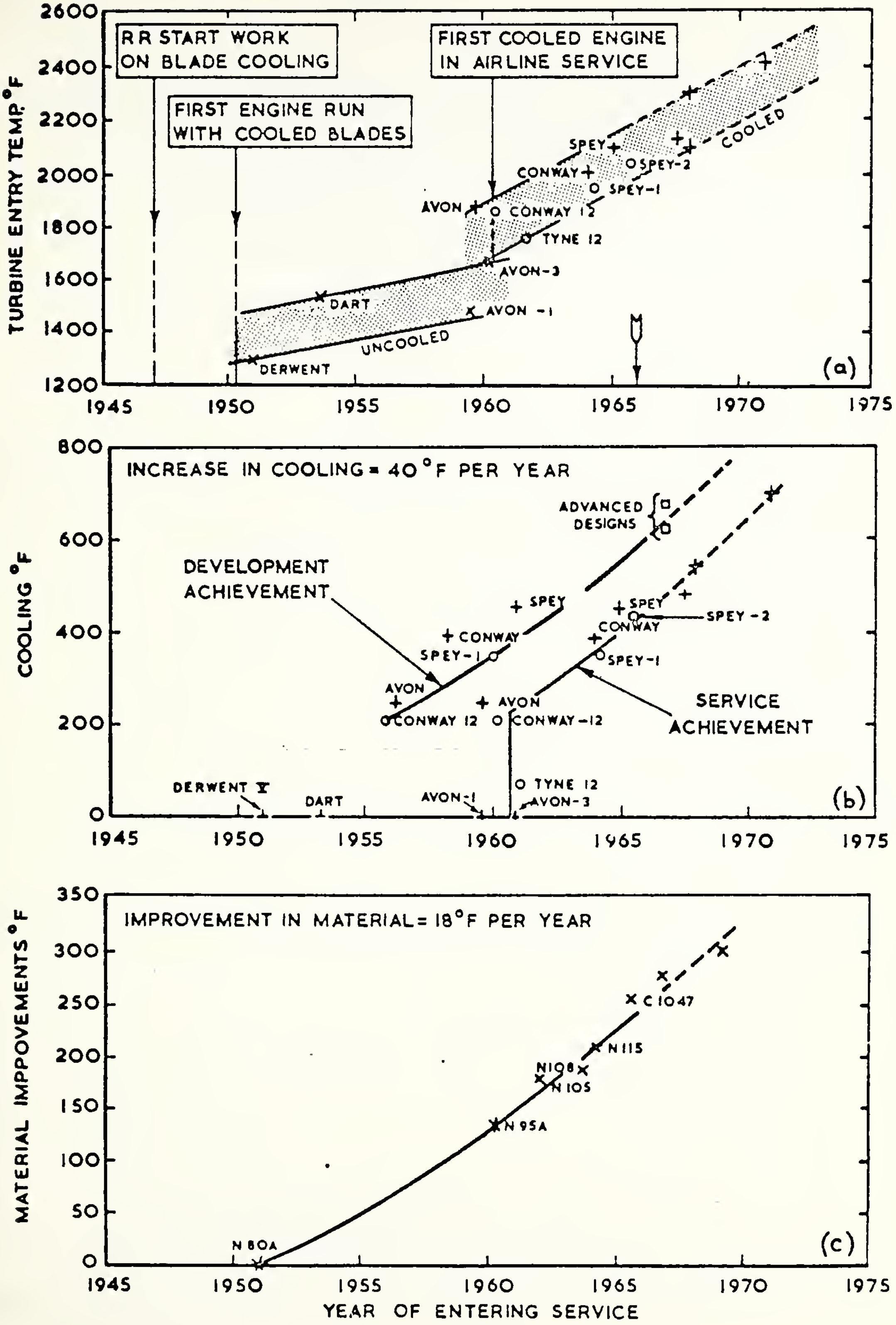

FIGURE 1.1 Cooled Gas Turbine Development Trends [1]

temperatures and corresponingly greater performance gains.

There exist other advantages attendant to the development and employment of cooled turbines. Increasing the turbine inlet temperature directly increases the cycle thermal efficiency, roughly as

$$\eta_{thermal} = 1 - \overline{T}_L/\overline{T}_H$$

where $\overline{T}_L$ and $\overline{T}_H$ are the average temperatures of heat removal and addition, respectively. The employment of cooling can increase specific power, allowing theoretical reductions in turbine size, weight and space. At higher turbine inlet temperatures a wider choice of pressure ratio is available where power output is little affected by the choice of pressure ratio (Figure 1.2). Other potential benefits include the possible improvement of gas turbine performance at part-load and the option of increasing efficiency and output with the simple, uncomplicated open-cycle arrangement [2]. However, increased demands for cooling air at high temperatures can cause power and efficiency losses in ways that are not always readily apparent [3].

1.2 COOLING SYSTEM GOALS AND DESIGN CRITERIA

As with any other practical engine design, the design of a gas turbine power system is a complicated

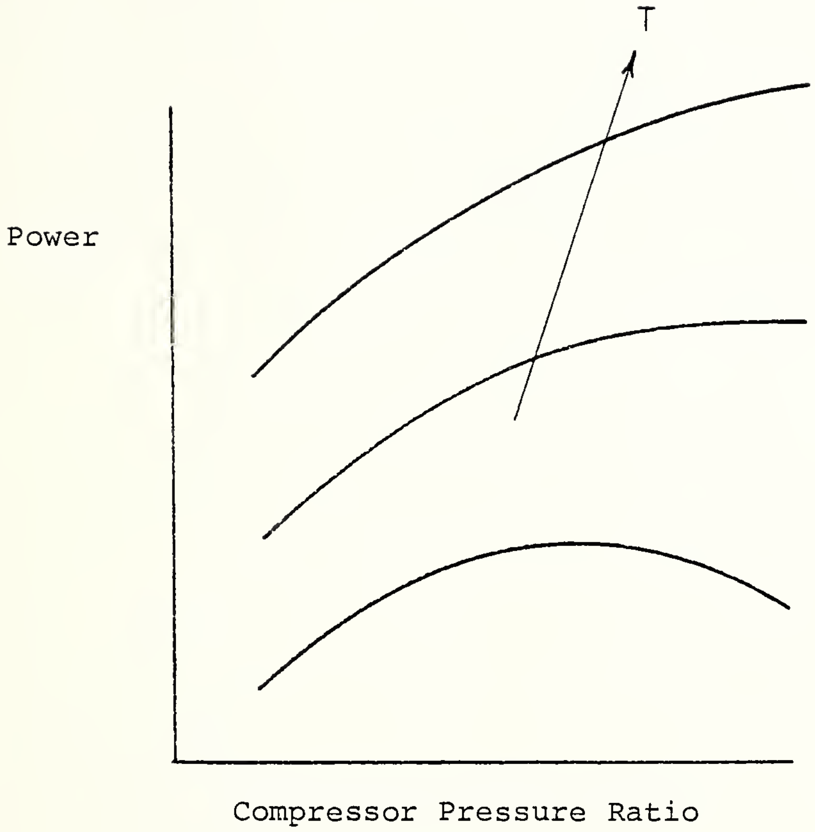

FIGURE 1.2 Open Cycle Power Versus Pressure Ratio [3]

engineering process requiring careful balance of advantages and problems. The selection of the most suitable cycle from thermodynamic aspects, even with a minimum number of components is not a straightforward matter of using the highest pressures and temperatures. A thorough understanding of component performance is needed to achieve the optimum effects of higher efficiency, high output, small size and low cost [4]. For many applications, blade cooling can offer substantial performance benefits but the cooling system itself must satisfy certain criteria. The optimum turbine cooling system must provide good stage efficiency and high cycle thermal efficiency plus yield a high specific power. An efficient cooling system should operate with low cooling losses and in the event of malfunction not result in catastrophic engine failure. Practical considerations of good mechanical designability, a minimum of mechanical complexity (coolant conduits), and capability of economic manufacture are important, in addition to minimizing in-service maintenance. The cooling system must operate to yield blade metal temperature levels and distributions that satisfy blade life and reliability requirements; it must respond to thermal transients in order to give satisfactory engine handling characteristics without unsatisfactory effects on blade life or

reliability. Providing satisfactory part load performance and satisfying vibration requirements are additional considerations, but the determining factor in cooling system selection is the overall economic justification for its use [3]. Thus the goals for cooling system design may be summarized as follows:

(1) improve thermal efficiency by permitting increases in turbine inlet temperature;

(2) maintain current reliability standards and low maintenance costs;

(3) retain the advantages of the gas turbine that have been responsible for its rapid growth and expanded application, principally its simplicity in the basic open cycle;

(4) provide acceptable turbine blade life for industrial and marine use;

(5) maintain or reduce current specific cost.

1.3 FUTURE REQUIREMENTS

The thermodynamic inducements to continue the development of stationary and aero-derivative gas turbines to permit the use of higher turbine entry temperature are strong. However, accompanying these trends is a

diminution in the ability of current cooling methods to properly protect hot engine components, the most critical of which are the blades. Most current production-model stationary and all aero-derivative gas turbines employ compressor-bleed air as the cooling medium. Higher thermal efficiencies in other than regenerative cycles demand an increase in compressor pressure ratio as well as increased inlet temperatures, resulting in a decrease in the specific thermal capacity of the cooling air. The thermal capacity of the coolant is also a function of the maximum temperature T_{co} attained by the coolant in the performance of its function. Figure 1.3 illustrates the declining effectiveness of air as a coolant at higher pressure and temperature levels. It is observed that more effective coolant utilization as reflected in a greater T_{co} can mitigate to some degree the effects of higher pressure; this is a function of design skill and the prevailing metallurgical temperature limit of the hot-section components. Projecting future requirements for thermal capacity leads to the general conclusion that this capacity must increase. As attempts to raise cycle temperatures proceed, the heat flux received by the turbine blades will increase; this heat flux is a function of the difference between the gas stream and

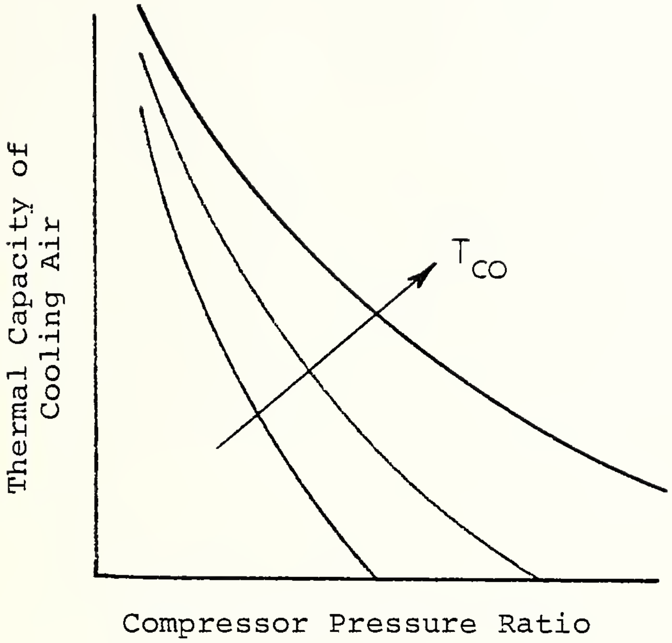

FIGURE 1.3 Effect of Maximum Cooling Air Temperature and Pressure Ratio on Cooling Air Thermal Capacity (After [2])

maximum permissible metal temperatures, and the mean heat transfer coefficient on the gas side. This heat transfer coefficient is influenced by Reynolds number, but offsetting effects of increased gas velocity with a reduction in the size of turbine required for a given power output can tend to limit the prospect of reducing heat flux by reducing the heat transfer coefficient. Thus the temperature difference will tend to increase as desired cycle temperatures outdistance metallurgical gains (see Figure 1.1). When this is considered in light of the reduced capability of coolant air at high pressures, it is clear that some means must be found to augment the cooling capability of current methods [2].

1.4 MARINE APPLICATIONS

The predominant marine application for gas turbines is in naval propulsion; at present there are over 20 million horsepower in service, of which 19.2 million are used to provide propulsion power. Naval users account for about 17 million horsepower in propulsion service. The attributes of the aircraft-type gas turbine, including low specific machinery weight, high reliability and corresponding reduction of personnel and maintenance requirements have been the primary reasons for increasing naval utilization. Merchant service needs

are dictated primarily by operating costs, and the relatively high fuel consumption of the earlier gas turbines discouraged rapid merchant marine gas turbine development in favor of diesel or steam plants. However, the development of regenerative versions of industrial-type turbines, such as the General Electric MS 5212R about 1972, has fostered continued applications of the industrial type turbine to merchant service.

The fundamental difference between naval and merchant gas turbine employment is based on operating profile. The typical naval plant for vessels of 1200 tons or larger has an operating profile such that over 35 percent of total operating time is spent at less than 50 percent full speed (1/4 power). To successfully and economically employ a gas turbine component as part or all of the main propulsion plant requires optimization at more than one power level, hence the development of CODOG and COGOG plants where separate prime-movers are utilized for different power levels. Typically this means that the gas turbine is installed as the boost or peaking unit for high power augmentation, supplementing a lower power cruising unit that may be another gas turbine of lower horsepower or a diesel. The aircraft-derivative gas turbine is particularly suited to this

peaking application. Merchant service, or naval auxiliary use, is characterized by a much more uniform operating profile, with over 90 percent of steaming time spent at full power; the higher specific fuel consumption of aero-type turbines (.45 to .51 lb/SHP-HR) is less attractive for this steady-state, base-load usage compared to industrial-type turbines with regeneration (SFC .39 - .40) or diesel plants (.38 - .42). Moreover, the longer lifetimes available in industrial-type gas turbines (80-100,000 hours) that derive from lower pressure ratios and operating temperatures are more suitable to merchant service goals of minimizing maintenance requirements and costs. Table 1.1 outlines the significant differences between aero and industrial gas turbines in marine use.

In gas turbines the efficiency of the compoents is extremely important since the power required by the compressor is relatively high, perhaps 20 to 40 percent of total power developed. Thus efficiency improvements of one to two percent in component efficiencies is reflected in about double that improvement to overall cycle thermal efficiency. Component efficiencies have been affected most significantly by the increase in turbine inlet temperatures permitted by metallurgical and cooling developments.

TABLE 1.1 Comparison of Industrial and Aero-Derivative Type Gas Turbines in Marine Use

ITEM	AERO TYPE	INDUSTRIAL TYPE
Weight	Lightweight	Heavyweight
Power to weight Ratio	Very High	Not so High
Pressure Ratio	High(20:1)	Medium(8:1)
Turbine Type	Multi-Stage Reaction	Impulse
Turbine Stage	Large Number of Lightweight, Air-Cooled Blades	Small Number of Large Section, Low Stress Blades
Life(HRS)	2-6000	80-100,000
Fuel Type	Restricted	Wider Range
Cycle	Usually Simple	Regenerative or Combined
First Stage Nozzles	Small Partitions Small Cooling Holes, Thin Trailing Edge	Large Partitions Air Cooled, Thick Trailing Edges
Turbine Inlet Temperature	2000 F	1700-1800 F

Source: [5]

It is logical to expect that future developments in gas turbine technology will enhance the usefulness of the gas turbine as a marine propulsion plant. Such future developments are aimed at improving reliability, increasing engine performance, reducing maintenance requirements and increasing engine life. The attainment of these objectives requires increasing turbine firing and inlet temperatures without decreasing present engine life. There are at least four ways to accomplish this goal: (1) through development of super alloys of sufficient mechanical and thermal properties to withstand rigorous service in the marine environment; (2) through development of producible ceramic components; (3) through application of barrier coatings to improve the thermal behavior of hot section components; and (4) through development of advanced blade and vane cooling techniques that offer simultaneous gains in engine life with improved performance in marine service. Although much work is in progress on items (1) through (3), less consideration has been given to (4) with respect to marine applications.

1.5 PURPOSE OF THE STUDY

It is the purpose of the study to: (1) review and describe the current state of the art in gas turbine cooling systems, particularly in rotating components;

(2) compare the performance costs and credits of several advanced cooling methods in simple and combined cycle use; and (3) briefly investigate the potential of these systems for a shipboard application.

A computer program is utilized to develop the performance characteristics and to compare the systems.

2. DESCRIPTION OF TURBINE COOLING METHODS

There exist various ways in which turbine cooling methods may be described and classified; these methods are usually related to the mechanical design of the system and have followed an historical progression from the early 1950's.

2.1 BACKGROUND AND METHODS OF CLASSIFICATION

Turbine cooling methods may be subdivided according to several criteria:

(1) whether the part cooled is moving or stationary;

(2) by the composition of the cooling medium gas, liquid or a combination of both;

(3) by the mechanical scheme employed;

(4) by the location of the cooling fluid as it performs its function, *i.e.* internal or external to specified engine components.

The engine components that require cooling are identified in Figure 2.1 and are lumped generally under the terms of hot-section components or hot parts. These include the combustor, nozzle guide vanes and diaphragms - all stationary components - and the blades and turbine

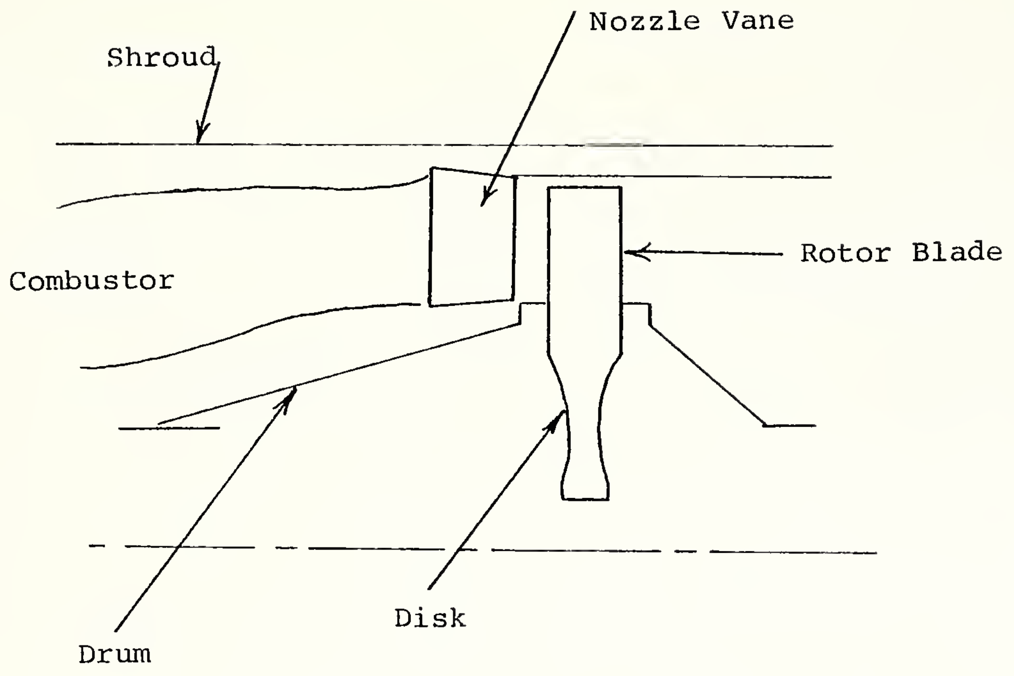
Nozzle Vane
Shroud
Rotor Blade
Combustor
Disk
Drum

FIGURE 2.1 Hot Section Components Requiring Cooling

disk - the rotating components. Additional cooling is required for bearings, shrouds and sealing systems. The problems of cooling stationary parts of modern turbines is important and is the object of considerable metallurgical research with ceramics; however, cooling stators is a much easier task than cooling rotating components. Combustor cooling technology is particularly well-developed and parallels the advanced attempts to provide additional cooling to blades through film and transpiration techniques [6]; however, the distinction between stationary and rotating parts remains and dominates the blade cooling problem.

2.2 BLADE COOLING METHODS

The incorporation of cooling into the rotating components of the axial flow turbine has presented a challenging technical problem to the turbine designer for almost thirty years. Turbine blades are subject to tremendous centrifugal and Coriolis forces which establish severe stresses within the blade that are further compounded by gas bending loads and temperature effects. The aerodynamic shape of the blades constrains the manufacturing problem of providing cooling passages and distributing and metering coolant flow. Figure 2.2

displays current practical, research and experimental blade cooling methods; this figure summarizes all of the significant mechanical factors involved. The physical characteristics and design philosophy vary significantly among the systems shown and will be described briefly.

2.2.1 Air Cooling Methods

All modern aircraft-derivative gas turbines and many industrial/stationary turbines employ air bled from the compressor as the blade and vane cooling medium. This practice developed historically as a result of concentrated efforts to increase the performance of the jet engine as an aircraft power plant. Considerations of weight and space dictated the use of air as the only acceptable coolant, although thrust-augmentation schemes utilizing injected water were investigated briefly prior to being abandoned as expensive and impractical [7]. The air-cooling development chain as outlined in Figure 2.2 is expanded in Table 2.1. Current production methods include elements (1) through (3); elements (4) through (7) are undergoing design and manufacturing research, while (8) and (9) are still in the laboratory stage of development. The simplest convection scheme involves passing bleed-air through a hollow blade and exhausting it into the gas stream; the blade thus acts

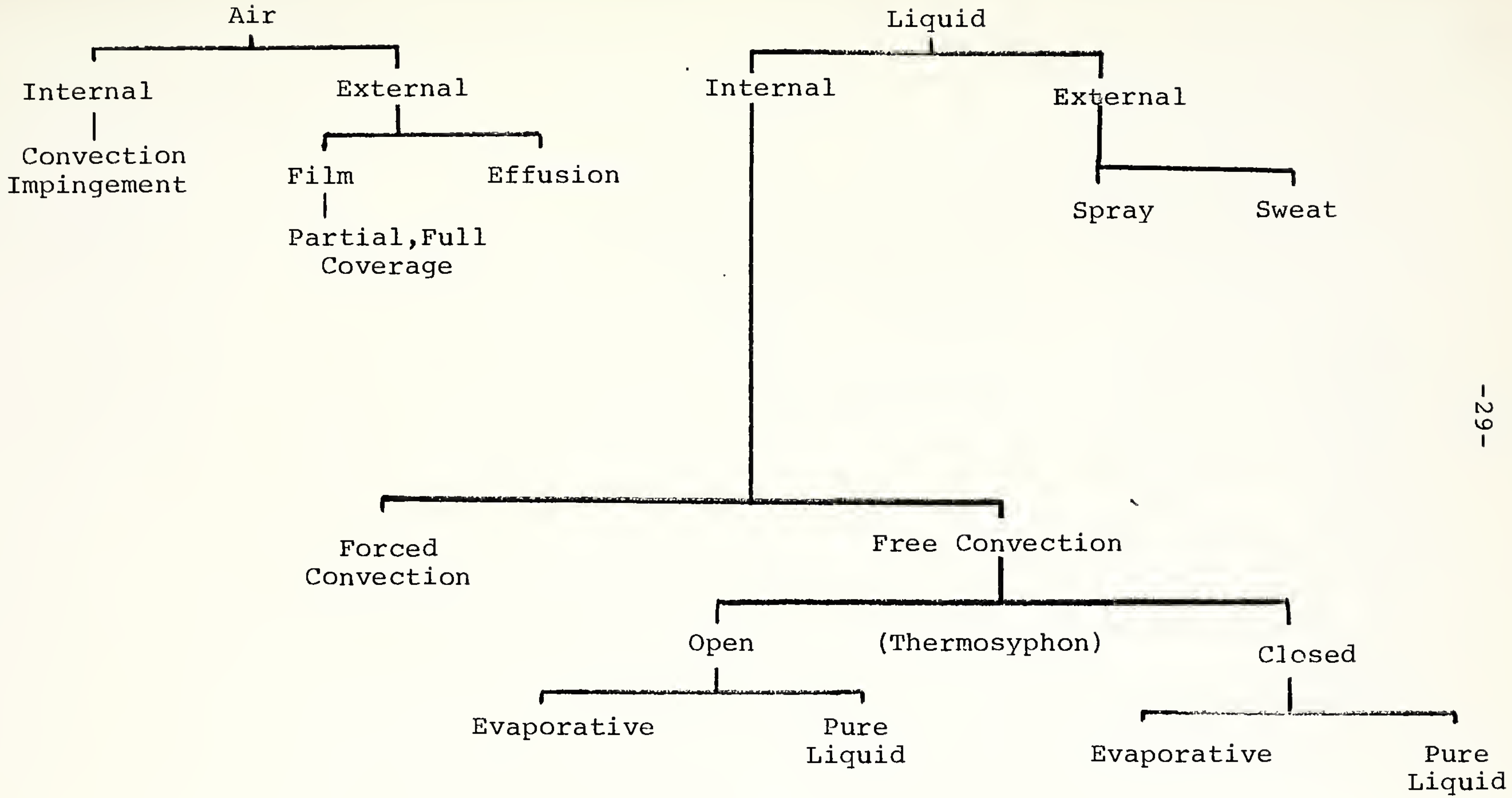
Air
Internal
Convection Impingement
External
Film
Partial,Full Coverage
Effusion
Liquid
Internal
External
Spray
Sweat
Forced Convection
Free Convection
Open
(Thermosyphon)
Closed
Evaporative
Pure Liquid
Evaporative
Pure Liquid

FIGURE 2.2 Blade Cooling Methods (After [3])

TABLE 2.1 Air Cooling Development Chain

(1) Simple convection

(2) Impingement (enhanced convection)

(3) Film cooling by localized injection through slots or holes

(4) Distributed injection through drilled sheets

(5) Coarse wire structures

(6) Multi-ply drilled sheets

(7) Fine wire mesh

(8) Uniformly porous materials developed through the techniques of powder metallurgy

(9) Porous materials with chord - and spanwise variations of porosity for coolant distribution control

(source: [6])

as a crossflow heat exchanger. Early attempts to improve the heat-exchanger effectiveness of convection-cooled blades concentrated on increasing the ratio of coolant-to-gas side heat transfer area. Circular passages were drilled radially to accomplish this but the blade geometry as dictated essentially by aerodynamic considerations limits the local effectiveness of this method, particularly in the region of the leading and trailing edges. The thin trailing edge requires excessively small cooling passages while the heat transfer requirements at the blunt end result in a deviation from optimal aerodynamic design in order to accommodate the desired coolant passage. Further attempts to improve on this idea included the assemblage of numerous tube bundles within the hollow blade, again to increase the effective heat transfer area of the coolant (Figure 2.3b). Although an improvement over the other methods, this technique still lacked sufficient effectiveness near the leading and trailing edges. The follow-on technique employed impingement jets in the leading edge region (Figure 2.3c) to augment the forced convection flow. This can be accomplished through the use of channeling inserts to redirect some portion of the main flow to the leading edge or along the chord; the use of impingement cooling is not practicable at the

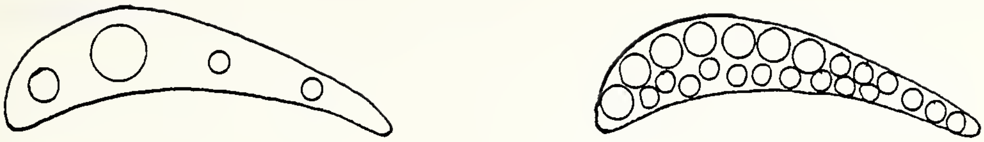

(a) Early Convection

(b) Improved Convection

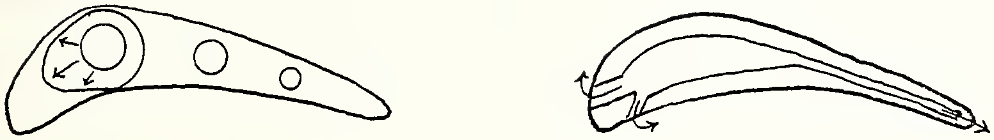

(c) Convection with Impingement

(d) Film (leading and trailing edge cooling)

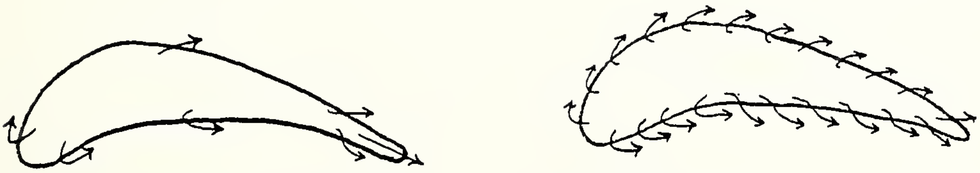

(e) Film (full coverage)

(f) Transpiration cooled

FIGURE 2.3 Hypothetical Blade Profiles Illustrating Blade Cooling Methods

trailing edge, however, due to geometry limitations. This impingement-convection technique can be augmented, however, with the presence of a slot through which the coolant can exhaust from the trailing edge and cool the region by convection; this results sometimes in a thickening of the trailing edge region, but has resulted in no undue aerodynamic losses in current designs. Additional attempts to improve on this composite convection and impingement design have been concerned chiefly with the passage shape and the subdividion of the blade cross-sectional area for optimal coolant metering (Figure 2.4).

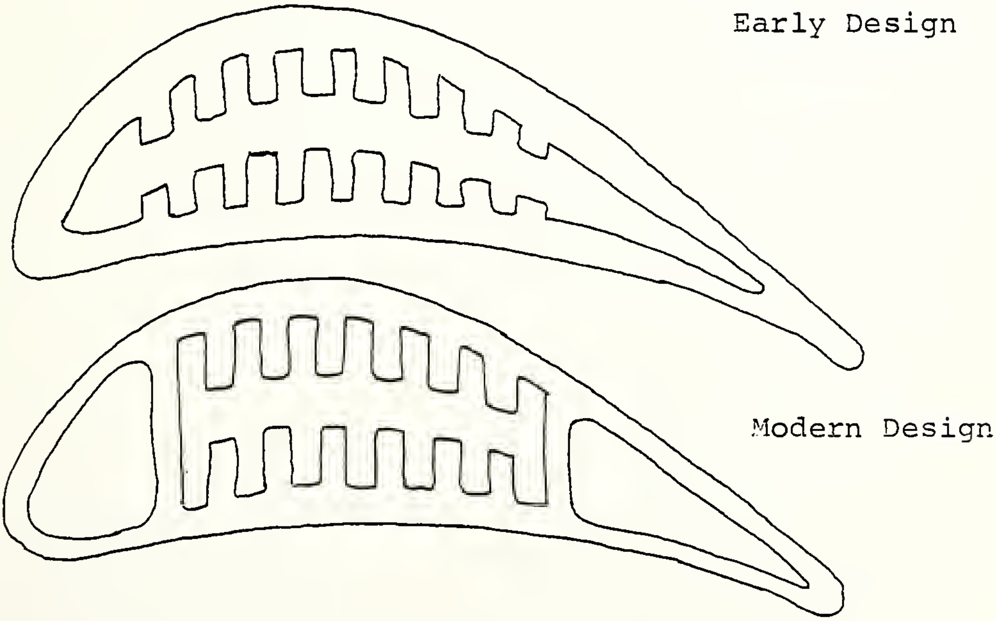

FIGURE 2.4 Convection Cooled Designs

The expansion of air-cooling techniques beyond the simple convection variations marked a major change in coolant system design philosophy. The employment of air over the external surface of a component is designed to reduce the heat transferred to the surface, while impingement and convection cooling methods attempt to maintain metal temperatures at a satisfactory creep-life level through internal heat transfer to the coolant. Film cooling is physically compatible with developed air-cooling methods; in practice the method has been used extensively to cool combustion-chamber linings and hot gas ducts. Film cooling is also employed in most aero-derivative turbines to supplement convection and impingement techniques, chiefly by improving the poor temperature distirbution at the blade leading and trailing edges. The film may be established in a number of ways; partial films for "spot-cooling" as described above are introduced through spanwise slots or through discrete injection ports of varying size, spacing, and spacing arrangement. Full coverage films require more complex metering systems and injection port arrangements to satisfactorily control the coolant distribution. In theory film cooling should result in improved cooled engine performance through more effective coolant utilization; there are a number of losses associated with this method, however, that

mitigate its positive impact on turbine and cycle efficiencies.

The logical extension of film cooling is achieved in transpiration air cooling, also known as effusion or aspiration cooling. Cooling air is supplied and distributed through a porous aerofoil surface. The porosity is determined by the fabrication materials and construction techniques. Drilled sheets provide the least porosity but are the easiest to manufacture. Additional porosity may be achieved by winding coarse or fine wire around a central support strut (Figure 2.5). Advanced powder metallurgy techniques involving sintered-mesh materials are in the industrial research stage [6]. The thermal design goal of transpiration-cooled blades is similar to that of film cooling-to reduce the heat flux to the blade. The anticipated gains of transpiration cooling over film cooling include more uniform blade metal temperature distribution and more effective coolant utilization; however, there are again penalties associated with its use that reduce theoretical performance gains.

2.2.2 Liquid Cooling Methods

The use of liquids in gas turbine cooling has long been investigated (Table 2.2) [9, 10]. However, progress has been very slow due to the extremely difficult technical problems associated with liquid-cooled blades.

TABLE 2.2 Experimental Cooled Gas Turbine Test Summary

Type of Cooling	Date	Cooling Fluid	Design Data	Remarks
Open Thermosyphon	1940-45	Water (Evaporation)	TIT 1470K; blade Temp 973K	Water near critical point, with passage pressures to 300 BAR
Open Thermosyphon w/stream formation	1950	Water (Evaporation)	TIT 1625K , steam pressure 573 psi; 19000 rpm	Vibration-limited at 60% design rpm; severe corrosion and oxide blockage
Open Thermosyphon	1950	Water (Bulk Flow)	TIT 1225K, blade temp 450K	No vibration; coolant leakage at tops, pumping power meas. at 2% turbine power
Forced Convection	1957	Air	TIT 1470K, 9000 rpm, 3:1 PR	Operated satisfactorily with high temperature vitallium alloy blades
Closed Thermosyphon	1957	Liquid metal, Nak (eutectic) plus water at root	TIT 1470K, blade temp 700K	Leakage of coolant and poor aerodynamic performance
Open Thermosyphon	1962	Water (evaporation)	TIT 1325K; 5.4:1 PR 7900 rpm	Vibration limited due flow instability in annular supply ring
Forced Convection	1960	Water		
Closed Loop Thermosyphon	1968	Water vapor, fuel at root	TIT 1600K, blade temp 1050K fuel press 8000 psi	Blade weld failures and fuel seal leaks; no catastrophic failure

TIT = turbine inlet temperature.

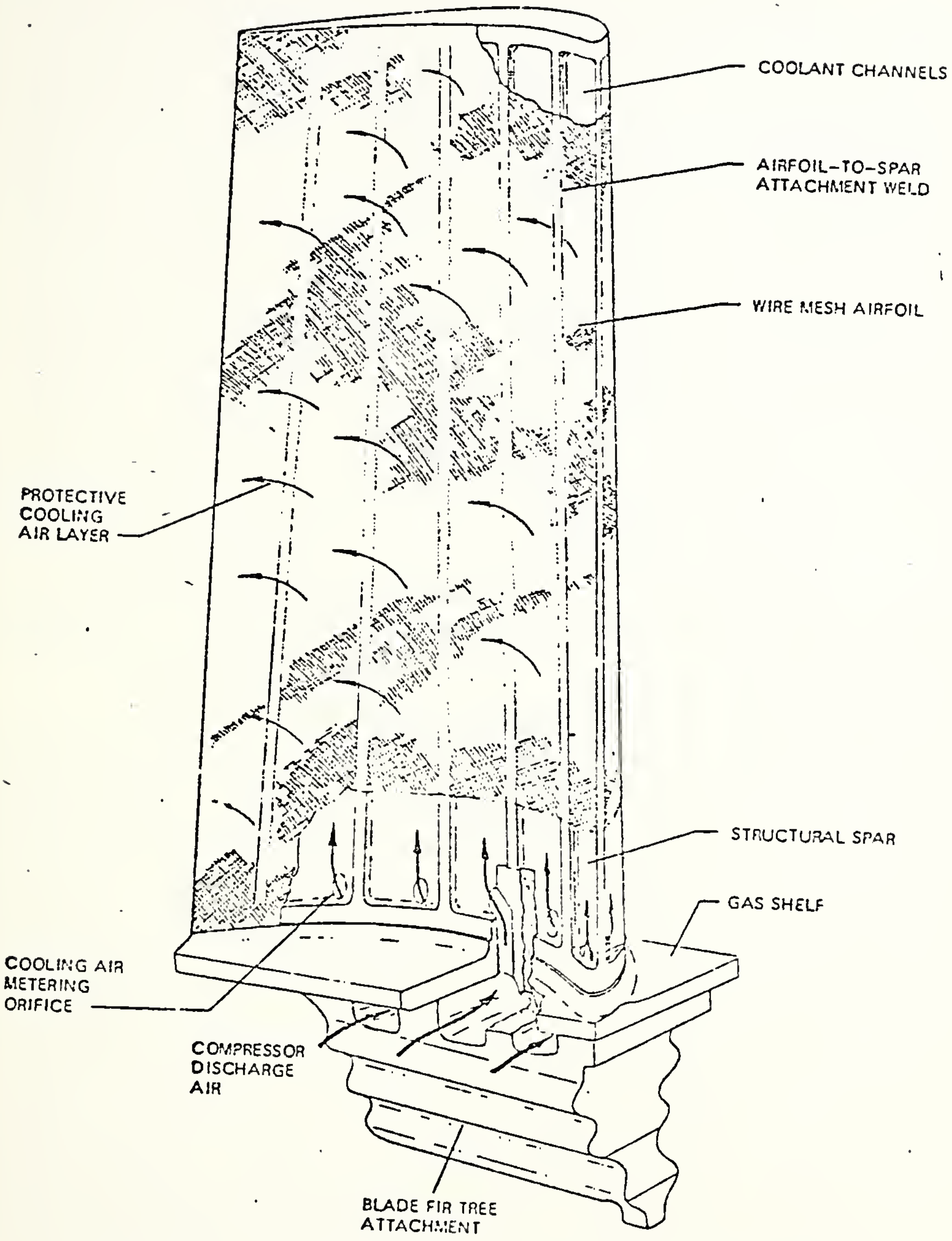
COOLANT CHANNELS
AIRFOIL-TO-SPAR ATTACHMENT WELD
WIRE MESH AIRFOIL
PROTECTIVE COOLING AIR LAYER
STRUCTURAL SPAR
GAS SHELF
COOLING AIR METERING ORIFICE
COMPRESSOR DISCHARGE AIR
BLADE FIR TREE ATTACHMENT

FIGURE 2.5 Transpiration Air Cooled Turbine Blade Concept [8]

The homogeneity of air with the turbine working fluid minimizes a number of problems that arise when a liquid, even water, is employed. Liquid cooling may be accomplished internally or externally as with air. Forced convection systems most commonly utilize a solid blade with interconnected radial holes; water enters the blade root from the turbine disk and follows a torturous path through the blade and is exhausted into the hub. The liquid can, alternatively, make a single pass through blade cooling passages and exhaust into the gas stream at some design quality. Recovery of some of the liquid is effected in a tip-shroud collecting ring for reuse, while the remainder is mixed with the gas stream.

Free-convection liquid cooling systems are commonly referred to as "thermosyphons" and several thermosyphon systems have been proposed for turbine blade cooling. The basic principle of the thermosyphon derives from the substantial free-convection velocities and effective heat transfer that result from the centrifugal-force field in a rotating turbine wheel. The Schmidt design [7] proposed radially drilled coolant passages open at the root and sealed at the blade tip. Coolant enters the passage at the root from an annular

supply and fills the entire passage. As the blade is heated by combustion gases, the layer of cooling fluid adjacent to the surface of the passages is heated and decreases in density relative to the fluid nearer the center of the cooling passage. The centrifugal body force per unit volume is $\rho r \omega^2$, where r is the radius from axis of rotation, ρ the coolant density and ω corresponds to the angular velocity. Thus the resultant body forces are smaller in the heated layer where the density is less than in the center; and the warmer fluid flows toward the axis of rotation. A continuous circulation is produced as hot fluid exiting from the turbine passage is replaced by cold fluid flowing outward from the core (Figure 2.6).

In an open thermosyphon, liquid water enters an exits from the turbine blade at the root water annulus carried in the rotor. Careful design of blade passages controls the pressure to avoid boiling within the blade unless specifically desired. Original designs [7] intended the water to flash to steam as it reentered the rotor hub, enabling additional extraction of work from the generated steam in an auxiliary turbine or heat exchanger. The open thermosyphon can employ partially or completely filled coolant passages, as can the closed thermosyphon. The closed system (Figure 2.7) seals

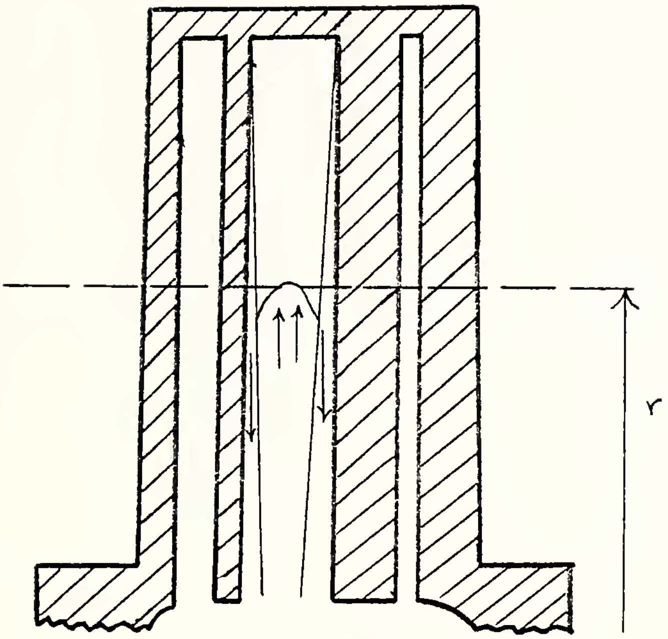

FIGURE 2.6 Free Convection Open Thermosyphon [11]

the blade at the root and tip, requiring a secondary coolant in the blade root and a heat exchanger. Consideration has been given to using fuel as the secondary coolant, but no working designs have evolved [12]. Another means of root cooling suggested is cooling by conduction through the rim of the disk [13] but this has not developed either.

The objective of using liquids in blade cooling is similar to convection with air, to reduce the metal temperature to a safe (lifetime-determined) level by the removal of heat through convection or boiling. External spray cooling has been considered for aircraft engines for short duration power augmentation on take-off or for emergencies, but the excessive water requirements and added weight ruled out further practical development of this system [3]. Water injection for shipboard turbines as a means of increasing the mass flow and power have been hindered by the problems of excess stack moisture that creates visible plumes that, in the case of naval vessels, can serve as an infra-red target [14].

The above description of the most common types of blade cooling systems has not attempted to compare them, as such a comparison relies on an evaluation of the abilities of the various systems to contribute to overall engine performance at reasonable economy.

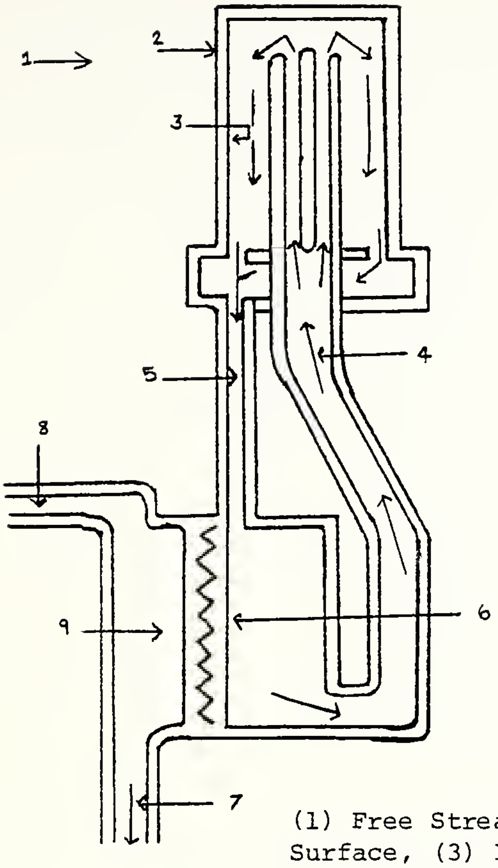

(1) Free Stream, (2) Outside Blade Surface, (3) Inside Blade Surface, (4) Secondary Coolant Inlet Conditions, (5) Secondary Coolant Exit Conditions, (6) Hot Side of Heat Exchanger, (7) Primary Coolant Exit Conditions, (8) Primary Coolant Inlet Conditions, and (9) Cool Side of Heat Exchanger.

FIGURE 2.7 Closed-Loop Thermosyphon Cooling System [12]

It is observed, however, that the liquid thermosyphon methods have been in the laboratory research stage for over thirty years without the appearance of a production model; the vibratory forces and coolant dynamics problems associated with liquid cooling have been thus far insurmountable. A revival of attempts at liquid system design for large industrial turbines is underway but remains in the conceptual design stage, awaiting test vehicle manufacture and operation [15].

3. THERMODYNAMICS OF COOLING

The thermodynamic effects of engine cooling on performance and efficiency vary with the cooling method and cooling system type; in particular some lossess associated with each system are a function of design and hence are controllable, whereas other losses are beyond the designers influence. This chapter shall (1) review the specialized nomenclature associated with the thermodynamic problems of turbine cooling; (2) discuss the general effects of cooling on performance and efficiency; and (3) examine the particular losses associated with the various cooling methods.

3.1 REVIEW OF THERMODYNAMICS

3.1.1 Temperature-Entropy Diagram

This diagram presents (explicitly) process lines of constant temperature and entropy plus (implicitly) lines of constant pressure and volume when the working fluid in the process is a gas. Several features of these last two process lines are important in analyzing gas turbine performance.

From the state relationship

$$Tds = c_v dT + Pd\nu$$

and the ideal gas law

$$Pv = RT \qquad (3.1)$$

Differentiating Equation 3.1,

$$Pdv = RdT - vdP$$

and substituting yields

$$Tds = c_v dT + RdT - \quad dP$$

The gas constant $R = c_p - c_v$ and with Equation 3.1

$$Tds = c_p dT - RT \frac{dP}{p}$$

and dividing by T

$$ds = c_p \frac{dT}{T} - R \frac{dP}{P} \qquad (3.2)$$

For a line of constant pressure $dP/P = 0$ and hence

$$\frac{dT}{ds} = \frac{T}{c_p} \qquad (3.3)$$

or a line of constant pressure on the T-s diagram has a positive increasing slope with T, although increasing values of c_p with T will diminish this somewhat.

Integrating Equation 3.2 between any two temperatures

$$s - s_o = \int_{T_o}^{T} c_p \frac{dT}{T} - R\ell n \frac{P}{P_o}$$

For an isentropic (ideal reversible) process, $s - s_o = 0$ hence from Equation 3.2, with c_p constant,

$$\bar{c}_p \, \ell_n \frac{T}{T_o} = R\ell_n \frac{P}{P_o}$$

$$\left(\frac{T}{T_o}\right)^{c_p} = \left(\frac{P}{P_o}\right)^{R}$$

$$\frac{T}{T_o} = \left(\frac{P}{P_o}\right)^{\frac{\gamma-1}{\gamma}} \qquad (3.4)$$

where $\gamma = c_p/c_\nu$. Knowledge of the variation of c_p with T or more usually the adoption of an average $\bar{c}_p$ over the temperature limits permits evaluation of the entropy change between two known states for any process. The important feature of isobars on the T-s diagram is their divergence as entropy increases, as shown in Figure 3.1.

3.1.2 Steady Flow Energy Equation

The total energy of a unit mass of fluid in steady flow is comprised of internal energy u, the flow work p , the kinetic energy $v^2/2$, and the potential energy due to position gz_1. The change of this total energy across a generalized rotor is due to shaft work W_s and heat Q being transferred into or out of the rotor. An energy balance between the inlet and outlet stations gives

$$u_1 + P_1 v_1 + V_1^2/2 + gz_1 + Q =$$

$$u_2 + P_2 v_2 + V_2^2/2 + gz_2 + W_s \qquad (3.5)$$

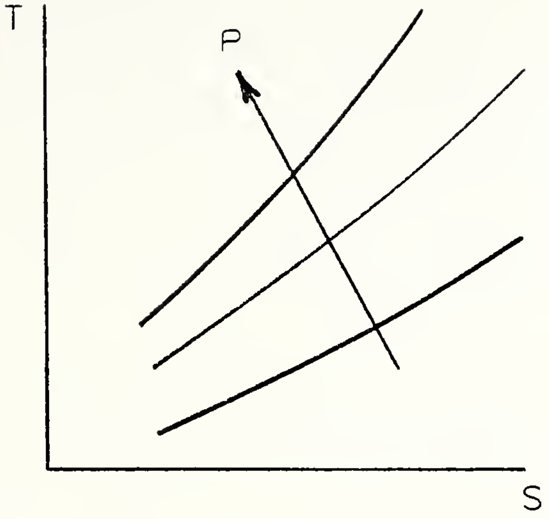

FIGURE 3.1 Isobars on T-s Diagram [4]

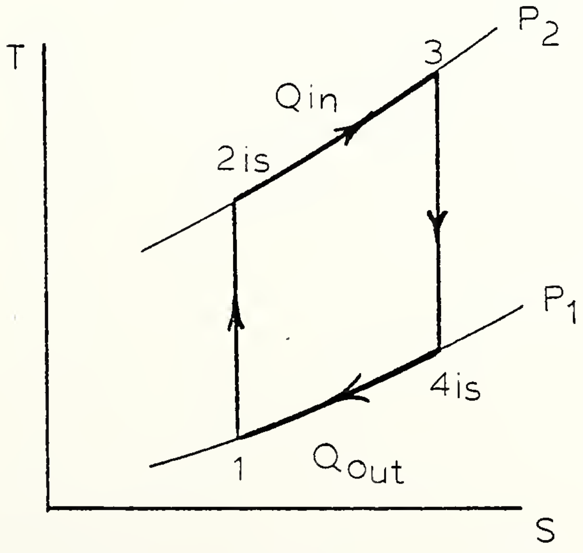
T
P2
3
Qin
2is
P1
4is
1
Qout
S

FIGURE 3.2 Brayton Cycle Representation

This relation is valid for any fluid and may be simplified considerably for an ideal gas. Potential energy changes are negligible and the internal energy and flow work terms may be combined as the fluid enthalpy h and expressed for a perfect gas as c_pT. Equation 3.5 reduces to

$$c_{p1}T_1 + V_1^2/2 + Q = c_{p2}T_2 + V_2^2/2 + W_s \qquad (3.6)$$

3.1.3 Ideal (Brayton) Cycle

The ideal cycle for the simple gas turbine is the Joule or Brayton cycle; heat addition and rejection is idealized at constant pressure as depicted in Figure 3.2. The relevant steady flow energy equation is

$$Q = h_2 - h_1 + \frac{1}{2}(V_2^2 - V_1^2) + W$$

where the heat transfer Q and the work transfer W are per unit mass flow. Applying this equation to each component and assuming no changes in kinetic energy between the inlet and outlet of each component

$$W_{12} = -(h_2 - h_1) = -c_p(T_2 - T_1)$$

$$Q_{23} = h_3 - h_2 = c_p(T_3 - T_2)$$

$$W_{34} = h_3 - h_4 = c_p(T_3 - T_4)$$

The cycle efficiency (net work output divided by heat supplied) is

$$= \frac{c_p(T_3 - T_4) - c_p(T_2 - T_1)}{c_p(T_3 - T_2)}$$

From the ideal gas relations for a reversible, adiabatic, process,

$$\frac{T_2}{T_1} = \left(\frac{P_2}{P_1}\right)^{\frac{\gamma-1}{\gamma}} = \left(\frac{P_3}{P_4}\right)^{\frac{\gamma-1}{\gamma}} = \frac{T_3}{T_4}$$

If r is defined as thepressure ratio $P_2/P_1 = P_3/P_4$, then the cycle efficiency can be shown to be given by

$$\eta = 1 - \left(\frac{1}{r}\right)^{\frac{\gamma-1}{\gamma}}$$

Thus the cycle efficiency of the ideal (loss-less) gas turbine open cycle is dependent only on the pressure ratio and the nature of the gas as reflected by the value for γ. For air γ is approximately constant at 1.4 although more rigorously it will vary slightly with temperature. The variation of cycle efficiency with pressure ratio is shown in Figure 3.3.

The specific work output W (work per unit mass of working fluid) is a function of maximum cycle temperature as well as pressure ratio:

$$W = c_p(T_3 - T_4) - c_p(T_2 - T_1)$$

The expression may be non-dimensionalized as

$$\frac{W}{c_p T_1} = t\left(1 - \frac{1}{r^{\frac{\gamma-1}{\gamma}}}\right) - \left(r^{\frac{\gamma-1}{\gamma}} - 1\right) \qquad (3.8)$$

where $t = T_3/T_1$. The maximum cycle temperature T_3 influences the specific work output considerably; the effect of increasing the temperature ratio of the cycle is demonstrated in Figure 3.4. For a fixed maximum temperature ratio, the specific work is maximized at a certain pressure ratio; this pressure ratio is determined by differentiating Equation 3.8. with respect to $(r)^{\frac{\gamma-1}{\gamma}}$ and equating the result to zero, and is less than the pressure ratio for maximum efficiency.

3.1.4 Stagnation Properties

For an adiabatic flow of a gas with no work transfers, the steady-flow equation reduces to

$$c_{p_1} T_1 + V_1^2/2 = c_{p_2} T_2 + V_2^2/2$$

which expresses the stagnation enthalpy h_o of the fluid. Physically, the stagnation enthalpy is the enthalpy which a gas stream of enthalpy h and free stream velocity V would possess when brought to rest adiabatically without work transfer. Thus,

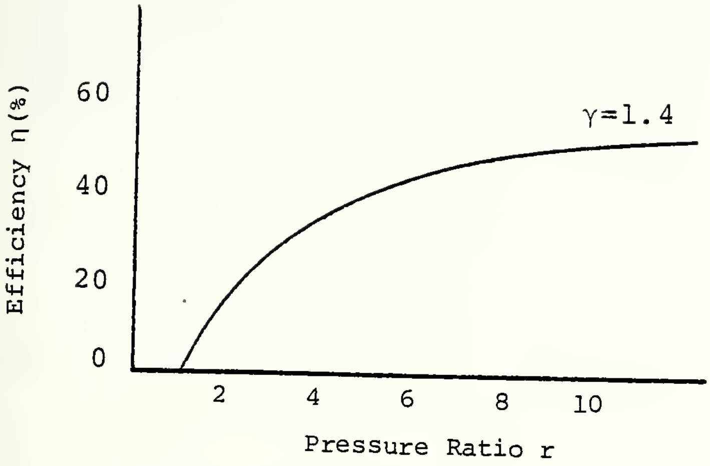

FIGURE 3.3 Simple Cycle Efficiency Variation with Pressure Ratio (Loss-Less) [16]

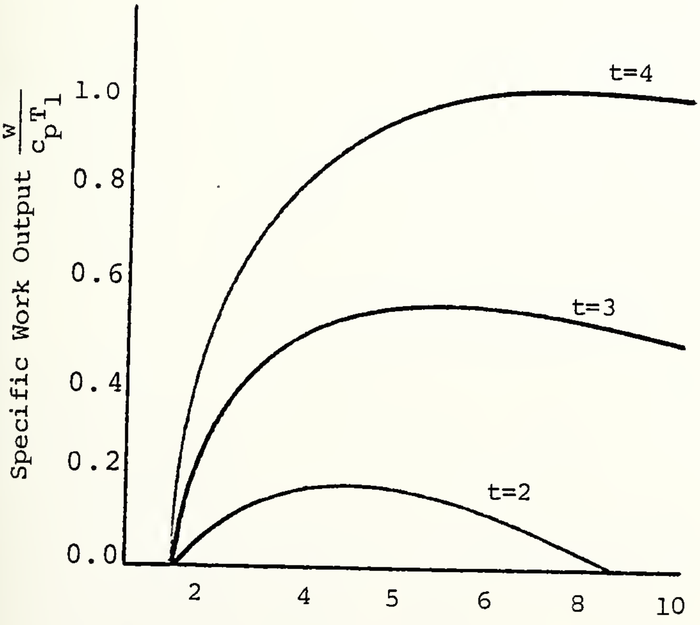

FIGURE 3.4 Simple Cycle Specific Work Output [16]

$$h_o = h + V^2/2$$

The stagnation enthalpy of a perfect gas ($h = c_p\ T$) is characterized by the stagnation temperature T_o

$$T_o = T + V^2/2c_p \tag{3.9}$$

Equation 3.9 expresses the total or stagnation temperature in a gas as the sum of the local free stream static temperature T plus a free stream dynamic temperature rise $V^2/2c_p$.

Thermodynamically, T_o represents the theoretical temperature that a flowing gas will attain when slowed adiabatically to zero velocity. In particular for a high speed gas following adiabatically across an insulated plate, viscous forces arising within the boundary layer slow the gas and dissipate the energy of the free stream, resulting in a temperature gradient normal to the plate.

If stagnation temperatures are employed in analysis, the kinetic energy terms in the steady flow equation are accounted for implicitly. Stagnation temperature is constant in a stream flowing without heat or work transfer; friction effects are accounted for between the static and dynamic terms. However, when the gas is slowed and the static temperature rises there is a simultaneous rise in pressure. The definition of stagnation pressure

P_O requires further restrictions that the gas is brought to rest adiabatically and also reversibly, hence in an isentropic manner; thus P_O is defined by

$$\frac{P_o}{p} = \left(\frac{T_o}{T}\right)^{\frac{\gamma}{\gamma-1}}$$

and is constant only if friction is absent.

3.1.5 Adiabatic Wall Temperature

A gas flowing past an insulated surface will cause the surface temperature to increase above the local gas temperature T but to less than the total temperature T_O. The actual temperature at an adiabatic surface is called the adiabatic wall temperature, T_{aw} and is related to T and T_o by the recovery factor R_t, which is a measure of the free stream dynamic temperature rise recovered at the wall;

$$R_t = \frac{T_{aw} - T}{V^2/2cp} = \frac{T_{aw} - T}{T_o - T}$$

The relationship among T, T_O and T_{aw} is illustrated in Figure 3.5 and becomes significant when considering heat transfer mechanisms in high-speed, turbulent fluid flow.

3.1.6 Isentropic Efficiency

Irreversibility in compression or expansion causes an increase in entropy as shown in Figure 3.6.

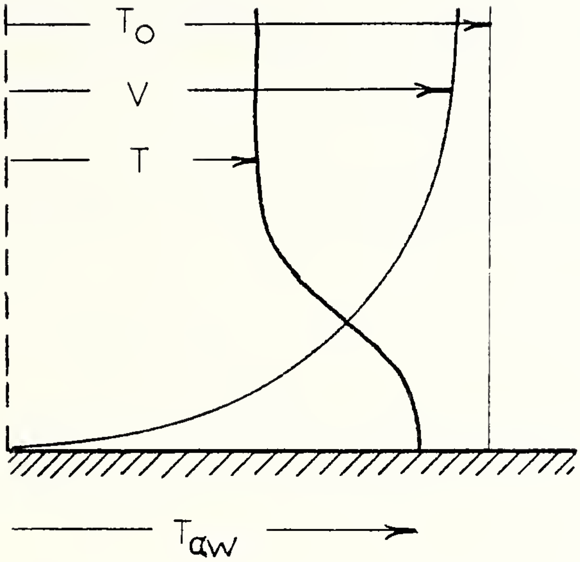

FIGURE 3.5 Temperature Relations in High-Speed Flow Over Insulated Plate [11]

The degree of irreversibility is expressed through the turbine or compressor efficiency η_T or η_c. For a turbine

$$\eta_T = \frac{\text{Actual Work}}{\text{Ideal Work}}$$

The evaluation of these quantities depends on whether the exit kinetic energy of the gas stream is utilized or not. If utilized (as in multi-stage turbine) the turbine isentropic efficiency is the total-to-total efficiency and is defined as

$$\eta_{TT} = \frac{h_{01} - h_{02}}{h_{01} - h_{02}\ \text{isen}}$$

For small differences in inlet and outlet kinetic energies (i.e. $\frac{1}{2} V_1{}^2 = \frac{1}{2} V_2{}^2$) then

$$\eta_{TT} = \frac{h_1 - h_2}{h_1 - h_2\ \text{isen}}$$

When exhaust kinetic energy is not utilized, the total-to-static efficiency represents the turbine isentropic efficiency

$$\eta_{TS} = \frac{h_{01} - h_{02}}{h_{01} - h_2\ \text{isen}}$$

For fixed stage pressure ratio, the irreversibility in expansion or compression results in higher exhaust and compressor exit temperatures.

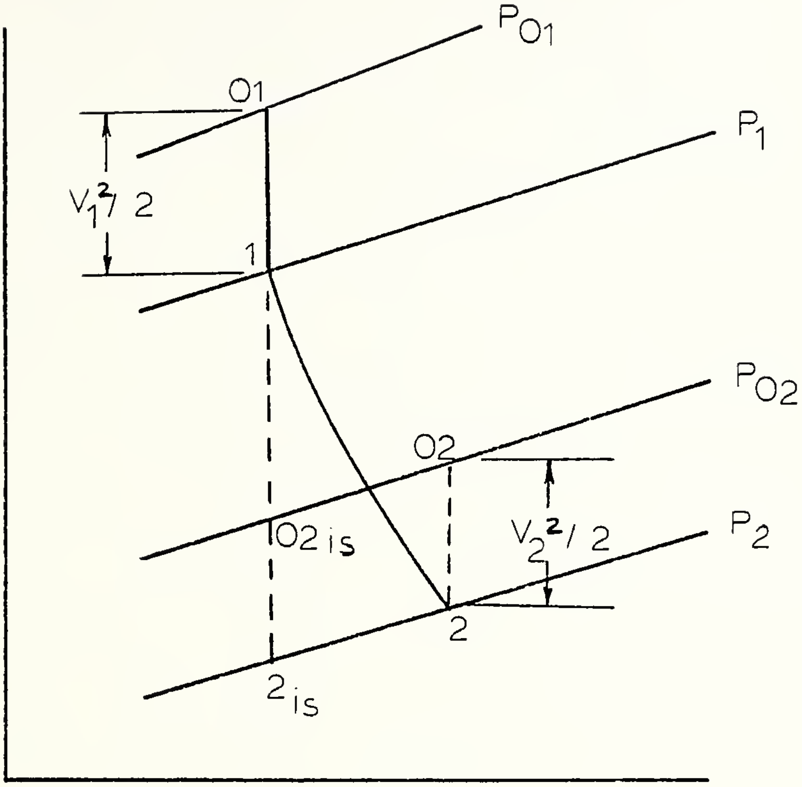
P_{01}
01
P_1
$V_1^2/2$
1
P_{02}
02
02 is
$V_2^2/2$
P_2
2
2_{is}

FIGURE 3.6 Turbine Isentropic Efficiency

3.1.7 Reheat Effects

Turbine efficiency has been described above in terms of the overall expansion pressure ratio; in an actual turbine this pressure ratio is achieved through multiple expansions or stages, each of approximately the same stage expansive efficiency η_s. In a turbine, the temperature at entry to each succeeding stage is higher than that due to isentropic expansion by virtue of the inefficiency of the proceding stage. Each successive stage therefore produces additional work output; the production of additional work for a given pressure ratio in a turbine is known as the reheat effect and is demonstrated in Figure 3.7. In expanding from initial state A to B', the overall isentropic efficiency is $\Delta T_{AB'}/\Delta T_{AB}$. If the overall pressure ratio P_A/P_B is achieved in three stages of equal stage isentropic efficiency η_s, the overall work remains $\Delta T_{AB'}$. This work is also represented by the sum of $\Delta T_{A1'}$, $\Delta T_{1'2'}$, and $\Delta T_{2'B'}$. From Figure 3.7,

$$\Delta T_{A1'} = \eta_s \, \Delta T_{A1}$$

$$\Delta T_{1'2'} = \eta_s \, \Delta T_{1'2''}$$

$$\Delta T_{2'B'} = \eta_s \, \Delta T_{2'B''}$$

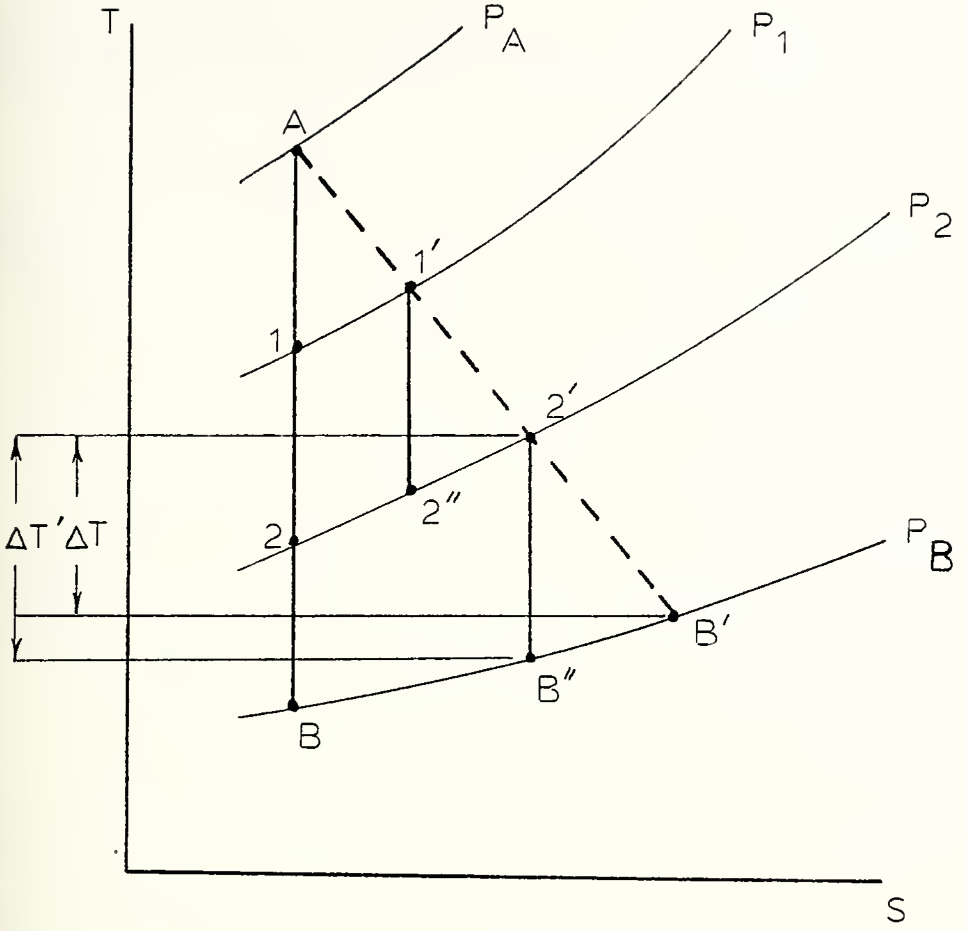
T
S
P_A
P_1
P_2
P_B
A
1
1′
2
2′
2″
B
B′
B″
ΔT′
ΔT

FIGURE 3.7 Reheat Effect in Turbine (Expansion) [4]

and therefore

$$\Delta T_{AB'} = \eta_s(\Delta T_{A1} + \Delta T_{1'2''} + \Delta T_{2'B''})$$

As the isobars diverge with increasing entropy,

$$\Delta T_{1'2''} > \Delta T_{12} \quad \text{and} \quad \Delta T_{2'B''} > \Delta T_{2B}$$

Therefore

$$\Delta T_{A1} + \Delta T_{1'2''} + \Delta T_{2'B''} > \Delta T_{A1} + \Delta T_{12} + \Delta T_{2b} = \Delta T_{AB}$$

or

$$\frac{1}{\eta_s} \Delta T_{AB'} > \Delta T_{AB}$$

and since

$$\Delta T_{AB'} = \eta_T \Delta T_{AB},$$

$$\frac{1}{\eta_s} > \frac{1}{\eta_T}$$

or

$$\eta_S < \eta_T$$

3.1.8 Polytropic Efficiency

The variation of turbine (and compressor) efficiency with pressure ratio as manifested in the reheat analysis complicates cycle calculations covering a range

of pressure ratios, hence the concept of polytropic (or small-stage) efficiency η_p. The polytropic efficiency of a process is the isentropic efficiency of an elemental stage in the process such that it is constant throughout the whole process. For a turbine,

$$\eta_p = \frac{dh}{dh\ isen}$$

For an isentropic process, Tds = 0 = dh_{IS} - vdp; hence,

$$\eta_p = \frac{c_p\ dT}{vdp} = \frac{c_p\ P\ dT}{RT\ dp} \qquad (3.10)$$

since v = R_T/P. Separating (3.10) into differential form

$$\frac{dT}{T} = \frac{R}{c_p}\ p\ \frac{dp}{p}$$

Substituting $c_p = \frac{\gamma R}{\gamma - 1}$ yields

$$\frac{dT}{T} = \left(\frac{\gamma-1}{\gamma}\right) \eta_p \frac{dp}{p}$$

Integrating across the whole turbine assuming equal efficiency for each infinitesimal stage

$$\int_{T_3}^{T_4} \frac{dT}{T} = \int_{p_3}^{p_4} \left(\frac{\gamma-1}{\gamma}\right) \eta_p \frac{dp}{p}$$

$$\frac{T_4}{T_3} = \left(\frac{p_4}{p_3}\right)^{\left(\frac{\gamma-1}{\gamma}\right)\eta_p} = \left(\frac{p_2}{p_1}\right)^{\left(\frac{\gamma-1}{\gamma}\right)\eta_p}$$

Isentropic efficiency for the entire expansion process is

$$\eta = \frac{T_3 - T_4}{T_3 - T_4 \text{ isen}}$$

Rearranging and substituting give

$$\eta_T = \frac{1 - r^{\eta_p(\gamma-1)/\gamma}}{1 - r^{(\gamma-1)/\gamma}}$$

where r is the turbine pressure ratio.

3.1.9 Heat Transfer

The principal mechanism of heat flow in solids and important to some extent in fluids is conduction, the process of heat transfer between high and low temperature regions through direct molecular communication. The governing relation for one-dimensional conductive heat flow is

$$\frac{q_k}{A} = - k \frac{dT}{dx}$$

where the proportionality constant, k, termed the thermal conductivity, links the heat flux and temperature gradient. The thermal conductivity is a material property with units W/HR m K (BTU/HR FT F): Convection is the process of energy transport by the combined action of heat

conduction, energy storage and mixing motion, and is the most important mechanism of energy transfer between a solid surface and a liquid or gas. Convection is classified according to the method of motivating flow in free or forced convection, depending on whether the flow results from density differences caused by temperature gradients or from pumping. The governing relation for convective heat transfer is Newton's Equation

$$q_c = \iint_A h_c \, dA \, (T_s - T_\infty)$$

where q_c = rate of heat transfer by convection w/HR (BTU/HR)

A = heat transfer area m^2 (FT^2)

h_c = local convective heat transfer coefficient w/m^2 HRK (BTU/HR FT^2 F)

T_s = surface temperature K(F)

T_∞ = fluid temperature K(F)

The evaluation of the convective heat transfer coefficient is extremely difficult due to the complex nature of the phenomenon; the value of h_c in a system depends if the surface geometry, fluid velocity and properties, and even on the magnitude of the temperature difference. The convective heat transfer coefficient may therefore vary

over the surface and hence must be specified locally. An average coefficient $\overline{h}_c$ can be defined in terms of the local value by

$$\overline{h}_c = \frac{1}{A} \iint_A h_c \, dA$$

and in fact for many engineering applications average values are sufficient.

3.2 HEAT TRANSFER IN TURBINE BLADES

3.2.1 Temperature Distributions

The temperature distribution around a typical blade is illustrated in Figure 3.8. The chordwise temperature differences result from several flow field factors, principally turbulence and (thus) Reynolds number. It is apparent from the figure that the critical temperature areas are the leading and trailing edges, which are also the most difficult areas to effectively cool. The distribution of the gas side heat transfer coefficient resembles that of Figure 3.9. The highest values occur at the leading edge stagnation point and on the after portion of the suction surface. The latter effect is due to the onset of turbulence usually within the first 25-30 percent chord that increases the heat flux to the blade through increased mixing.

The temperature distribution within a turbine blade has significant (often critical) impact on maximum

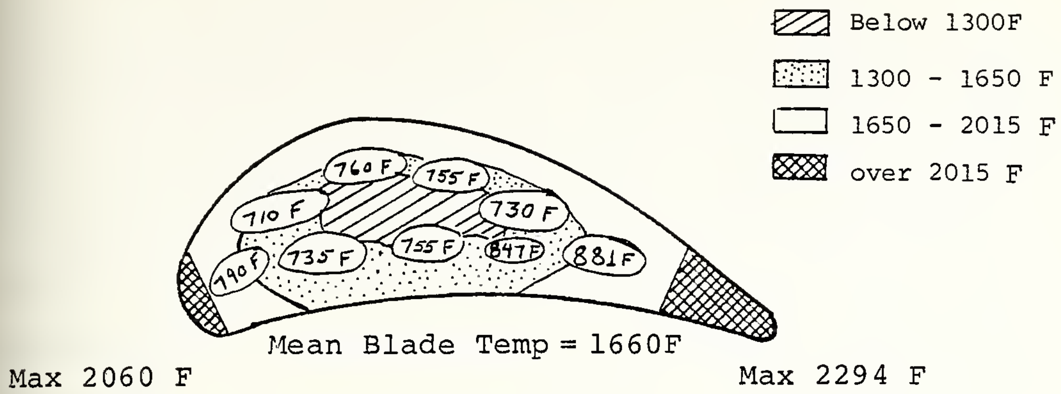
▨ Below 1300F
░ 1300 - 1650 F
☐ 1650 - 2015 F
▩ over 2015 F
760 F
755 F
710 F
730 F
790 F
735 F
755 F
847F
881 F
Mean Blade Temp = 1660F
Max 2060 F
Max 2294 F

FIGURE 3.8 Typical Cascade Blade Temperature Distribution [17]

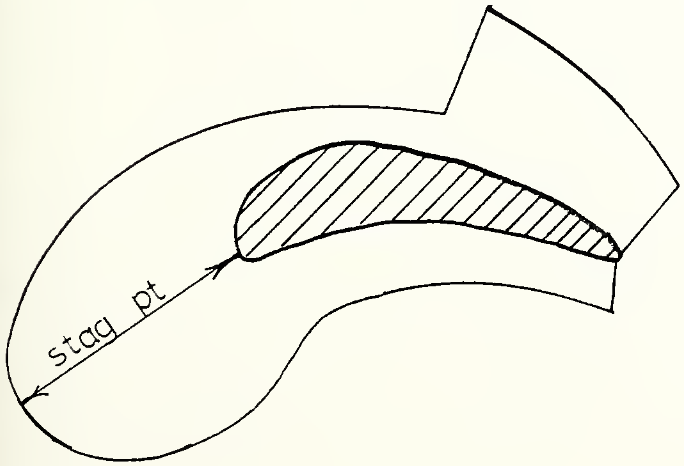

FIGURE 3.9 Typical Turbine Blade Heat Transfer Coefficient Distribution [18]

operating temperature and lifetime, due to thermal stresses and low cycle fatigue. The cooling system therefore is a major variable in attempts to minimize thermal stress and improve blade life characteristics. When a turbine blade is heated, the outer surface layers develop compressive stresses while the core remains cool (condition at startup). As the blade core heats up a stress reversal occurs and tensile stresses are induced in the surface layers. Cool-down repeats the pattern and if the stress changes are rapid and cyclic, surface cracking will be inducued, usually at the leading or trailing edges. Blade cooling can aggravate the situation if uneven chordwise and spanwise temperatures develop. Transpiration cooling has demonstrated the capability to significantly smooth out such gradients (Figure 3.10) throughout the blade; film cooling can reduce the spanwise temperature gradient but establishes its own chordwise distribution. The limit of a poor temperature distribution results in excessive oxidation and corrosion, leading ultimately to failure. Liquid cooling has demonstrated significant distribution ability [24] but excessive cooling that can result with liquids can intensify the low-cycle fatigue problem.

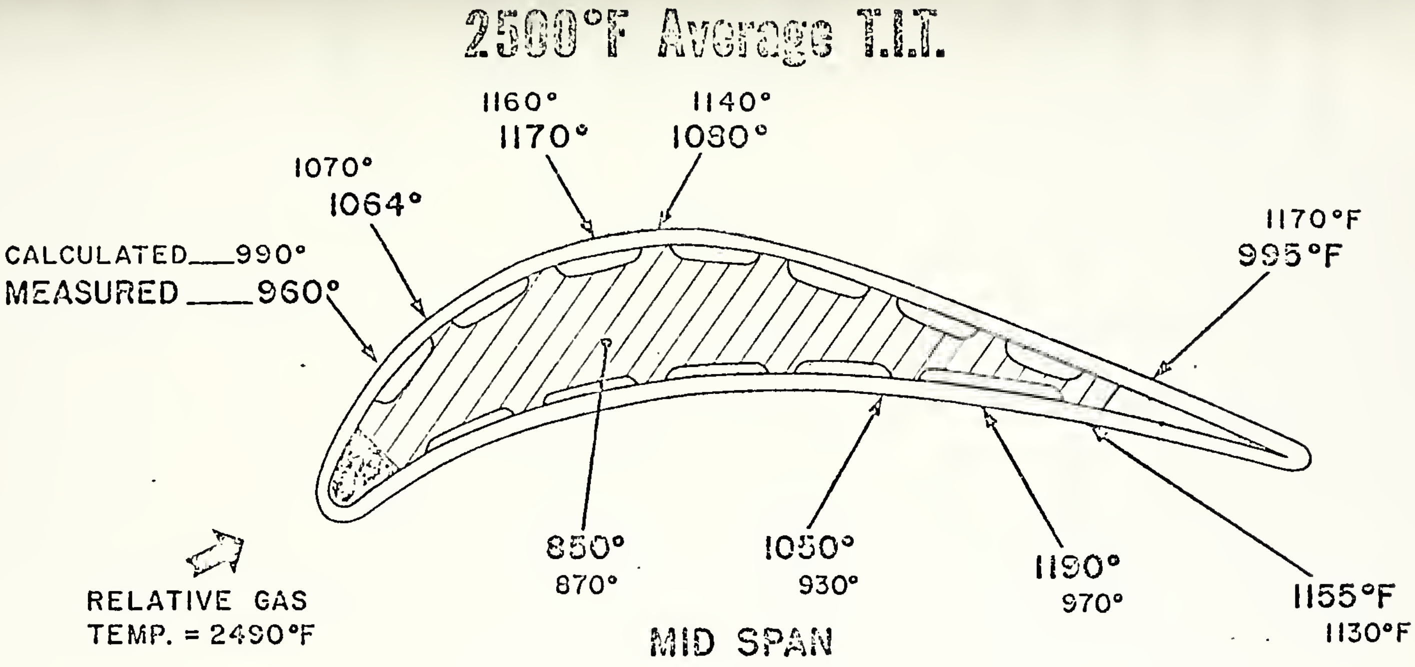
2500°F Average T.I.T.
CALCULATED___990°
MEASURED____960°
1070°
1064°
1160°
1170°
1140°
1080°
1170°F
995°F
RELATIVE GAS
TEMP. = 2490°F
850°
870°
1050°
930°
1190°
970°
1155°F
1130°F
MID SPAN

FIGURE 3.10 Chordwise Thermal Gradients with Transpiration Cooling

3.2.2 Gas Side Heat Transfer

Blade cooling methods are usually considered independently of gas side heat transfer since this factor is common to both cooled and uncooled blades. There have been numerous attempts to measure the gas side heat transfer coefficient for varying conditions, as shown in Figure 3.11. The Nusselt number Nu represents the non-dimensionalized heat transfer coefficient

$$Nu = \frac{h_c}{k}$$

where c is the blade (or stator) chord. From the figure it is apparent that much disparity occurs in values for Nu at a given Re, as much as 150 percent variation over the range of Re shown. Thus prediction of gas side heat transfer is an inexact procedure at best. For laminar conditions

$$Nu \propto (Re)^{0.5}$$

(assuming air with constant Pr) and with turbulence

$$Nu \propto (Re)^{0.8}$$

These derive from flat plate correlations and an actual turbine maybe expected to lie between these values, tending towards turbulence assuming normally high levels of ambient turbulence must exist in real engines.

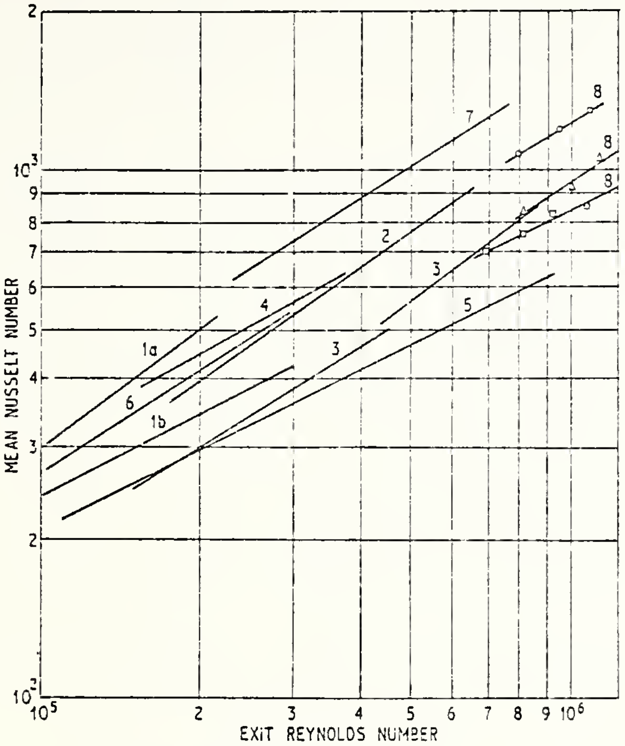

1*a* Ainley turbine
1*b* Ainley cascade
2 Wilson and Pope
3 Hodge
4 Bammert and Hahnemann
5 Andrews and Bradley
6 Fray and Barnes
7 Halls
8 Turner

Symbol	Turbulence
○	5·9%
△	2·2%
□	0·45%

FIGURE 3.11 Gas Side Heat Transfer Correlations for Turbine and Cascades [6]

The location of the transition point from laminar to turbulent flow is quite variable, usually within the initial 30 percent chord on the suction surface. Along the pressure surface the flow may remain very nearly laminar throughout.

There is conflicting evidence that transpiration cooling in particular may have some determinable effect on gas side heat transfer coefficients; although Bayley [6] suggests little variations from convection cooling consistent with the normal variation as in Figure 3.11, some experiments suggest that the cooling blanket from uniformly porous materials trips the boundary layer into turbulence at a lesser distance along the chord, increasing the heat transferred to the coolant [19].

3.2.2 Coolant Side Heat Transfer

Coolant side correlations take similar form as for gas side relations

$$Nu \propto Re^{0.8}$$

for turbulent flow through a pipe. For natural convection systems (thermosyphons) the relevant correlations are of the form

$$Nu = \phi(Gr), \psi(Pr)$$

where Gr is the Grashof number and represents the ratio of buoyant to viscous forces

$$Gr = \frac{g\beta \ \Delta T}{\nu^2} L^3$$

where β = coefficient of thermal expansion of the fluid and g the acceleration of gravity. For a turbine the driving field is the contrifugal acceleration $r\omega^2$ instead of g; hence

$$Gr = \frac{r\omega^2\beta \ \Delta T \ L^3}{\nu^2}$$

where L is the length of the cooling passage. For typical blade dimensions and turbine rpm with water cooling, the heat transfer coefficients can be quite large, on the order of 16-20,000 BTU/HR FT^2 F [11]. The internal cooling heat transfer coefficients h_c are usually one to two orders of magnitude greater than the gas side coefficient; hence if the blade or vane material conductivity is not so low as to cause a large temperature drop between the outer surface and the cooling passage, the surface can be cooled adequately.

The increased values of Nuc with turbulence have prompted the employment of turbulence stimulators as integral parts and inserts to cast blade sections.

3.3 COOLED TURBINE LOSSES

The cooling process incurs a number of losses to cycle efficiency; some of these losses can be accounted for directly in calculating cycle efficiency while others require additional methods of accounting. The sources and approximate magnitudes of cooling losses in air-cooled turbines are described below. When compressor air is utilized for cooling there is a net reduction in turbine mass flow. Although some reduction in compressor work can be realized if cooling flows are extracted before the compressor exit, reintroduction of these flows at varying stages in the turbine reduces the net work extracted from the gas stream per stage. This loss is proportional to cycle pressure and coolant flow rate and can be quite large, from 1-20 percent in turbine efficiency. Another direct loss associated with cooling flows is a reduction in turbine exhaust temperature; this factor becomes very significant in cycles with heat exchange or exhaust heat recovery systems, as the lower temperature lessens the heat exchanger effectiveness.

Other losses that are not so easily accounted for include: (a) the expansion is no longer adiabatic; the result of heat extraction at each turbine stage is a progressive reduction in the gas temperature through

the turbine, reducing the turbine reheat factor R and therefore reducing overall turbine efficiency η_T since

$$\eta_T = R\,\eta_s$$

where η_s is stage efficiency; obviously reducing the number of stages helps to minimize efficiency loss; (b) there is a pressure loss and a reduction in enthalpy of the gas stream due to mixing of exhausted cooling air with the main stream; (c) some pumping work is done on the blades by the coolant as it passes radially outwards through the coolant passages. If exhausted at the blade tip additional mixing loss occurs but may be partially offset by reduction in tip leakage loss. This pumping work may include an "acceleration" loss as the coolant moves from near-rest conditions to full turbine speed; this loss is proportional to coolant flow rate and to the square of the turbine wheel speed. Magnitudes of this acceleration loss for convection cooling systems are estimated between zero and 5 percent [3]; (d) a final ill-defined loss experienced in cooled turbines is aerodynamic loss due to departure from optimal blade shapes to accommodate coolant flow passages, especially in the vicinity of the leading and trailing edges, where thickness of the cross-section must increase to provide

adequate flow area for the coolant. Estimates for the magnitude of this loss range from nil to 2 1/2 - 3 percent in turbine efficiency [3].

Not all of the losses listed above are applicable to all cooling systems. For liquid closed thermosyphons the negative reheat effects dominate while there are no mixing and minimal pumping losses. For open thermosyphons, there is considerable mixing loss and gas stream enthalpy drop, so much so that these systems are no longer considered practical [7,20]. The tendancy of all liquid cooled blades is excessive reduction of the metal temperatures and exaggerated negative reheat. One of the principle goals of liquid cooling system design has been the limitation on the degree of cooling applied to the blade to prevent this effect.

The losses listed in (a) through (d) are accounted for in cycle calculations through a reduced value of turbine efficiency. Several methods have been employed to assess this reduction; pertinent sections of the analysis of Hawthorne, Brown and May are presented below.

3.4 COOLING LOSS PARAMETERS

Brown [21] defined a non-dimensional cooling loss factor

$$\ell = \frac{\text{heat loss by gas/unit time}}{\text{turbine work/unit time}}$$

and developed a formula to relate ℓ to turbine isentropic efficiency. In a multi-stage turbine the stage efficiency closely approximates the polytropic efficiency and in an uncooled turbine of this type the heat equivalent of energy losses occurring in any given stage is returned to the working fluid in the stage. This reheat effect raises the outlet temperature of the stage to a value greater than that due to adiabatic expansion and thereby increases the total work output and turbine efficiency. From Figure 3.12 the uncooled turbine efficiency

$$\eta_T = \frac{h_1 - h_2}{h_1 - h_2 \text{ isen}}$$

for a polytropic process of an ideal gas becomes

$$\eta_T = \frac{1 - (p_2/p_1)^{\eta_s \left(\frac{\gamma-1}{\gamma}\right)}}{1 - (p_2/p_1)^{\frac{\gamma-1}{\gamma}}}$$

If the stage efficiency is not appreciably affected by the heat loss due to blade cooling, a cooled stage efficiency η_s' may be defined as

$$\eta_s' = \frac{\text{stage total heat drop}}{\text{stage adiabatic heat drop}}$$

to give the actual expansion line obtained in the cooled turbine. From Figure 3.12

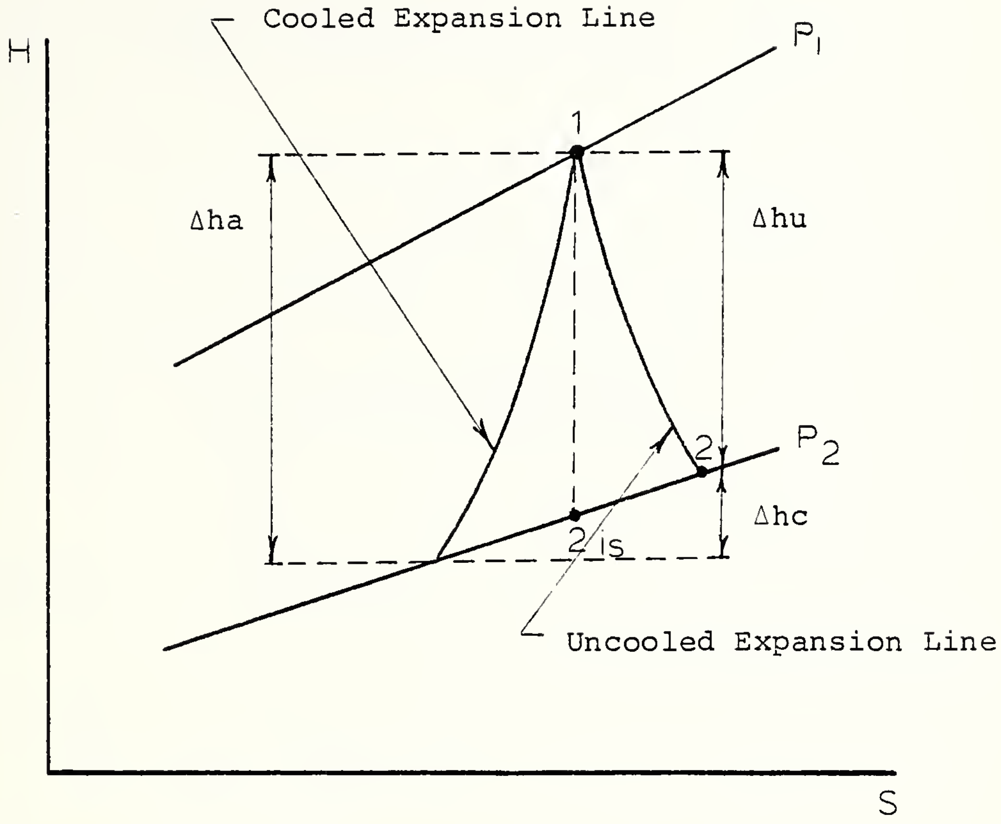
Cooled Expansion Line
H
P_1
1
Δha
Δhu
2
P_2
Δhc
2_{IS}
Uncooled Expansion Line
S

Δha = stage adiabatic heat drop

Δhu = stage useful work

Δhc = stage cooling loss

FIGURE 3.12 Effect of Cooling Losses on Turbine Efficiency [21]

$$\eta_s' = \frac{\Delta h_u + \Delta h_c}{\Delta h_a}$$

$$= \frac{\Delta h_u}{\Delta h_a} \cdot \frac{\Delta h_u + \Delta h_c}{\Delta h_u}$$

$$= \eta_s \ (1 + \ell)$$

For a constant ℓ throughout the turbine then the turbine efficiency η_T may be related to ℓ as follows:

$$\eta_T' = \frac{\text{turbine total heat drop}}{\text{turbine adiabatic heat drop}}$$

$$= \eta_T \ (1 + \ell)$$

expressing η_T' in similar form as η_T

$$\eta_T' = \frac{1 - (p_2/p_1)^{\eta_s' (\frac{\gamma-1}{\gamma})}}{1 - (p_2/p_1)^{\frac{\gamma-1}{\gamma}}}$$

Substituting the expressions for η_s' and η_T' gives

$$\eta_T = \frac{1}{1+\ell} \cdot \frac{1 - (p_2/p_1)^{\frac{\gamma-1}{\gamma} \eta_s \ (1+\ell)}}{1 - (p_2/p_1)^{\frac{\gamma-1}{\gamma}}}$$

Typical values of ℓ calculated for liquid cooled turbines [21] range from 0.12 to 0.25 for laminar flow conditions on a single rotor blade; turbulence will increase ℓ somewhat.

In his original analysis Brown showed ℓ to be primarily dependent on the temperature difference between gas and blade, a blade setting parameter and a gas property parameter for gas conditions in the stage. The cooling loss factor is found to be lower at higher gas pressures, Figure 3.13. Since high inlet temperatures require high pressure ratios to optimize efficiency the cooling loss factor will minimize in future high temperature turbines and illustrates the decreasing losses associated with increasing specific output.

Hawthorne [22] examined the effect of cooling on turbine and stage efficiencies in an analysis that closely paralleled Brown [21]. His analysis confirmed the assumption [21] that stage efficiency is relatively unaffected by cooling unless large amounts of cooling are applied to stators (one to three percent maximum). Impulse stages suffer only slight degradations in stage efficiency with applied cooling, and generally the impact of cooling on stage efficiency is much less important than the lost work due to negative reheat.

The enthalpy - entropy diagrams relevant to the cooling process are shown in Figure 3.14 for the ideal reversible cooled stage and the irreversible cooled stage.

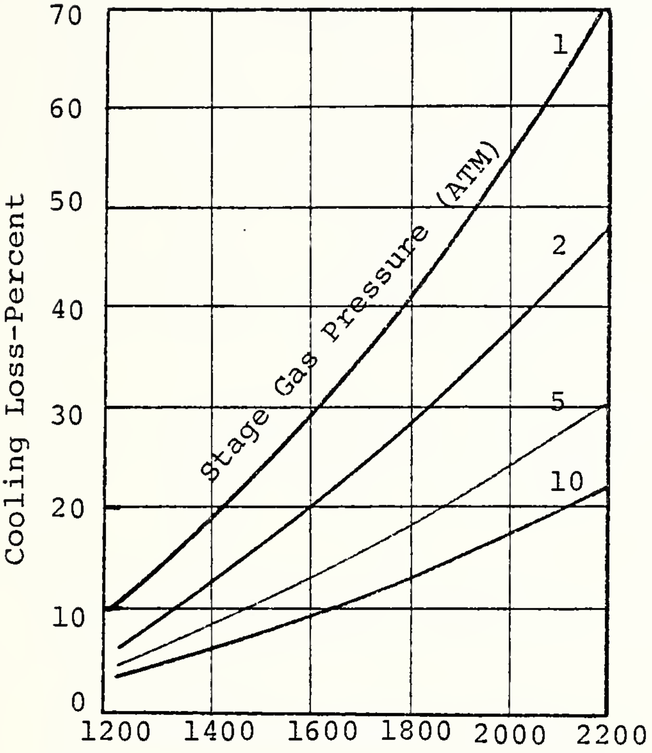

FIGURE 3.13 Estimated Cooling Loss Per Stage at Various Pressures [21]

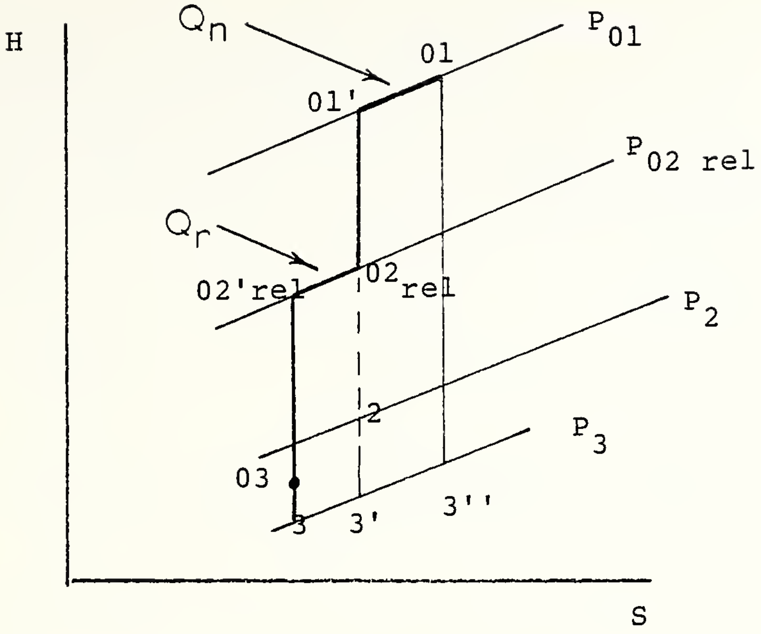
H
S
Q_n
Q_r
P_{01}
01
01'
$P_{02\ rel}$
02'rel
02_{rel}
P_2
2
P_3
03
3
3'
3''

(a) Reversible Cooled Stage

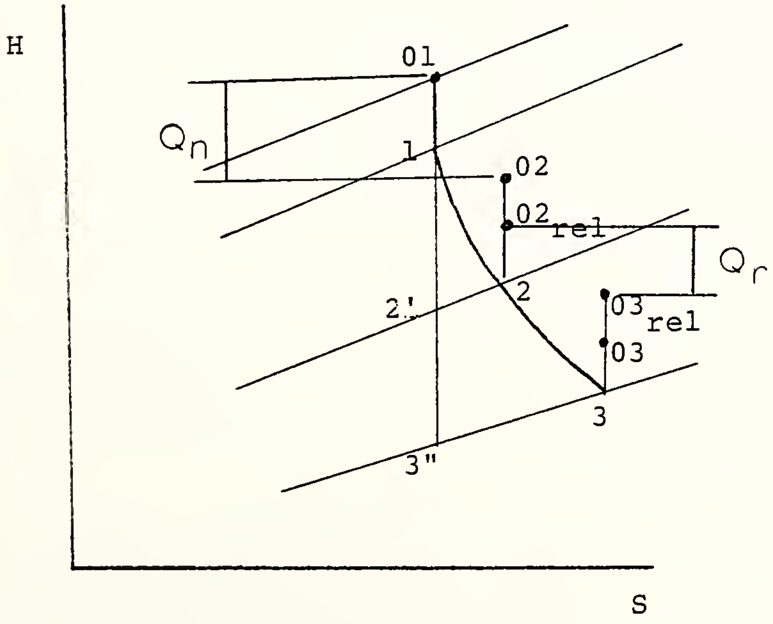
H
S
01
Q_n
1
02
02_{rel}
Q_r
2
2'
03_{rel}
03
3
3"

(b) Irreversible Cooled Stage

FIGURE 3.14 Cooling at Constant Stagnation Pressure.(22)

The heat transferred due to cooling may also be modeled as occurring at constant outlet pressure.

Heat losses can also be accounted for by using a cooling number [24]. For an expansion with friction and heat transfer,

$$p = \frac{dh}{vdp}$$

expresses the customary polytropic efficiency and

$$\xi_c = \frac{\delta q}{vdp}$$

is cooling number representing the heat removed by the coolant and is the ratio of the heat loss to coolant in the turbine to the isentropic enthalpy drop in the turbine. Recalling that the cooling loss factor ℓ represents the heat loss by the gas to the turbine work, the relation of ξ_c and ℓ is

$$\xi_c = (\ell)\ (\text{turbine isentropic efficiency})$$

An expression for ξ_c in terms of the usual stage parameters was developed in reference [24]:

$$q_c = \frac{\xi_c}{\xi_c + \eta_p} \left(\frac{\gamma}{\gamma-1}\right) R_{T1} \left[1 - \left(\frac{p_2}{p_1}\right)^{(\eta_p+\xi_c)\frac{\gamma-1}{\gamma}}\right]$$

Knowledge of the heat transfer per stage q_c obtained from experiment in terms of gas and blade temperature differences and blade setting parameters, plus the assumption of a polytropic efficiency η_p enables the determination of the cooling number ξ_c. ξ_c has been shown to depend on gas conditions and cooling system design and generally increases with increasing gas temperature and decreasing pressure ratio at a fixed blade temperature, similarly to the cooling loss factor. Typical values at gas temperature 2192F for ξ_c and 0.7 at PR = 8 to 0.4 at PR = 14, with turbine efficiency losses around 3.2 and 2.7%, respectively.

An additional heat loss parameter employed in current experiments [3] is a cooling loss number, CLN that is the ratio of the sum of all the heat extracted from the gas through the turbine to the net useful specific power output. This parameter is especially useful in that it gives directly the heat loss to the coolant and can give an indication of the potential for heat recovery in an auxiliary cycle.

4. COOLING SYSTEM EFFECTIVENESS

4.1 MEASURING EFFECTIVENESS

There are several performance parameters in use which describe the efficiency with which a given design employs its coolant. For air cooled turbines the most significant factor relating cooling system efficiency to turbine and cycle performance is the temperature difference ratio

$$TDR = \frac{T_g - T_m}{T_g - T_c}$$

where T_g is the effective gas temperature, T_m is the metallurgical limiting temperature and T_c is the coolant temperature. For internal convection cooled stators and blades this is a local measure of how well the coolant is able to control the heat transfer to the metal surface. The TDR varies between zero (for no cooling of the metal) to unity for equal wall and coolant temperatures. Local gas temperature varies with Reynolds number which will vary around the blade according to the pressure distribution established by the stream and airfoil; the coolant temperature rises from inlet to exit as it passes through the blade cooling passage. Allowable metal temperature is normally assumed uniform and established by creep-life limitations and material properties. For most

applications, however, the TDR is evaluated at average conditions. Metal temperatures should be set at the maximum permitted for the desired creep life; T_g becomes the mean effective gas temperature or mean adiabatic wall temperature and for rotor blades is measured relative to the rotating surface. T_c is normally measured at its inlet value, T_{cr}.

A related cooling performance parameter is the wall temperature ratio

$$\frac{T_m - T_{cr}}{T_g - T_{cr}}$$

which for rotor blades becomes the blade relative temperature

$$BRT = \frac{T_{BL} - T_{cr}}{T_g - T_{cr}}$$

with blade and gas temperatures measured at mean and mean relative values, respectively. BRT and TDR are related as follows:

$$1 - BRT = TDR$$

The factors influencing the blade relative temperature are examined in the following analysis.

For an internally-cooled, forced convection design utilizing air as the primary coolant, a one

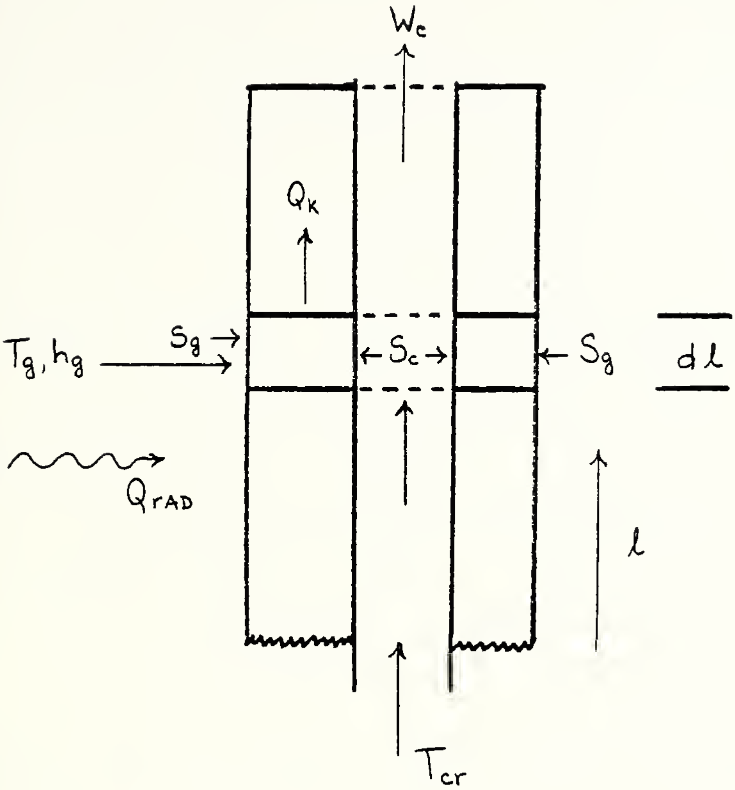
W_c
Q_k
S_g
T_g, h_g
S_c
S_g
$d\ell$
Q_{RAD}
ℓ
T_{cr}

FIGURE 4.1 Heat Balance on Air Cooled Blade [16]

dimensional heat balance on an elemental length of blade $d\ell$ at distance ℓ from the root is shown in Figure 4.1. It is known that cooled blades of this type develop a spanwise temperature gradient [16]; this is principally due to the rising temperature of the coolant in the spanwise direction which reduces its effectiveness. The effect of this temperature gradient is the conduction of heat along the blade. The low thermal conductivity of many turbine blade alloys permits the neglecting of the conduction term, and radiation effects are negligible for all but the first stage inlet guide vanes of most turbines. The heat transferred to the coolant is:

$$W_c \; c_{pc} \frac{dT_c}{d\ell} = h_c \; S_c \; (T_b - T_c) \qquad (4.1)$$

The coolant and blade temperature gradient may now be determined and an expression for the local temperature difference ratio derived:

$$T_c = T_b - \frac{h_g \; S_g}{H_c \; S_c} (T_g - T_b)$$

$$\frac{dT_c}{d\ell} = \left(1 + \frac{h_g \; S_g}{h_c \; S_c}\right) \frac{dT_b}{d\ell}$$

Since $\frac{dT_b}{d\ell} = - \frac{d(T_g - T_b)}{d\ell}$, from Equation 4.1 with $T_g - T_b = \theta$

$$\left(1 + \frac{h_g\ S_g}{h_c\ S_c}\right) \frac{d\theta}{d\ell} + \left(\frac{h_g\ S_g}{W_c cpc}\right) \theta = 0$$

The solution to this equation with boundary condition

$$T_b(o) = T_{br}$$

is

$$\theta = (T_g - T_{br})e^{-k\ell/L}$$

where

$$k = k_g\ S_g\ L/W_c\ cpc\ [1 + h_g\ S_g/h_c\ S_c]$$

Similarly,

$$T_g - T_c = T_g - T_b\ [1 + h_g\ S_g/h_c\ S_c]$$

and combining yields

$$\frac{T_g - T_b}{T_g - T_{cr}} = \frac{e^{-k\ell/L}}{[1 + h_g\ S_g/h_c\ S_c]}$$

For fixed geometry the primary variable influence the local temperature difference ratio is W_c cpc, which also influences the magnitude of h_c in proportion to coolant flow Reynolds number. The temperature difference ratio is therefore not explicit in terms of coolant flow rate or, equivalently, coolant-to-gas mass fraction W_c/W_g. In general increasing W_c/W_g is effective in improving

the temperature difference ratio but cycle efficiencies will suffer due to dilution effects after some level. The variation of the specific heat of the coolant flow with temperature also affects the temperature difference ratio, particularly where compressor bleed air at high pressures is utilized. The other factors influencing the temperature difference ratio are the gas and coolant side heat transfer coefficients. In general, the cooling effectiveness of a particular cooling design is improved by decreasing h_g and increasing h_c; this is logical since the goal of the coolant is to maintain metal temperature at a specific level and reducing the heat flux to the blade or increasing it to the coolant accomplishes this.

4.2 FACTORS AFFECTING COOLING EFFECTIVENESS BY METHOD

Different cooling methods attempt control of metal surface temperatures in varying ways; it has been seen that simple-convection designs make no attempt to limit heat flux to the blade and rely on the thermal capacity of the coolant air to convey sufficient heat from the blade or vane to keep the allowable metal temperature within creep-life limits, usually defined as one percent creep in some specificd number of hours

of operation at a given temperature. For aircraft engines this ranges from 400 to 4000 hours, while heavy duty industrial turbines require 80,000-100,000 hours continuous operation without overhaul. Thus the principal attempts at improving cooling effectiveness for this type of system consist of improving the coolant-to-gas wetted surface ratio or increasing the coolant side Nusselt number. Nu_c is principally affected by coolant velocity and temperature; the potential for heat transfer is improved by decreased coolant temperature although an accompanying decrease in thermal conductivity of the cooling gas will partially (though not significantly at lower temperatures) offset this. The geometrical limitations on cooling leading and trailing edges of blades have been previously described. Typical values of cooling effectiveness (temperature difference ratio) for simple convection cooling are about 0.5 at 6 percent coolant mass fraction [25]. This has been improved to 0.6 to 0.72 for advanced impingement-convection methods [26].

In film cooling, the gas-to-metal heat flux is minimized through the shielding action of the air blanket. The low thermal conductivity of the cooling air provides good insulation; however, some of this effectiveness is lost due to mixing and resulting

turbulence downstream that will increase gas side heat transfer coefficients for subsequent stages. A principle parameter affecting film cooling effectiveness is the injection angle [19]; when the coolant is injected normal to the mainstream through the relatively large film injection sites, the boundary layer along the surface is disrupted and the heat shield is diminished through mixing and entrainment (Figure 4.2) of free stream fluid particles with coolant air along the blade surface. The blowing rate ($\rho_c V_c / \rho_\infty V_\infty$) of the film normal to the surface becomes important and when limiting values are exceeded (defined by the gas and coolant temperatures and the location of the injection port along the surface) cooling effectiveness is decreased and heat flux to the blade increases. This effect is illustrated in Figure 4.3 where surface heat flux is plotted as a function of blowing rate for several coolant temperatures [27]. For the upper curve the film and stream temperatures are equal and the heat flux to the surface increases with coolant mass fraction primarily due to mixing in the boundary layer. When the cooling air is at wall temperature the heat flux is reduced for small coolant flows but increases (due to mixing) at larger flows.

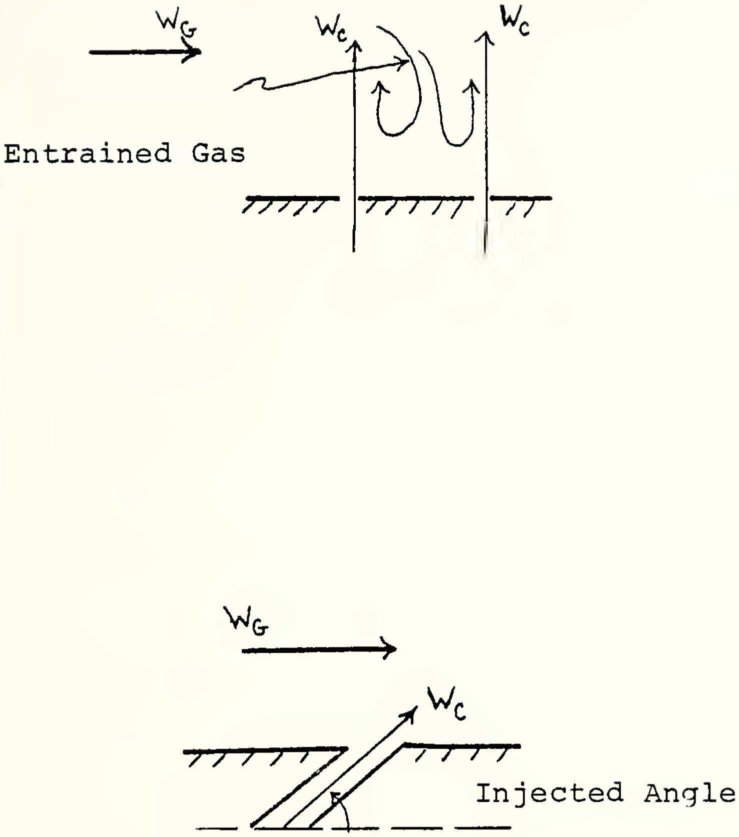
W_G
W_c
W_c
Entrained Gas
W_G
W_c
Injected Angle

FIGURE 4.2 Normal and Angled Injection of Cooling Air [19]

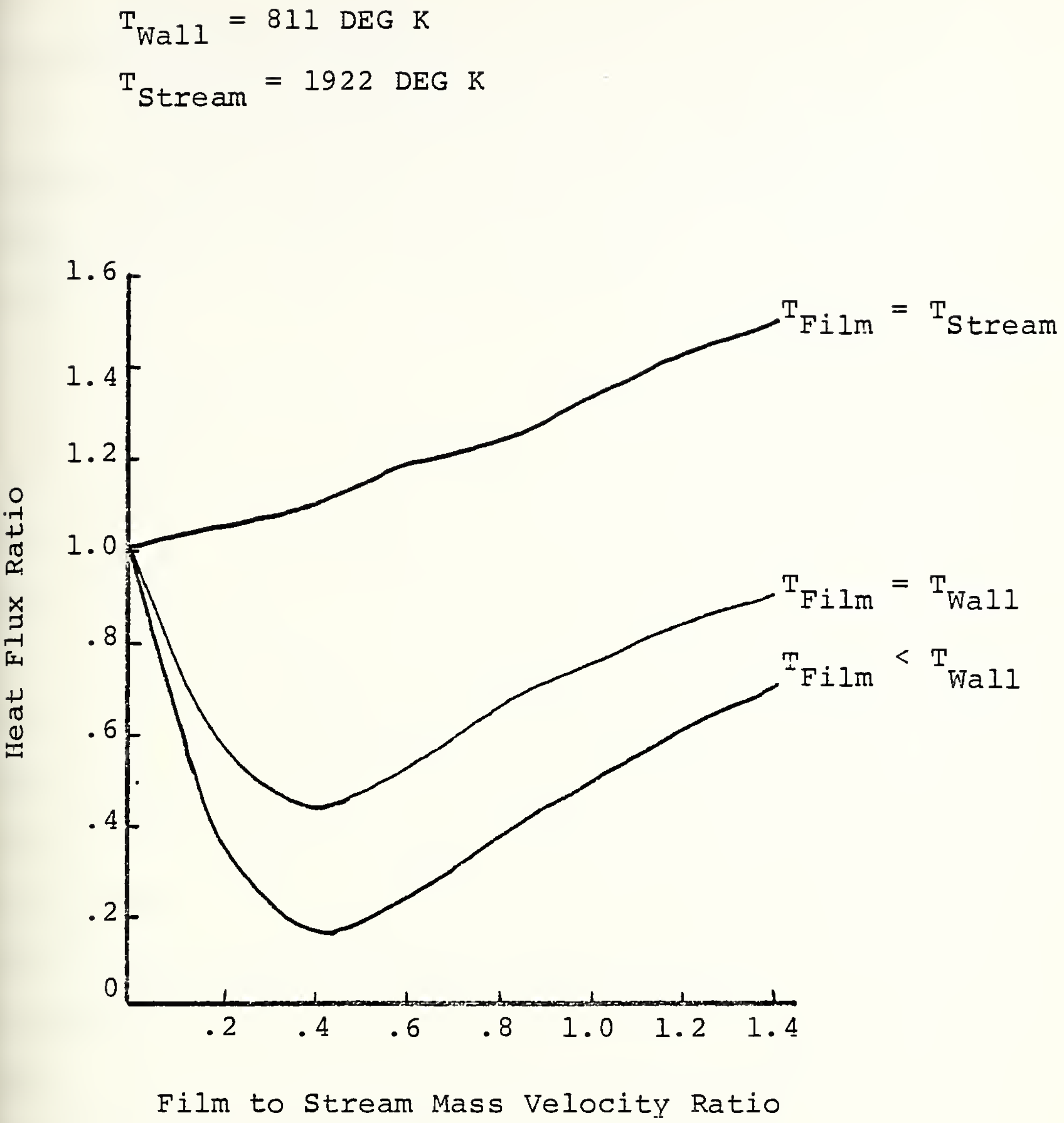

FIGURE 4.3 Effect of Film Blowing Rate on Surface Heat Flux [27]

For a cooling air temperature below wall temperature, the cooling is more effective.

A boundary layer separation criterion for normal injection has related the skin friction coefficient (without coolant flow) to the normal mass injection rate [28]:

$$\frac{\rho_c V_c}{\rho_\infty V_\infty} \leq 2\, c_{fo}$$

For realistic conditions of coolant and gas flow, this value is small, on the order of 10^{-3}.

For angled injection of coolant the blowing rate can be increased beyond the normal blowing rate for the same separation criterion proportionally to the sine of the injection angle. The angled injection permits quick reattachment of the coolant film to the surface and thereby improves the shielding effect [19]. It has been suggested [19] that increasing the blowing rate near the rear of the suction surface of a turbine blade (where an adverse pressure gradient exists) may delay separation and thus reduce drag losses. Experiments at NASA, however, have indicated that these gains are offset by the resultant increase in gas-stream turbulence, which, for even light blowing, trips the boundary layers on downstream blades from laminar to transitional or turbulent

and increases the heat transfer to these surfaces [29]. The presence of film cooling holes near the leading edge of a foil surface has been shown to trip the boundary layer into turbulence and increase the rate of heat transfer to the trailing edge region of the same surface.

One positive effect that a high blowing rate can accomplish is the diminution of radiant heat flux in first stage vanes and blades [30]. Typical values of cooling effectiveness with large-hole coolant injection in practical blades are 0.6 to 0.7 at a coolant mass fraction of about 6% [25]; the effects on turbine efficiency for full-coverage film blades are uncertain at present since film cooling has been principally employed to supplement convection impingement techniques.

Transpiration cooling effectiveness depends on the shielding action of a protective air blanket as with film cooling. The convective heat flux to the porous surface is more effectively reduced due to the improvement in uniformity of blowing sites, requiring reduced coolant velocity. These lower wall velocity gradients reduce the recovery temperature and hence the heat transfer to the surface [12]. The most significant factor in improved effectiveness for transpiration cooling is the increase in coolant temperature rise that occurs within

the porous wall itself. For coolant flow through a porous wall, a significant amount of heat is transferred to the coolant within the wall and this heat transfer rate may be expressed with an interstitial heat transfer coefficient:

$$h_i = \frac{\text{rate of heat transfer per unit volume of porous material}}{(\overline{T}_c - \overline{T}_m)}$$

where $\overline{T}_c$ and $\overline{T}_m$ are average coolant and metal temperatures, respectively. In terms of a conventional heat transfer coefficient h,

$$h_i = h\left(\frac{S}{V}\right) = \frac{Q}{A\Delta T}\left(\frac{S}{V}\right)$$

where S is the internal surface area and V the material volume [6]. For porous materials including drilled sheets and mesh, S/V is high, yielding high effective heat transfer from the surface to the coolant. Since this occurs at every injection site along the surface, the coolant attains the surface temperature at exit. This complete utilization reduces required coolant flows for a fixed desired blade temperature and correspondingly reduces mixing losses and negative reheat. Turbine efficiencies should therefore improve significantly over convective and film cooling methods. Transpiration cooling effectiveness theoretically then attains a value

of unity rapidly with low blowing rates. Maximum values in industrial and research use have typically been about 0.85 [25].

4.3 DEVELOPMENT OF EFFECTIVENESS CORRELATIONS

In order to compare the cooling system effectiveness among advanced air cooling methods, expressions relating temperature difference ratio to coolant mass fraction are relevant. As seen above (Section 4.1) cooling effectiveness is essentially a local phenomenon and is a complex function of coolant and gas side heat transfer coefficients and area ratios plus the thermal capacity of the coolant ($\dot{W}_c$ cpc). There have been numerous experiments that have attempted to measure this effectiveness for varying cooling methods. Yeh [31] developed a general correlation for local effectiveness

$$\frac{T_g - T_m}{T_g - T_c} = \left[1 + \alpha\left(\frac{W_c}{W_g}\right)^{\beta}\right]^{-1}$$

where α and β varied according to location with a general range of $0.1 < \alpha < 0.2$ and $-0.5 < \beta < -0.75$. On the basis of a one-dimensional heat transfer analysis similar to that above, Gladden [29] suggested

$$\frac{T_g - T_m}{T_g - T_c} = \left[1 + \frac{h_g\ S_g}{h_c\ S_c}\left(\frac{W_c}{W_g}\right)\right]^{-1}$$

for average temperatures and heat transfer coefficients for convection and film methods. These forms suggest that cooling effectiveness correlations may take, in the absence of knowledge of detailed heat transfer characteristics, this form

$$\frac{T_g - T_m}{T_g - T_c} = A \left(\frac{W_c}{W_g}\right)^b$$

and technical data is often published in this form. This form is especially conducive to computer application in determining coolant flow requirements for prescribed temperature levels and ultimately the impact of various cooling methods on turbine efficiency and cycle performance.

For this study, coolant mass fraction and temperature difference ratio data were collected from several sources [12 ,26 ,32] and correlated for advanced impingement-convection (2 curves), full-coverage film and transpiration methods.

The correlations developed from the data are as follows, where ψ represents the temperature difference ratio:

$$\left(\frac{W_c}{W_g}\right)_{\text{composite 1}} = 0.1768 \ (\psi)^{2.0833}$$

$$\left(\frac{W_c}{W_g}\right)_{\text{composite 2}} = 0.1977\ (\psi)^{2.1375}$$

$$\left(\frac{W_c}{W_g}\right)_{\text{film}} = 0.0905\ (\psi)^{1.3698}$$

$$\left(\frac{W_c}{W_g}\right)_{\text{transpiration}} = 0.0826\ (\psi)^{2.1277}$$

These results plus a curve of theoretical film cooling effectiveness developed in reference [33] are shown in Figure 4.4; the plotted relations indicate that transpiration cooling is the most effective cooling method at all coolant flow rates. At 6 percent coolant mass fraction (a typical value for present designs and temperatures) transpiration effectiveness exceeds that of composite 1 by 44 percent and film by 17 percent $(\frac{\eta - \eta_{ref}}{\eta_{ref}})$. The differences between composite curves one and two are small except for vary high coolant flow rates.

4.4 COMMENTS ON CORRELATIONS

The derived correlations indicate the anticipated results that transpiration cooling followed by film cooling

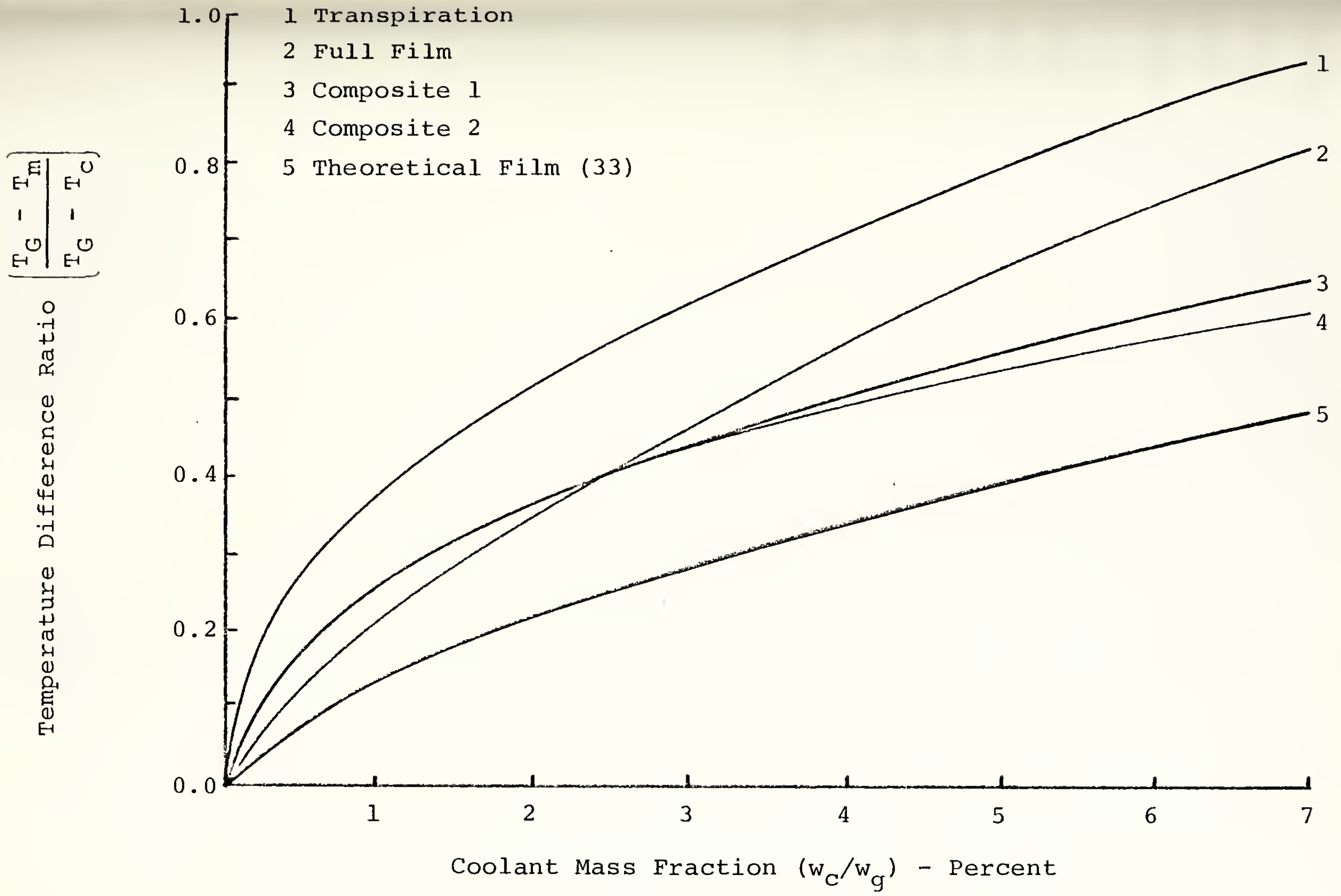

FIGURE 4.4 Air Cooling Effectiveness Versus Coolant Mass Fraction for Various Methods

is superior in terms of effectiveness for a given flow rate of coolant to composite (convection-impingement plus hot spot film cooling) methods. The full-coverage film expression is developed from relatively few data points (12) averaged from spot-cooling data between leading and trailing edges [32]; it reflects the better local effectiveness of films at the trailing edge especially. The data from [32] generally indicate that composite cooling is at least as effective as full-coverage film cooling for most coolant flow rates; this may be so because full film coverage may under-utilize the film air prior to ejection in a convective or impingement role. It is very difficult to isolate a full-coverage film case as in most turbines the film air is always employed in some other mode before ejection. The significant conclusions to be drawn from Figure 4.4 are:

(1) Transpiration is clearly the most effective air cooling method in terms of conservation of cooling air;

(2) Full-film data, although limited, indicates much better results than those analytically predicted some years ago;

(3) Composite cooling as presently developed achieves significantly high effectiveness through optimizing the local effectiveness

of individual air cooling methods, re-emphasizing the fact that cooling effectiveness is a highly local phenomenon;

(4) There are errors of approximation inherent in attempting to employ average temperatures in a simplified correlation; as shown above, effectiveness is a complex function of the coolant-to-gas mass fraction.

The impact of each method of cooling on turbine and cycle efficiencies is not directly proportional to effectiveness due to the complex mixing and gas temperature effects occurring at injection. To assess the ultimate affects of employing advanced air cooling methods on cycle performance and efficiency, a computer program was employed utilizing the above correlations. A description of the program and results obtained by varying key parameters follows in the next chapter.

5. COMPARISON OF AIR COOLING METHODS

5.1 COMPUTER MODEL UTILIZATION

A digital computer model was utilized to compare the effects of cooling system modification on various cycle parameters. The existing model permits the detailed simulation of a combined Brayton-Rankine cycle (COGAS) plant with the options of feedheating and reheating on the Rankine cycle. This model was modified to permit the substitution of alternative gas turbine models within the basic program and to permit the simulation of the gas turbine only. Thus, the variations of cooling system type on the key performance parameters of the gas turbine could be compared on the bases of simple and combined cycle utilization.

5.1.1 Description and Features of the Model

The combined cycle model (library name "RANKINE") avoids detailed modelling of the working fluid flow and thereby avoids the compounding effects of assumptions about boundary layer flow. However, the working fluid properties (enthalpy, entropy, specific heat) are modelled in detail utilizing polynomial representations that incorporate the effects of current gas composition. Steam properties are evaluated analytically from relations in [34].

The gas turbine is modelled in three separate subroutines - compressor, combustor and turbine; the major variables are compressor pressure ratio and turbine inlet temperature. The compressor and turbine performances are modelled as polytropic processes with assumed polytropic efficiencies. Pressure losses at inlet and exhaust can be specified. The compressor subroutine computes values of temperature and enthalpy at the compressor exit and at the intermediate bleed pressures required for turbine cooling. The combustor determines the fuel rate of known heating value required for a specified gas temperature at the turbine inlet. The cooled gas turbine subroutine (GTUR) expands the gas polytropically through stages of equal enthalpy drop, providing cooling air to the stators and rotors as a function of cooling effectiveness for a limiting metal temperature. Gas properties are adjusted at each stage to allow for the mixing of gas with coolant. GTUR determines the net work and efficiency of the entire gas turbine model and establishes the exhaust gas conditions at entry to the waste heat recovery unit (WHRU) when applicable. For combined cycle employment, a pressure loss in the exhaust duct accounts for both duct loss and that due to the WHRU. Principal variables in the steam plant include the WHRU pressure and the

options of feedheating (single stage) and reheat. The feedheating deaerator raises the feedwater temperature to 422 K (300 F); this level is sufficient to protect against the formation of corrosive products in the exhaust gas while allowing effective heat transfer from the exhaust gas in the WHRU. Condenser temperature is variable, as is the "pinch point" and the difference between the maximum gas temperature and maximum steam temperature.

5.1.2 Modifications to RANKINE

A simple modification to RANKINE was required to permit simulation of the Brayton cycle only; this was accomplished through a change in the initializing subroutine. Options now available with RANKINE include: (1) open cycle gas turbine, with various alternate gas turbine models (with cooling alternations); and (2) combined cycle simulation with any gas turbine model, Rankine cycle options as before. For this study, the basic gas turbine model GTUR was modified by the substitution of cooling effectiveness curves as previously described to model alternative air cooling methods (full-coverage film and transpiration). This procedure was adequate for comparing the impact on cycle efficiency, specific fuel

consumption and specific power of similar cooling systems (i.e. utilizing air) but was not compatible when the basic cooling method changed. Therefore a first generation, liquid-cooled gas turbine model was developed with the general structure of GTUR in order to enable interfacing with RANKINE. This model is described in Chapter 6.

5.2 COMPARISON OF AIR COOLING METHODS

5.2.1 Open Cycle Results

Open cycle conditions were established as in Table 5.1

TABLE 5.1 Simple Cycle Parameters

Compressor inlet pressure (N/m^2)/psi	101325/14.7
Compressor inlet temperature ($^{\circ}$K)	300
Inlet pressure loss (inches water)	2
Compressor flow loss (% inlet flow at PR=20)	1.25
Compressor polytropic efficiency	0.88
Combustor pressure loss (% inlet)	5.0
Heating value (kcal/kg/Btu/lbm)	10000/18000
Combustor efficiency	0.99
Turbine polytropic efficiency	0.90
Exhaust duct pressure loss (inches water)	5.0

and the primary cycle parameters (pressure ratio and turbine inlet temperature) were varied to determine the effects of cooling and/or cooling conditions on cycle performance.

The cooling effectiveness correlations plotted in Figure 4.4 indicate a potential conservation in cooling air flow requirements among composite, film and transpriation cooled turbines. Figure 5.1 illustrates the reduction in cooling air observed as a function of turbine inlet gas temperature. The reduction due to the film cooling is markedly less significant than from transpiration cooling, and at small to moderate temperature rises, film cooling is not as effective as composite methods. A temperature limit for each type of cooling is discernable.

The reduced cooling air flow experienced at higher temperatures with the advanced cooling methods improves the cycle efficiency by reducing the mixing losses that reduce the gas stream temperature at each stage and by minimizing the reductions in turbine hot gas flow resulting from compressor bleed-off. The gains in efficiency and specific fuel consumption for compressor pressure ratio 16 are shown in Figure 5.2. The optimum inlet temperature at this pressure ratio is increased to 1660 K from 1480 K with transpiration cooling, with a percentage increase in efficiency of 4.1% over composite cooling. Film cooling results were less significant as noted in Table 5.2. The reductions in specific fuel consumption are comparable.

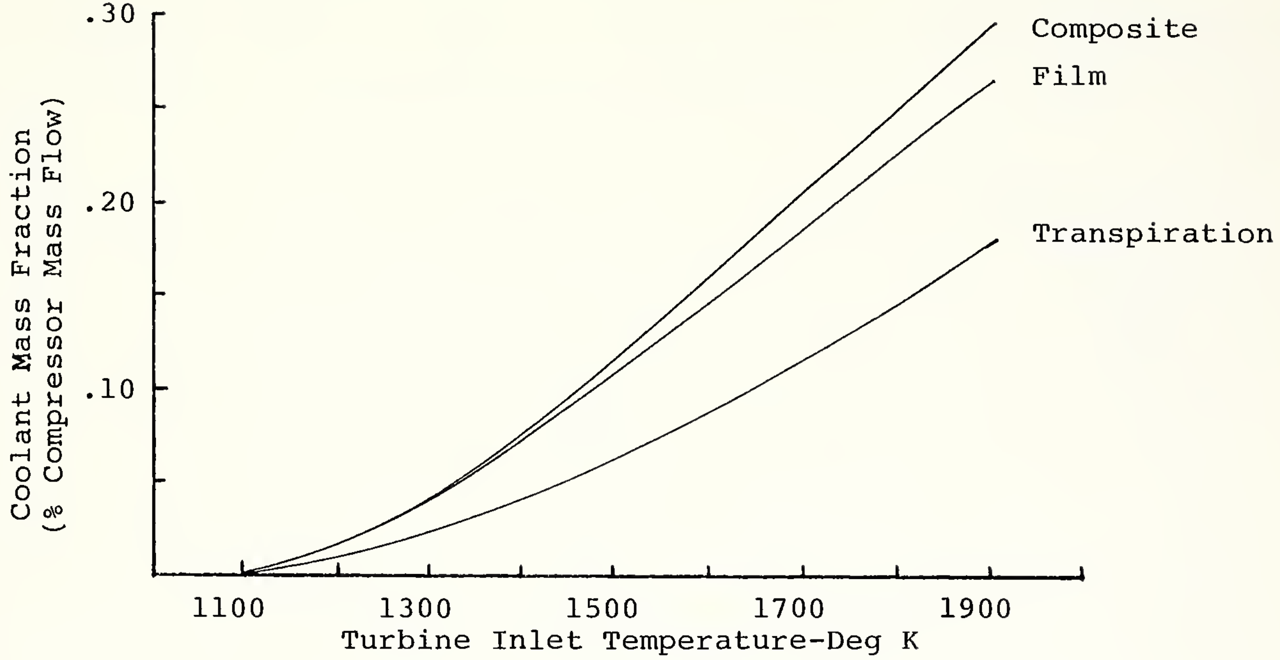

FIGURE 5.1 Cooling Air Requirements For Various Cooling Methods

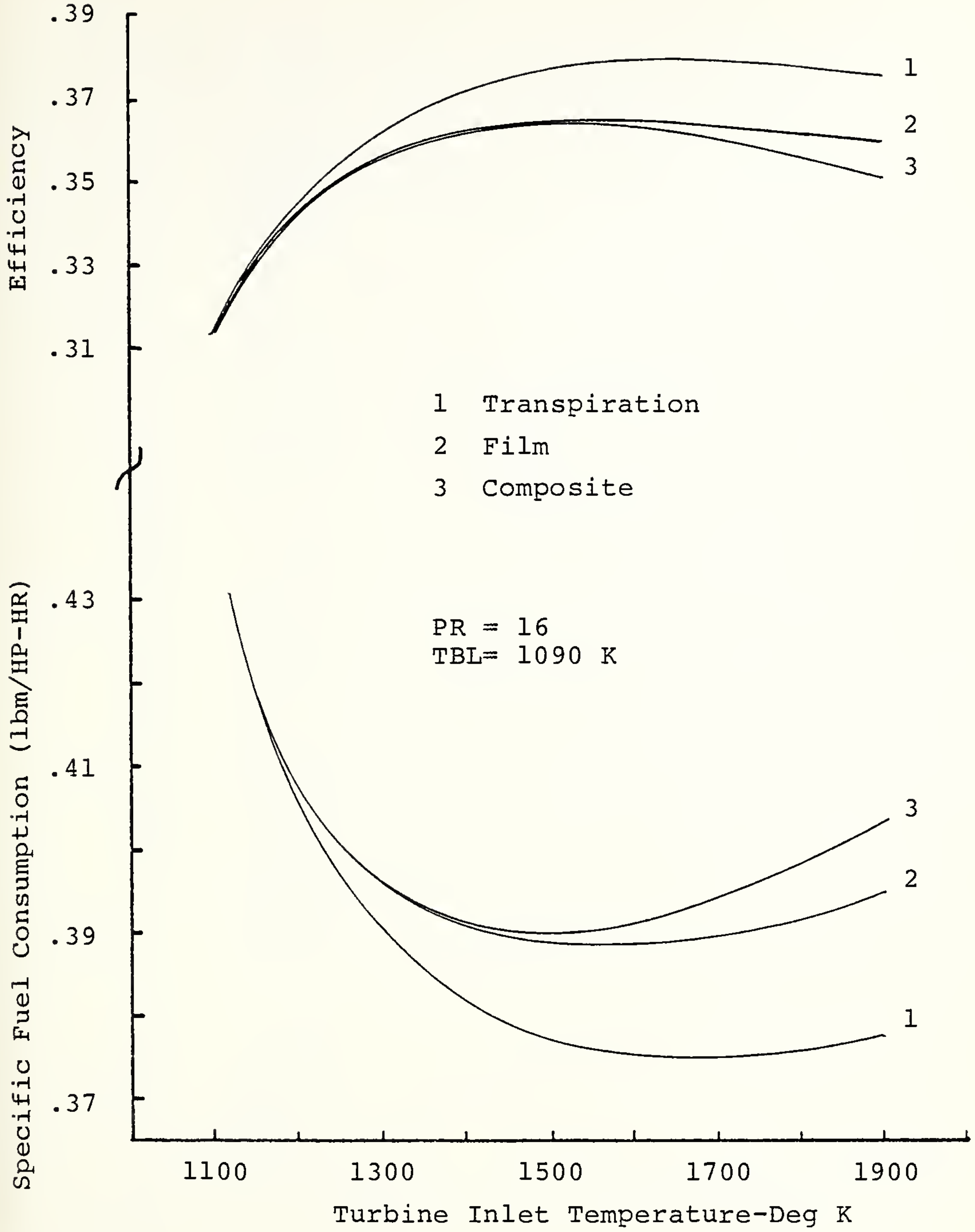

FIGURE 5.2 Comparison of the Effects of Cooling Method on Efficiency and Specific Fuel Consumption (Simple Cycle).

TABLE 5.2 Comparison of Performance with Cooling Method (Open Cycle); PR = 16, Metal Temperature 1090 DEG K.

Cooling Method	Maximum Cycle Efficiency	Turbine Inlet Temperature (^{o}K)	SFC (lbm/HP-HR)	Specific Power (HP/lbm-sec)	Exhaust Temperature (^{o}K)
Composite	.363	1480	.388	186	790
Film	.364	1550	.387	204	825
Transpiration	.378	1660	.374	304	900

A major gain in specific power was observed with transpiration cooling, increasing 34.4% over composite cooling (Figure 5.3). This results primarily from increased turbine high temperature gas flow, and a related effect is the rise in turbine exhaust gas temperature with advanced cooling methods. At optimum inlet temperature, the exhaust gas from the transpiration cooled turbine is over 100K (13.9%) hotter than with current cooling methods. The loss in potential energy that this represents for open-cycle arrangements enhances the attractiveness of a transpiration cooled turbine in a combined plant.

The attainment of high efficiencies through increased turbine inlet temperatures requires progressively higher pressure ratios as illustrated in Figure . A transpiration cooled turbine achieves peak efficiency at a specified maximum cycle temperature at a lower pressure ratio than with other methods. The higher cost of porous surfaces in the transpiration turbine (currently about twice as expensive as convection-impingement air-cooled blading) may thus be offset partially or completely by the savings in compressor development costs, especially since variable components will be required to achieve pressure ratios greater than 30.

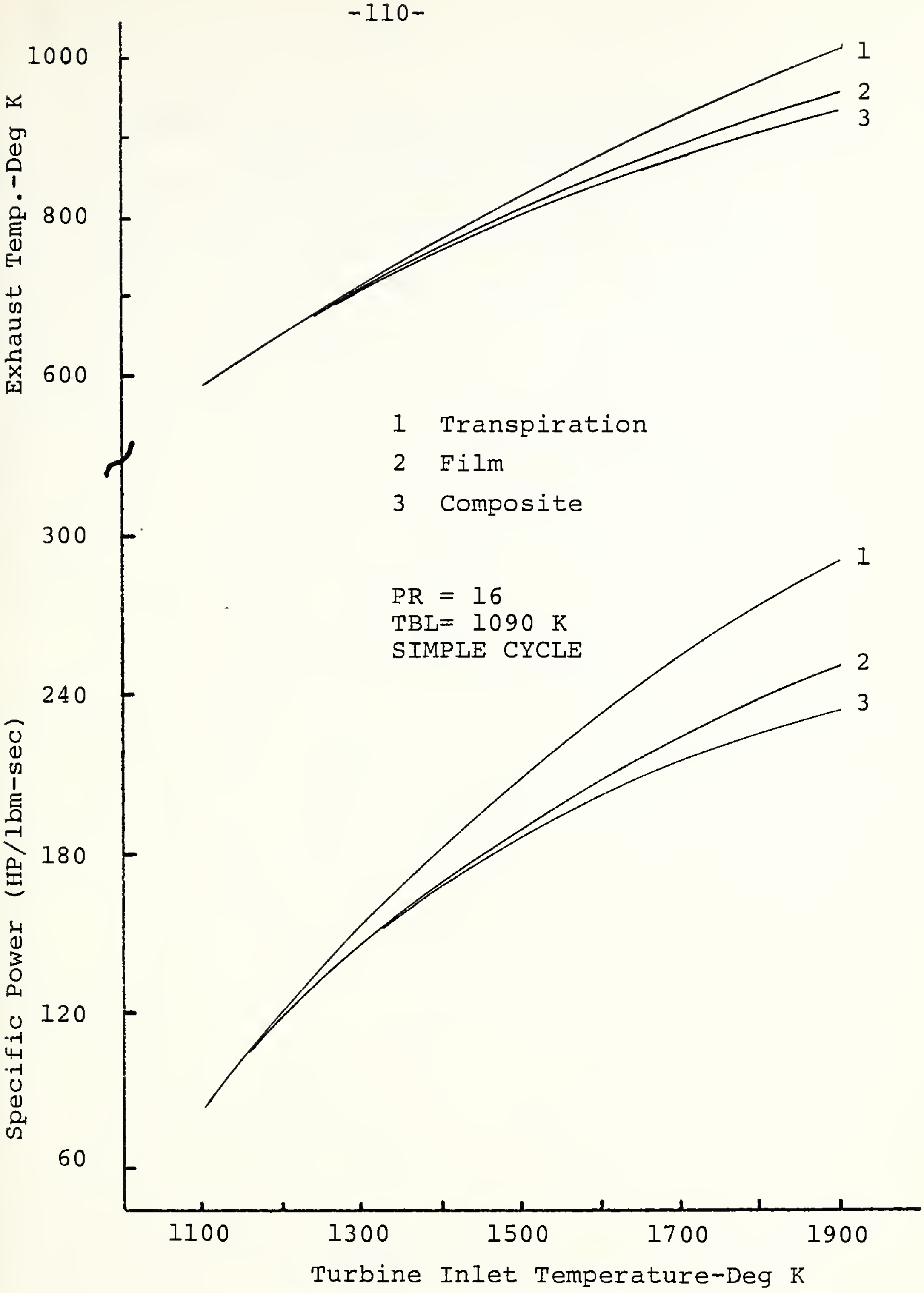

FIGURE 5.3 Variation of Exhaust Temperature and Specific Power with Cooling Method.

As developing compressor technology permits the economical use of higher pressure ratios, transpiration cooled turbines will enable the attainment of greater efficiencies and specific powers through the use of higher inlet temperatures. Figure 5.4 compares current cooling with transpiration results at PR 32. Transpiration cooling at this pressure ratio permits an optimum temperature of 2100K with corresponding efficiency of 41.8 percent, an increase over standard cooling methods of 4 points or over 10.6 percent.

The small magnitude of performance gains achieved with transpiration cooling at currently available pressure ratios suggests that alternative means of attaining higher temperatures may be worthwhile. Comparisons for two separate cases have been made; in case (1), reduction in cooling air temperature to all turbine stages is affected by a heat exchanger. Case (2) postulates an increase in allowable metal temperature to 1255K based on barrier coating development supported by projected metallurgical gains (Figure 1.1). Table 5.3 compares the effects of precooling and metallurgical progress for transpiration and composite cooling methods. For each method, average coolant temperature is reduced

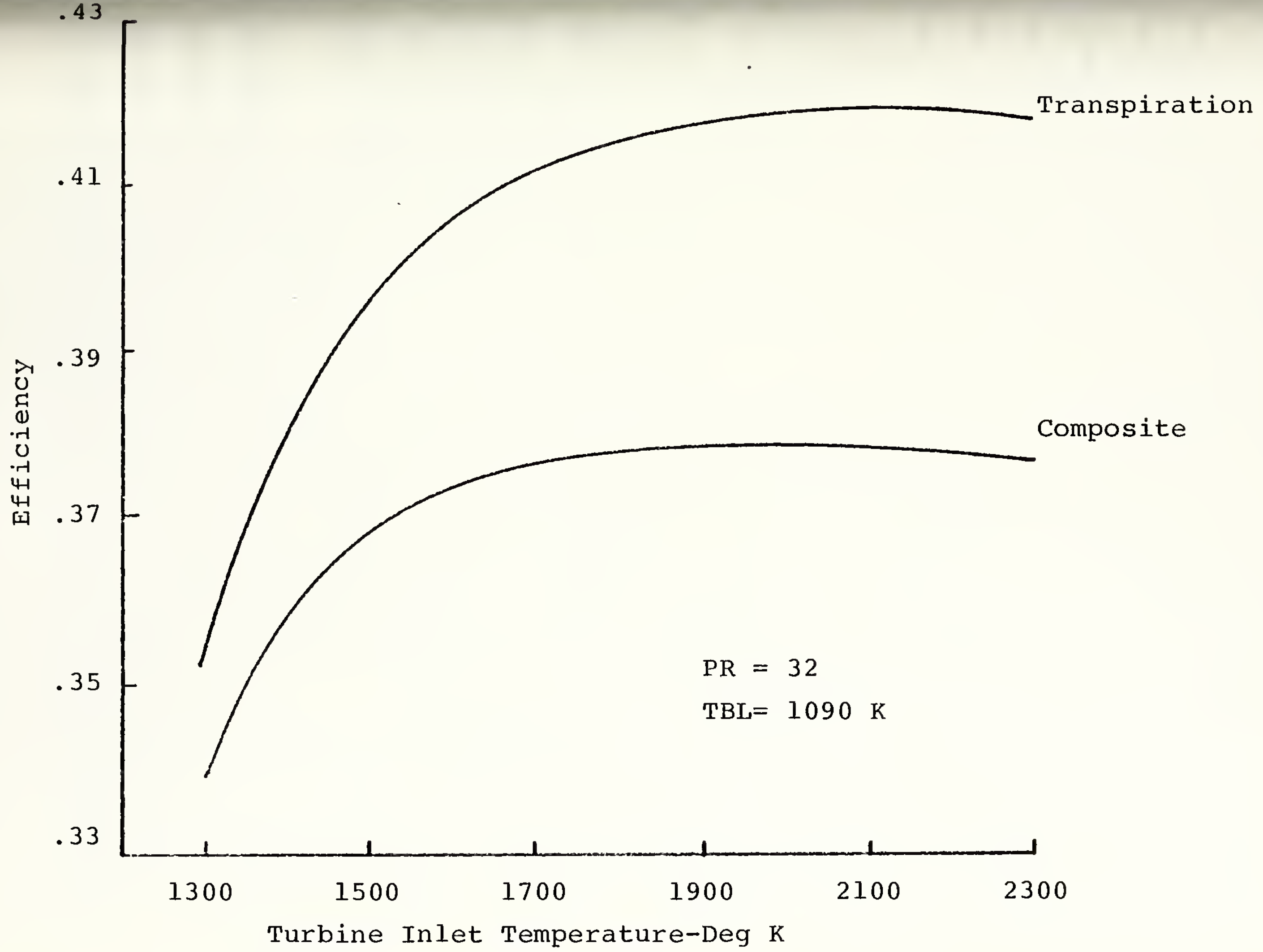

FIGURE 5.4 Transpiration versus Composite Cooling Efficiency (Simple Cycle).

approximately 280 DEG (K) for comparison with increased metal limiting temperature of 165 DEG K.

As evidenced by the tabulated results, greater reductions in coolant mass flow can be achieved through materials progress than with precooling (about 75 percent compared to 52 percent) for each type of cooling. The corresponding percentage gains in cycle efficiency with the transpiration method, however, are approximately half of those for composite cooling; these diminishing returns to efficiency and fuel consumption would require that a marginal analysis be performed to balance the total costs of materials improvement and precooling hardware with cycle benefits for transpiration cooling. The improvements in fuel consumption and efficiency that derive from precooling a state-of-the art blade are approximately one third those experienced from incorporating transpiration cooling methods (1.1 percent to 3.5 percent). Specific power increases are comparable, however (approximately 9 percent).

Precooling requires additional heat exchanger equipment and considerable modification to the compressor hardware, and any potential savings in machinery weight and volume derived from a reduced air rate for a fixed power level must be balanced against these costs.

TABLE 5.3 Comparison of Effects of Precooling and Increasing Allowable Metal Temperatures with Cooling Method (Open Cycle, PR=16, Turbine Inlet Temperature = 1500 K)

Blade Temperature (^{O}K)	Average Coolant Temperature (^{O}K)	Cooling Method	Coolant-Gas Mass Fraction (%)	Cycle Efficiency	SFC (lbm/HP-HR)	Specific Power (HP/lbm-sec)	Exhaust Temperature (^{O}K)
1090	607	Composite	.117	.363	.389	190	800
1255	650	Composite	.031	.381	.371	220	831
1090	324	composite	.057	.367	.385	206	811
1090	613	transpiration	.064	.376	.376	210	821
1255	652	transpiration	.014	.384	.368	225	837
1090	324	transpiration	.029	.378	.374	218	827

5.2.2 Combined Cycle Results

The higher exhaust temperatures experienced with transpiration cooling offer greater potential for waste heat recovery in a combined cycle. There are many configurations of recovery units, including multi-pressure, waste heat recovery units (WHRU) and supplementary fired exhaust gas boilers. This study employs the unfired WHRU in a Rankine cycle with options of single-stage feedheating and steam turbine reheat. The thermodynamic interconnection between the gas turbine and steam cycles improves the combined cycle efficiency and specific fuel consumption by taking advantage of the facility of gas turbines to add heat at high temperatures and the facility of condensing steam plants to reject heat at low temperatures; the primary disadvantage of gas turbine plants - the inability to reject heat at low temperatures - is minimized by transferring exhaust gas heat to steam. Combined cycle parameters were established as in Table 5.4 and the variation of cycle performance with cooling methods was investigated. The presence of the steam cycle adds additional restrictions to performance variables - the moisture content of the steam in the last stage of expansion must not exceed about 12 percent and the pressure

TABLE 5.4 Combined Cycle Parameters

Compressor inlet pressure (N/m^2)	101325
Compressor inlet temperature (^oK)	300
Inlet flow loss (inches water)	2
Compressor flow loss (% inlet flow at PR=20)	1.25
Compressor polytropic efficiency	0.88
Combustor pressure loss (%)	5
Heating value (Kcal/kg/Btu/lbm)	10000/18000
Combustor Efficiency	.99
Gas turbine polytropic efficiency	0.90
Exhaust duct pressure loss (inches water)	5
Pressure loss due WHRU (inches water)	15
Condenser temperature (^oK)	299.8
Condenser pressure (vacuum, inches Hg)	27.5
Pinch point temperature difference (^oK)	19.4
Maximum gas-steam temperature difference (^oK)	16.6
Pump efficiencies	0.88
Steam turbine efficiency (dry region)	0.89
Feedheating temperature (^oK)	427

of the WHRU has significant impact on the size and weight of the unit and the moisture content of the expansion. The WHRU exhaust temperature must remain above about 422 DEG K to prevent exhaust duct corrosion.

The combined cycle results for pressure ratio 16 with composite and transpiration cooling methods are shown in Table 5.5 and Figure 5.5. Combined cycle efficiencies exceeding 50 percent are achievable through transpiration cooling and comparison with the open cycle results of Table 5.2 indicates that for a fixed pressure ratio the maximum cycle temperatures required are significantly less (for this case, approximately 100 DEG K). With the combined cycle, transpiration cooling allows an increase in maximum temperature of 140 DEG K, and this is reflected in improved efficiency and specific power.

Figure 5.6 relates the gas turbine exhaust temperature to the proportion of work contributed by the Rankine cycle. As expected the steam cycle work increases with increasing exhaust gas temperature, but an unexpected result is the less proportionate increase with transpiration cooling at higher temperatures. The implication is that as maximum cycle temperatures exceed the optimum, the decline in performance of the transpiration-cooled gas

TABLE 5.5 Comparison of Performance with Cooling Method (Combined Cycle); WHRU Pressure 400 PSIA; PR 16, Single Stage Feedheating

Cooling Method	Maximum Cycle Efficiency	Optimum Turbine Inlet Temperature (°K)	Optimum SFC (lbm/HP-HR)	Specific Power (HP/lbm-sec)	Exhaust Temperature Gas Turbine/WHRU (°K)
Composite	.465	1380	.310	223	750/485
Composite (Precooled to 324 K)	.491	1440	.294	260	788/481
Transpiration	.505	1540	.286	309	849/473
Transpiration (Precooled to 324 K)	.524	1590	.275	344	882/469

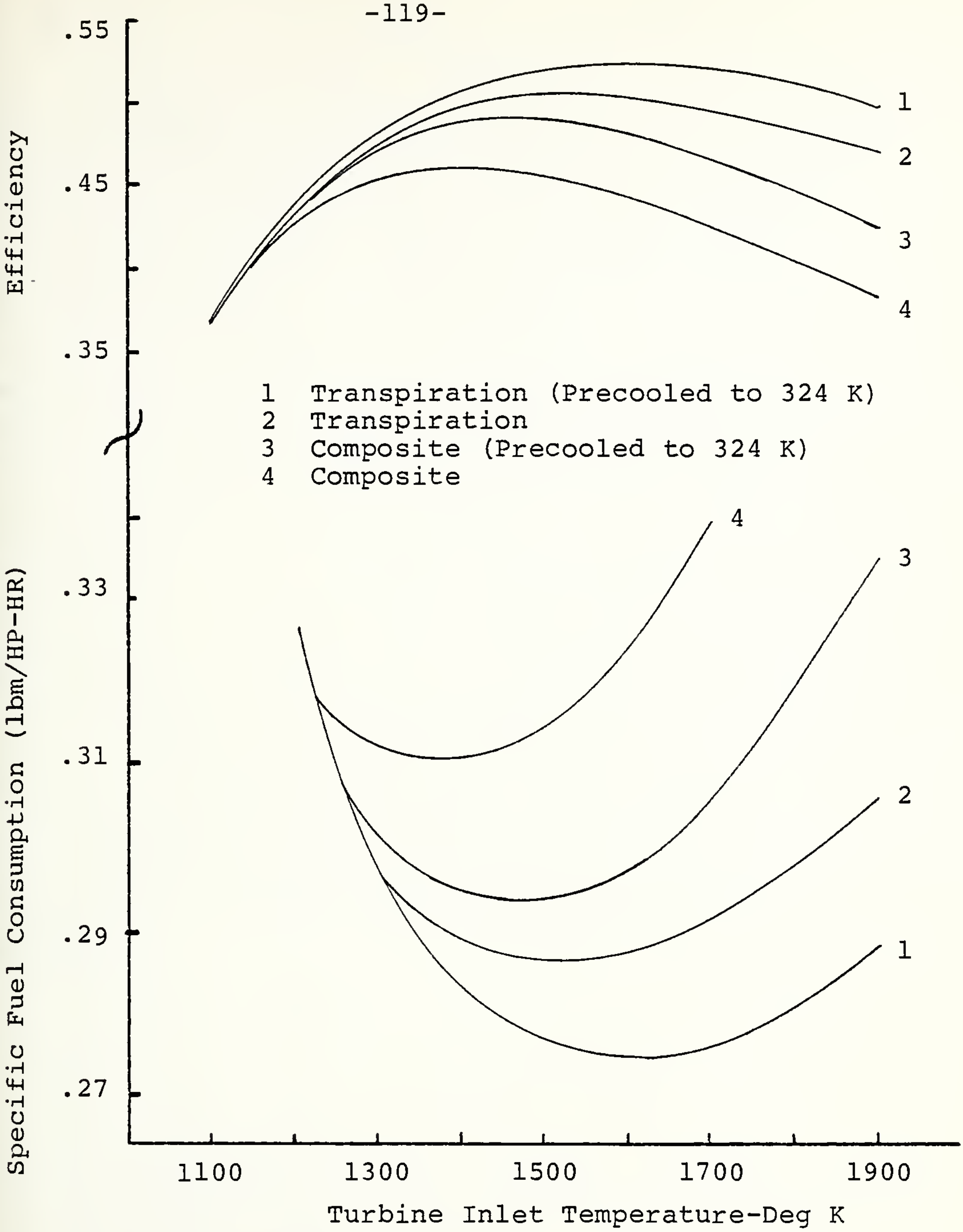

FIGURE 5.5 Combined Cycle Performance Variations with Cooling Method. (PR= 16, TBL= 1090 K, WHRU Pressure= 400 psia)

turbine proceeds at a greater rate (for a fixed boiler pressure). The effect of increasing boiler pressure with the transpiration-cooled combined cycle arrangement is also shown in Figure 5.6 (dashed line) and summarized in Table 5.6. The transpiration cooled gas turbine has greater compatability at higher boiler pressures with acceptable moisture as maximum cycle temperatures increase; higher boiler pressures allow reductions in steam component size (although cost increases) and the implication is that where size is critical (shipboard applications) the transpiration/combined cycle system is more suitable if minor cycle efficiency losses are permitted. The moisture content can be reduced to negligible proportions with the use of reheat in the steam turbine, at considerable cost in machinery complexity.

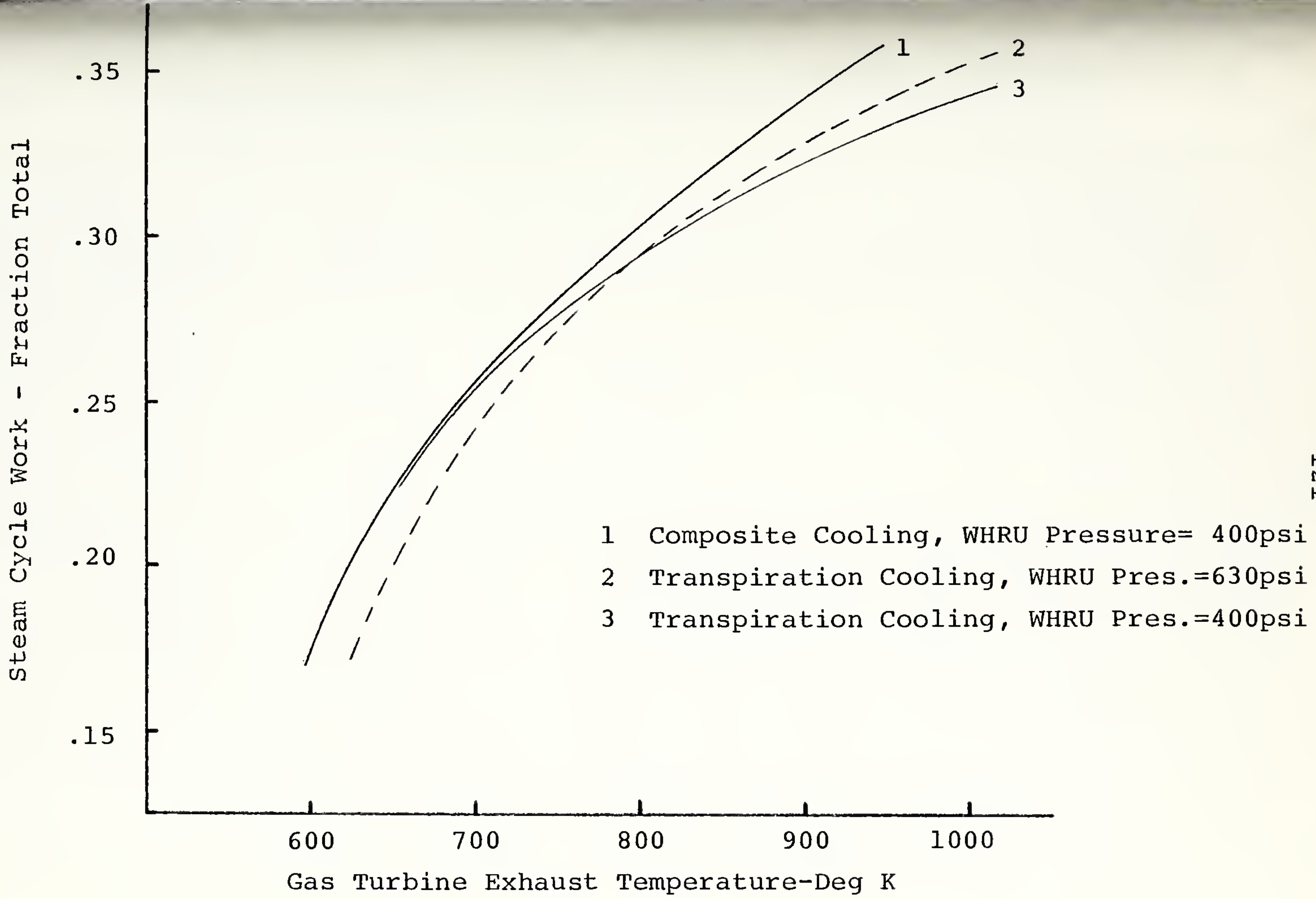

FIGURE 5.6 Steam Cycle Work versus Gas Turbine Exhaust Temperature.

TABLE 5.6 Effect of Boiler Pressure on Transpiration-Cooled Gas Turbine Performance (Combined Cycle); PR=16; T metal = 1090 (K); Single Stage Feedheating

WHRU Steam Pressure (psi)	Maximum Cycle Efficiency	Turbine Inlet Temperature (DEG K)	Gas Turbine/WHRU Exhaust Temperatures (DEG K)	Moisture (Percent)	Gas Turbine Work (Percent Total)
400	.505	1540	849/473	10.3	69.0
	.493	1700	928/463	8.5	67.2
	.469	1900	1016/449	8.5	65.5
630	.505	1550	853/482	12.7	68.7
	.499	1700	928/470	10.9	66.4
	.476	1900	1016/451	10.9	64.5

6. WATER-COOLED GAS TURBINE

6.1 BACKGROUND

As outlined in Table 2.2 much research effort been expended in the effort to produce a workable design of a non-air cooled gas turbine. Many of the motivating performance goals attendant with air cooling methods apply to liquid cooling also, such as increased specific output, reduced fuel consumption and increased efficiency. There are additional benefits deriving from water cooling however, chiefly involving the mechanical design of the blades and vanes. The greatly increased thermal capacity of water over air reduces sharply the differential expansion and thermal gradients within the blades, provides greater uniformity of chordwise temperature distribution over the metal surface (reducing "hot spots") and increase the blade operating life. Water is cheap, plentiful, possesses good heat transfer characteristics and is safe. A solid blade surface may be used, reducing the changes of overheating due to film-port blocking from debris and particulates and permitting the gas turbine to burn lower quality fuels. The principal drawbacks in water-cooling techology have also been mechanically oriented, with the higher pressure closed circuit systems requiring thick blade walls constraining the manufacturing

of the aerofoil shape, plus excessive feed rates and water treatment requirements. The effective transporting and collecting of the rotor coolant is a major design problem of proposed water-cooled industrial turbines, compounded by the generally insufficient knowledge of heat transfer systems over a wide range of operating conditions to permit a comparative assessment of performance [15].

Alternative methods to air cooling offer the possibility of reducing mixing losses and increasing effective turbine work through the reheat effect. Control of metal temperatures is important to limit the heat rejected from the gas steam to that required to provide adequate cooling to maintain the blade limiting temperature. Evaluation of the thermodynamic capabilities and limitations of a water-cooled turbine may be accomplished in the absence of detailed design information with a computer model. The first step in developing a liquid-cooled turbine model is the determination of the effects heat rejection from the gas stream to the stator/rotor surface.

6.2 METHOD OF MODEL DEVELOPMENT

An air cooled turbine model shall be modified to reflect the heat rejection processes at each stage plus

the effects on performance and efficiency resulting from no bleed-air requirements or coolant-mainstream mixing. The current model assumes a constant stage work of 31.0 kcal/kg (55 BTU/lbm) manifested as a change in stagnation temperature of the gas across the stage. The gas attains an assumed kinetic energy across the stator before entering the rotor, which gives the relative stagnation temperature into the rotor.

For this modification to the model these assumptions (constant stage work and assumed kinetic energy) are maintained. Expressions for heat transfer to the stator and rotor of each stage are developed from one dimensional heat balances of a single vane/blade considering continuity through a pair of vanes/blades. The governing consideration of the analysis is that only cooling produces a change in stagnation enthalpy across the stator and a change in relative stagnation enthalpy across the rotor. Heat is assumed transferred at constant stagnation pressure based on stator/rotor exit conditions.

In the notation of Appendix I, the mass flow of gas per unit blade height is

$$\dot{m}_g = \rho_2 W_2 \cos \beta_2 \cdot s \tag{6.1}$$

and continuity requires this constant through a pair of blades. The change in relative stagnation enthalpy h_R across the blade is due to cooling and is

$$\dot{m}_g \, (h_{01R} - h_{02R}) = h_{gR} \, \ell \, (T_{REL} - T_{BL}) \qquad (6.2)$$

where h_{gR} = average gas side heat transfer coefficient to rotor

T_{REL} = blade relative stagnation temperature (chordwise avg)

T_{BL} = metal limiting temperature

then

$$h_{01R} - h_{02R} = \frac{h_{gR} \ell (T_{REL} - T_{BL})}{\rho_2 \, W_2 \, \cos \beta_2 \, s} \qquad (6.3)$$

Similarly for a stator

$$h_{01} - h_{02} = \frac{h_{gs} \ell (T_{GAS} - T_{BL})}{\rho_1 \, V_1 \, \cos \alpha_1 \, s} \qquad (6.4)$$

where h_{gs} = average gas-side heat transfer coefficient to stator.

The values for α_1, β_1, V_1, and w_2 are determined from the computer program assumptions; the complete velocity diagrams are developed in Appendix I. Representative values for ℓ/s were extracted from Reference [15] and determined as

$$\left(\frac{\ell}{s}\right)_{rotor} = 3.303$$

$$\left(\frac{\ell}{s}\right)_{stator} = 3.155 \qquad (6.5)$$

The gas side heat transfer coefficients were expected to be of the form

$$N_u = \phi(R_e)^a \; \psi(P_r)^b$$

Flat plate values for a and b are 0.5 and 0.33 (laminar) and 0.8 and 0.33 (turbulent), respectively. For an actual turbine it is expected that the value for a is closer to 0.8. An expression by Hawthorne for Nu for turbine blades [35] was selected:

$$N_u = (0.14) R_e^{.68} \; Pr^{.33} \tag{6.6}$$

for air at high temperatures this reduces to

$$h = \frac{k}{c} (.1212) Re^{.68} \tag{6.7}$$

where k is the gas conductivity and c the blade chord.

Conductivity is primarily an increasing function of temperature, little affected by pressure expect at extremely high temperatures (greater than 2800 DEG K); for the range of 811-2250 DEG K k may be linearly approximated (within 1%) by

$$k = 1.4056 \times 10^{-5} + 1.31598 \times 10^{-8} (T-811) \frac{\text{kcal}}{\text{s-m-K}} \tag{6.8}$$

T in degrees K

Stator and vane chords were assumed equal at a value of .0508 m which is a reasonable first approximation assuming a small number of cooled stages.

Densities were determined within the computer program; in the notation of Figure 6.1 for the stator

$$\rho = \frac{P_{01}}{R\ T_{GAS}} = \frac{P_{01}}{c_p\left(\frac{\gamma-1}{\gamma}\right)\ T_{GAS}} \qquad (6.9)$$

for the rotor with heat removed at constant relative stagnation pressure

$$\rho_{REL} = \frac{P_{REL}}{R\ T_{REL}} \qquad (6.10)$$

From the gas laws

$$\frac{P_{01}}{P_{REL}} = \left(\frac{T_{02}}{T_{REL}}\right)^{\frac{\gamma}{\gamma-1}} \approx \left(\frac{T_{GAS}}{T_{REL}}\right)^{\frac{\gamma}{\gamma-1}} \qquad (6.11)$$

Since $T_{GAS} - T_{REL} \approx T_{02} - T_{02\ REL}$. Substituting for the gas constant R and from Equation 6.11

$$\rho_{REL} = \rho_{01} \div \left[\left(\frac{T_{GAS}}{T_{REL}}\right)^{\frac{\gamma}{\gamma-1}} c_p\left(\frac{\gamma-1}{\gamma}\right)\ T_{REL}\right] \qquad (6.12)$$

To determine the dynamic viscosity μ, an expression by Walz [36] was employed with temperatures evaluated at actual (vice film or bulk) values:

$$\mu = \frac{C_1\ T^{1/2}}{C_2 + T} \quad \left(\frac{N\text{-}s}{m^2}\right) \qquad (6.13)$$

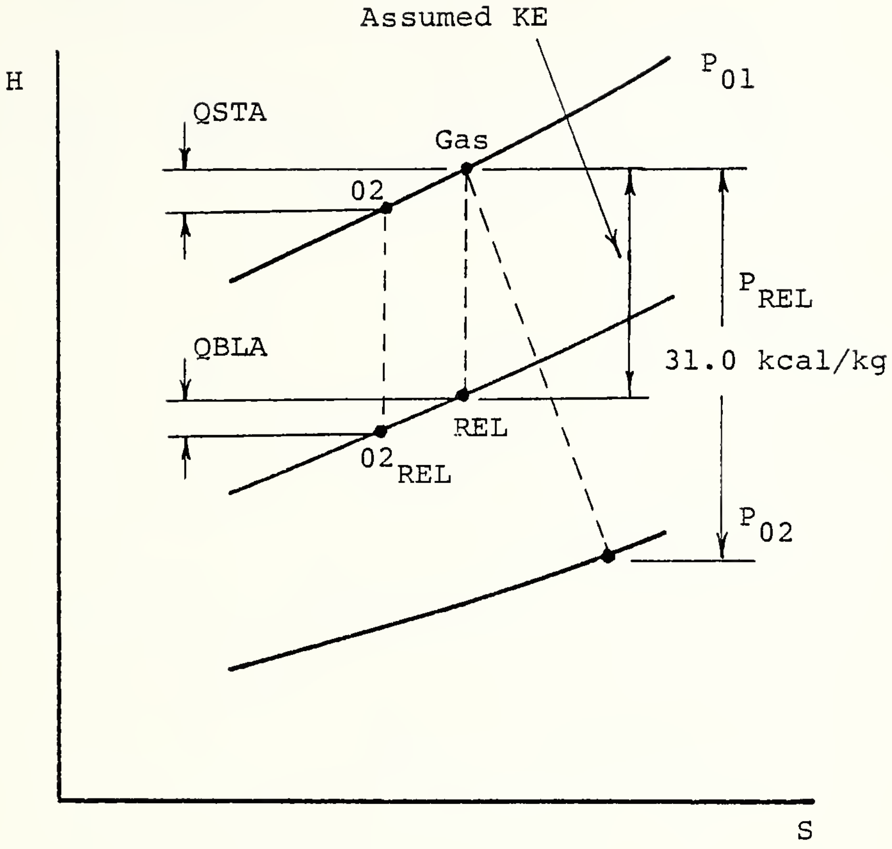
Assumed KE
H
QSTA
Gas
P_{01}
02
P_{REL}
QBLA
31.0 kcal/kg
REL
02_{REL}
P_{02}
S

FIGURE 6.1 Computer Model Heat Transfer Diagram

where $C_1 = 1.486 \times 10^{-6}$

$C_2 = 110.6$

T in degrees K.

The appropriate temperatures T are T_{GAS} for stators and T_{REL} for blades. The kinematic viscosity ν is then evaluated from

$$\nu = \frac{\mu}{\rho} \tag{6.14}$$

All quantities are therefore known to evaluate Re for the stator and rotor and to determine the heat losses (stagnation enthalpy changes) from Equations 6.3 and 6.4. The stage enthalpy drop is then

$$h_{01} - h_{02} = 31.0 - QSTA - QBLA \left(\frac{\text{kcal}}{\text{kg air}}\right)$$

Appendix I contains a listing of the water-cooled turbine subroutine modified to reflect the units of the model.

6.3 COOLING WATER REQUIREMENTS

Blades and stators are assumed cooled with pressurized water in a closed system (no mixing with gas stream). Assumptions are as follows:

(a) No temperature drop in blade;

(b) No boiling occurs in coolant;

(c) Allowable temperature rise of cooling water is 80% of the saturation-inlet temperature difference (for factor of safety).

The heat transferred to the metal is determined; an allowable coolant temperature rise is postulated and the mass flow rate of coolant is determined as follows

$$Q_{TOT} = Q_{STA} + Q_{BL} \left(\frac{\text{kcal/s}}{\text{kg air/s}}\right) \text{ per stage}$$

$$Q_{TOT} = \dot{m}\, c_p (\Delta T)$$

where $$\dot{m} = \frac{\text{mass flow rate coolant}}{\text{mass flow rate of air}} \left(\frac{\text{kg water/s}}{\text{kg air/s}}\right)$$

$$c_p = 1 \,\frac{\text{kcal}}{\text{kg K}} \text{ for water}$$

$$T = \underbrace{\text{safety coefficient}}_{0.8} \times (T_{SAT} - T_{\text{Coolant in}})$$

Thus for a particular power level the mass flow of air may be established (based on required specific work from the program) and this determines the coolant flow rate required. A further refinement could recognize

$$\dot{m} = \rho VA$$

and for some determined area with prescribed inlet conditions (ρ fixed), the coolant velocity is established. This requires detailed assumptions in blade design for the required area A which is beyond the scope of the study.

As a first trial, coolant conditions are established as follows:

Water Inlet Pressure		1000 Psia
	T_{IN}	124 K
	T_{SAT}	558 K
	c_p	1 kcal/kg K
then	ΔT	185 K

6.4 PERFORMANCE RESULTS

6.4.1 Open Cycle Results

The cycle conditions specified as Table 5.1 were duplicated for this model; the coolant is distilled water at inlet conditions 1000 psia and 324 K. The impact on open cycle performance at pressure ratio 16 is summarized in Table 6.1 and Figure 6.2. Figure 6.3 illustrates the reason for the rapid decline in efficiency; the heat absorbed by the coolant increases sharply as the gas temperature increases. This is anticipated as the temperature difference is the principal driving "force"

TABLE 6.1 Water Cooled Gas Turbine Simple Cycle Performance

Pressure ratio	16
Metal temperature (DEG K)	1090
Inlet temperature (DEG K)	1350
Cycle efficiency	.466
SFC (lbm/HP-HR)	.300
Heat loss (% turbine work)	1.5
Total cooling water required[1]	1.57/81
Specific power (HP/lbm-sec)	220

---

[1] % air flow rate/lbm per min. for 20000 HP.

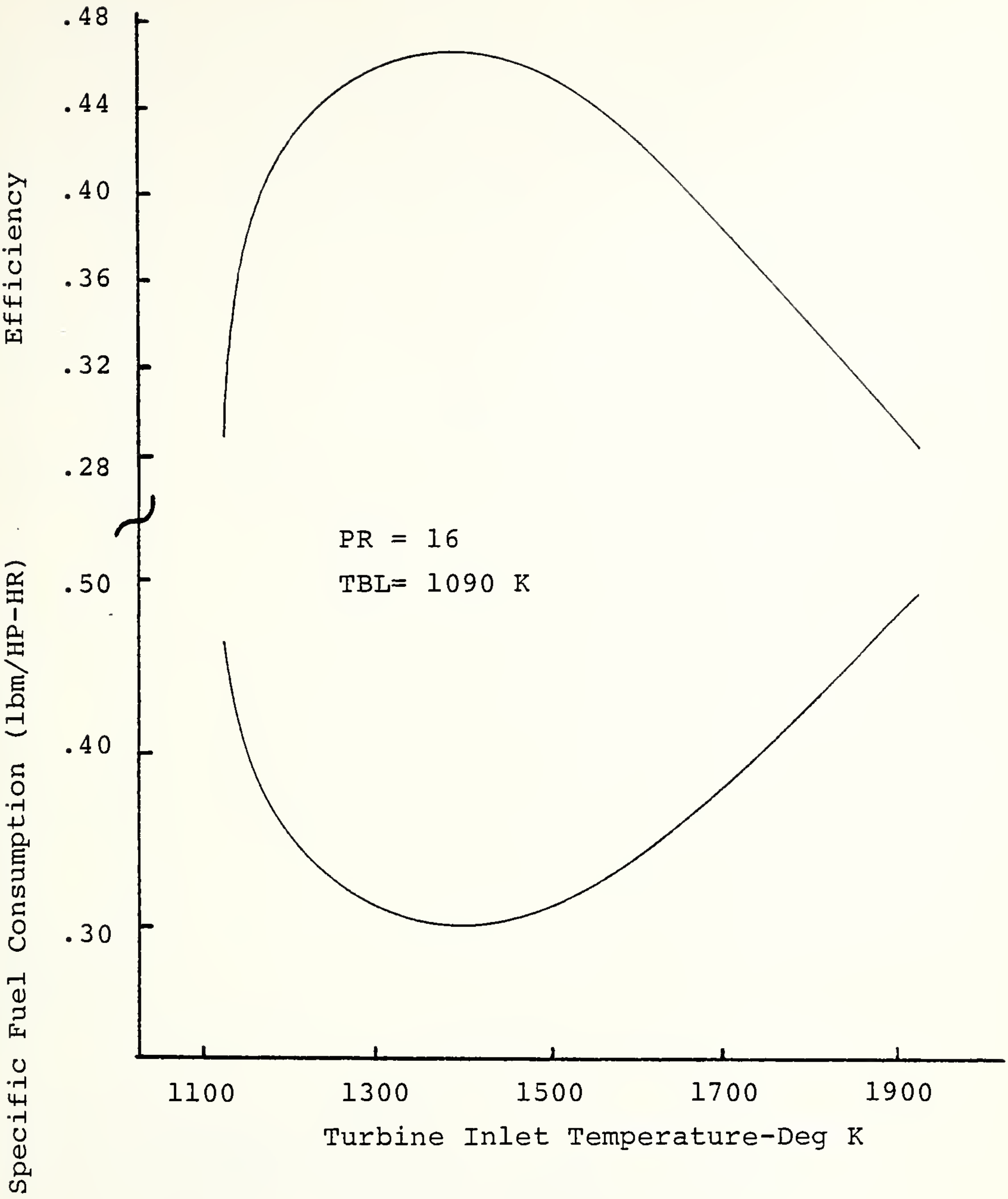

FIGURE 6.2 Simple Cycle Water-cooled Turbine Efficiency and Specific Fuel Consumption.

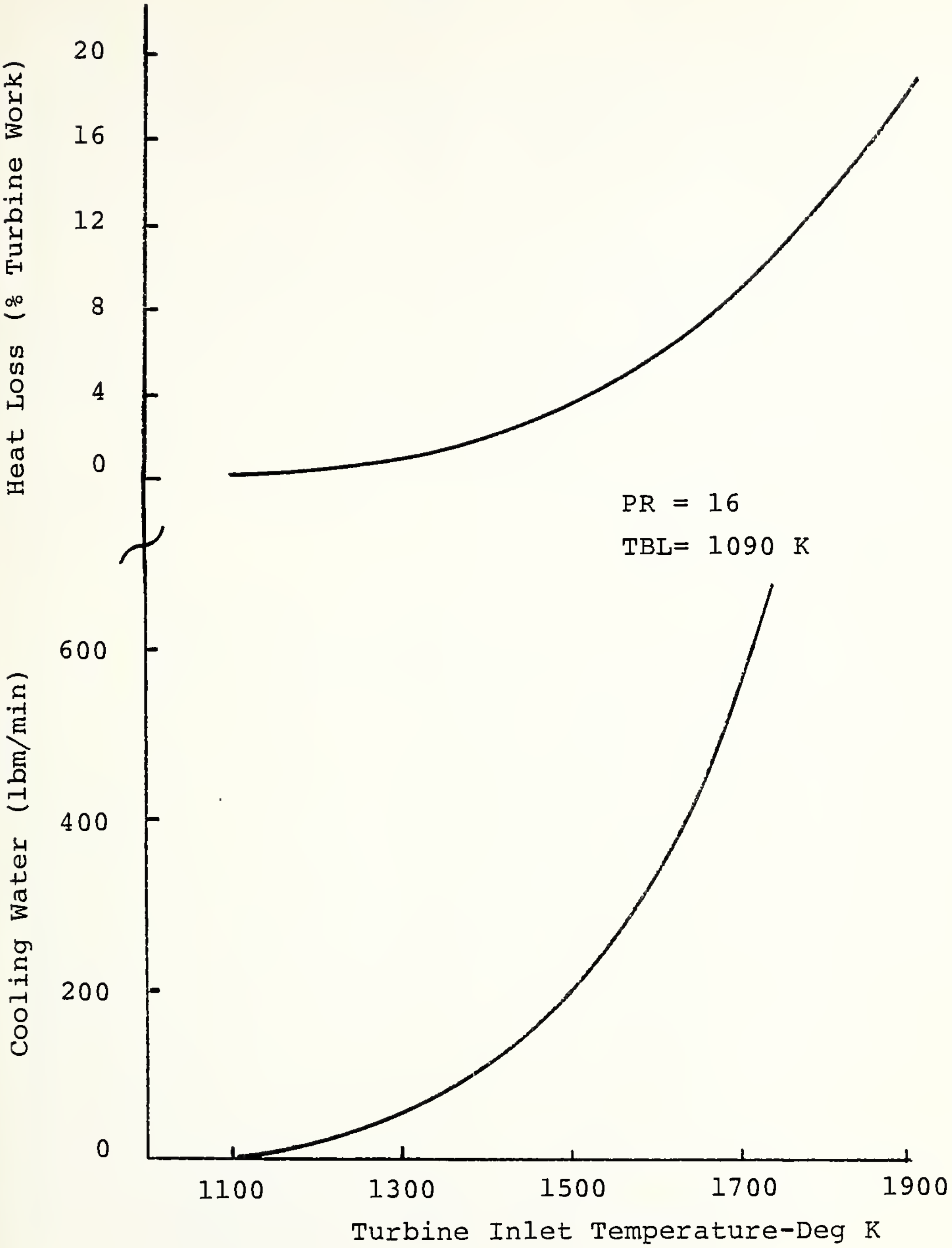

FIGURE 6.3 Water-cooled Turbine Heat Loss and Coolant Flow Rate. (Simple Cycle; Coolant Flow for 20000 HP)

for heat transfer. Increased heat fluxes require compensating cooling water flows as also illustrated in Figure 6.3.

The efficiency attained by the water-cooled turbine is noteworthy not only for its magnitude which approaches combined cycle efficiencies, but as well for the low optimum cycle temperature, fully 130 DEG (K) less than the optimum for a current air cooled turbine (Table 5.2).

6.4.2 Combined Cycle Results

The potential performance attainable with water-cooled turbines in combined cycle applications is indicated in Figure 6.4 and in Table 6.2 (combined cycle parameters as indicated in Table 5.4). As with the transpiration-cooled turbine, increases in boiler pressure are an available option to improve the steam cycle work ratio. The advantages of water cooling in both simple and combined cycle arrangement are indicated by the trends of Figure 6.5.

6.4.3 Evaluation of Water-Cooling Results

Assessment of the performance gains and additional costs of water-cooling gas turbines requires

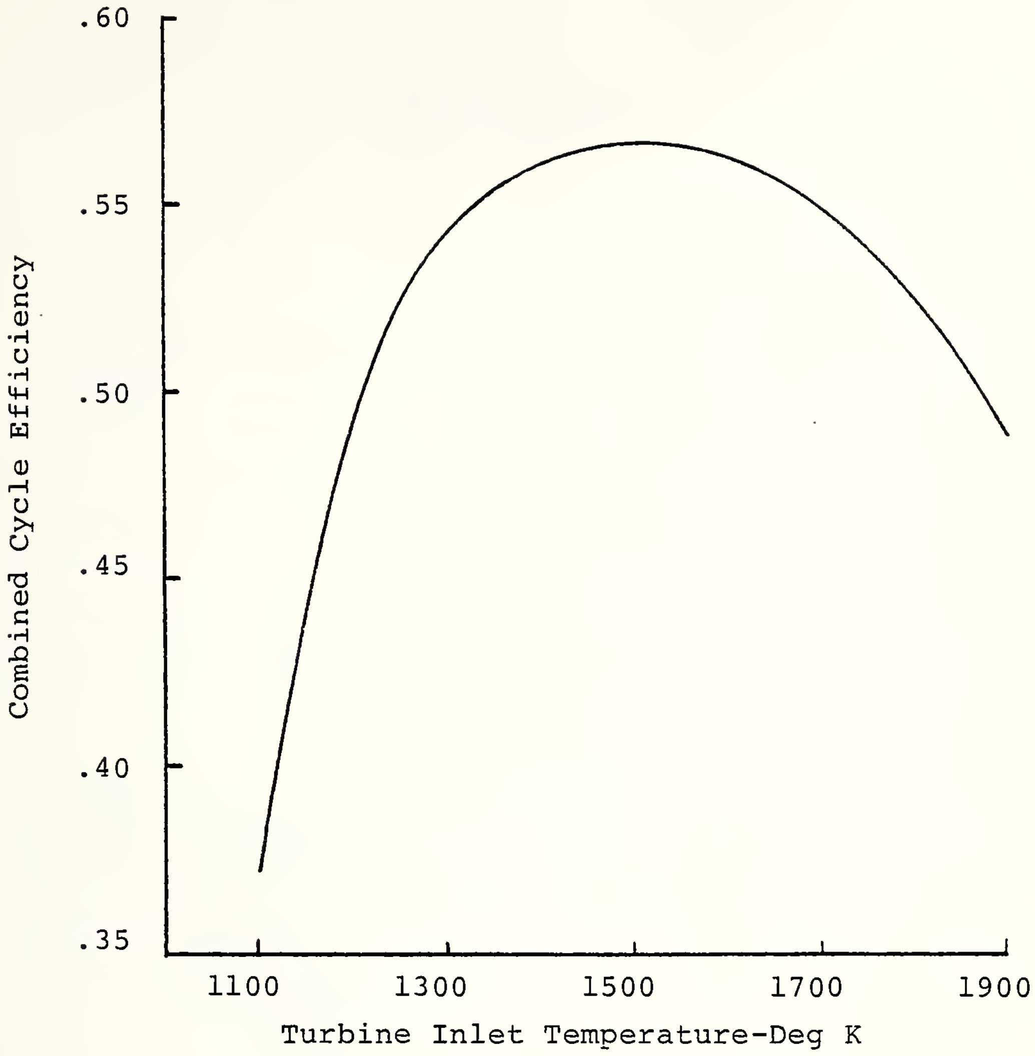

FIGURE 6.4 Combined Cycle Efficiency for Water-cooled Turbine. (PR= 16, TBL = 1090 K, WHRU Pressure = 400 psi.)

TABLE 6.2 Water Cooled Gas Turbine Combined Cycle Performance

Pressure ratio	16
Metal temperature	1090
Inlet temperature (DEG K)	1500
Cycle efficiency	.565
Specific power (HP/lbm-sec)	330
SFC (lbm/HR-HR)	.255
Work gas turbine (% total)	78.6
Boiler pressure (psi)	400
Moisture (%)	13.0
Temperature leaving gas turbine (DEG K)	772
Temperature leaving WHRU (DEG K)	482.5
Cooling water flow (lbm.min for 20000 HP)	155

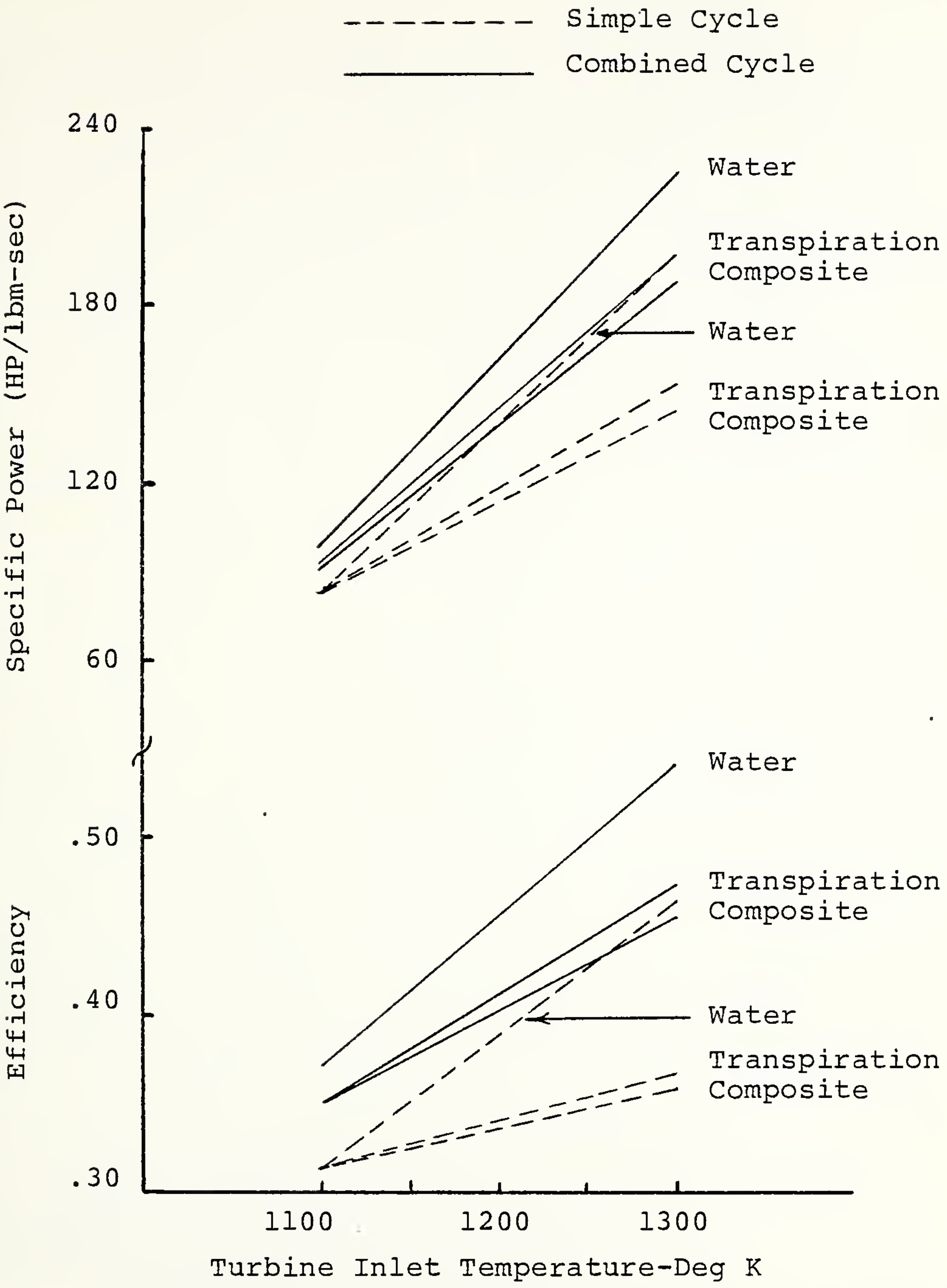

FIGURE 6.5 Effect of Cooling Method on Performance for Moderate Temperature Increases (Trend Diagram).

consideration of the limitations and idealizations of the model plus the paucity of full-scale prototype plants to develop approximate working comparisons. The derived equation for conductivity is accurate to within 1 percent for the optimum temperatures determined in this analysis; the low values of heat transferred for temperatures with 300 (DEG K) of metal limiting temperature are consistent with the usual assumption of adiabatic expansion. A comparison of blade Nusselt number with experimental data from actual engines indicates realistic agreement (Figure 6.6). A manual computation of the effects of neglecting to evaluate fluid properties (density and viscosity) at film temperature (averaged surface and gas temperature) indicated about 1% error (high). Determining the heat flux temperature difference based on gas temperature as opposed to adiabatic wall temperature was considered acceptable at the elevated temperatures involved, given the expected recovery factors (proportional to $P_r^{1/3}$) of 0.86 to 0.91; a brief computation at a turbine inlet temperature of 1700 DEG K indicated a 1 percent discrepancy in stage heat flux (high).

The prediction of coolant flow rates was highly idealized; the coolant flow map of Figure 6.7 when compared with values of a preliminary design of an industrial water-cooled gas turbine [15] indicates that

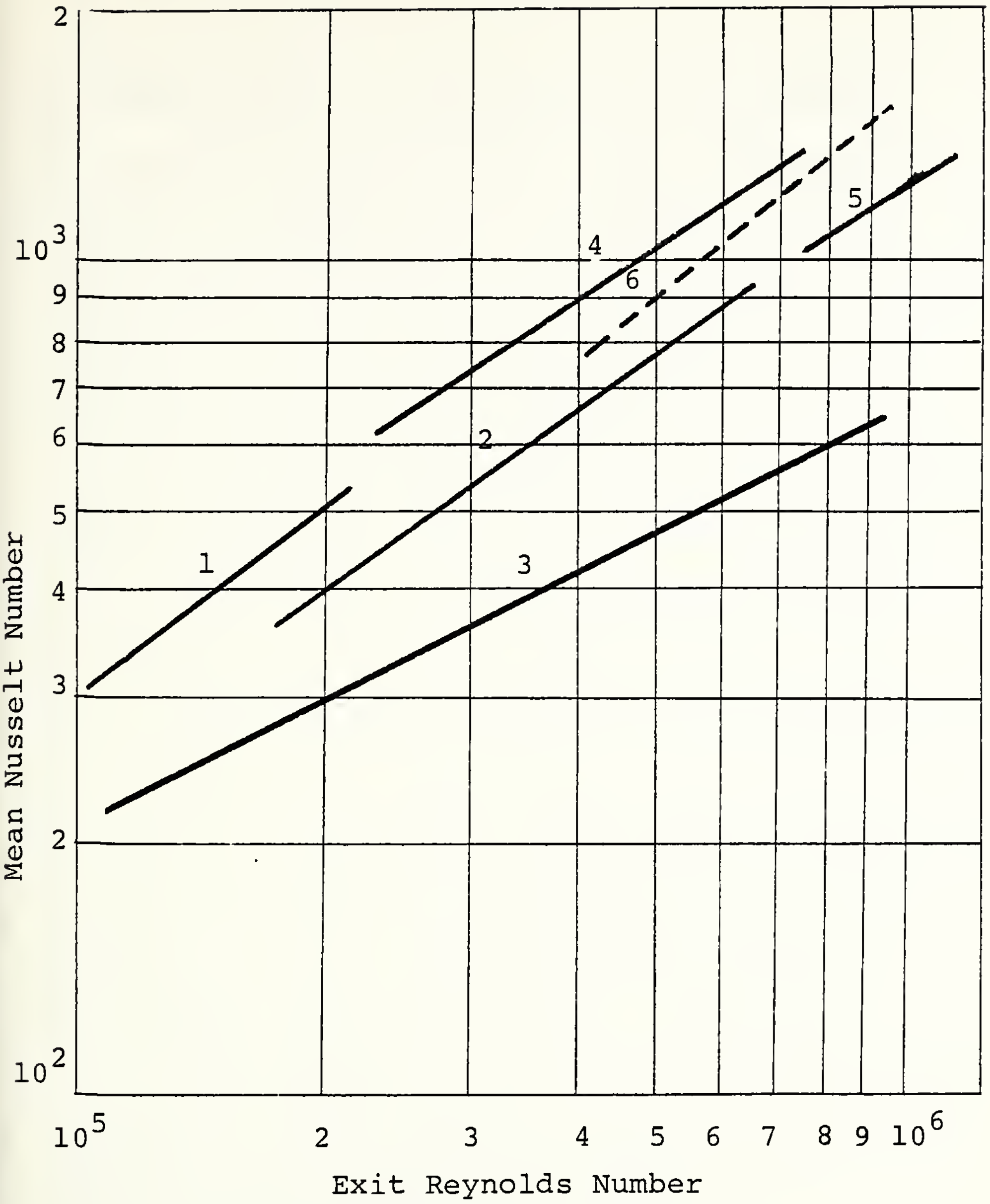

1 Ainley turbine
2 Wilson and Pope
3 Andrews and Bradley
4 Halls
5 Turner
(Reference 6)
6 Model predicted (water-cooled simple cycle)

FIGURE 6.6 Mean Heat Transfer Predictions

The coolant flow as a percentage of compressor air flow is very low for the nozzles (one order of magnitude) with not as large a discrepancy for the rotors. The total feed flow for the detailed design was 16.7 percent compressor air flow, compared to 1.57 percent for this model. Although coolant system pressures (1000 psi versus 1250 psi) and gas temperatures are similar, the design of reference [15] is an evaporative system that recovers only one third of its coolant; the heat tansfer capability per unit mass of coolant in such a system is many times that in which no phase change occurs and therefore it is anticipated that the coolant flow proportion for the model would be much higher than in the detailed design. This significant variation in flow rate is unexplained and indicates that more detailed modelling of coolant side heat transfer (and blade design) is probably required.

An additional noticeable result is that the maximum cycle temperature obtained with the water-cooled combined cycle exceeds that of the simple cycle configuration which is contrary to the trends indicated with air-cooled versions. The reason for this result is not understood, but may further indicate some discrepancy or inadequacy of the water-cooled model.

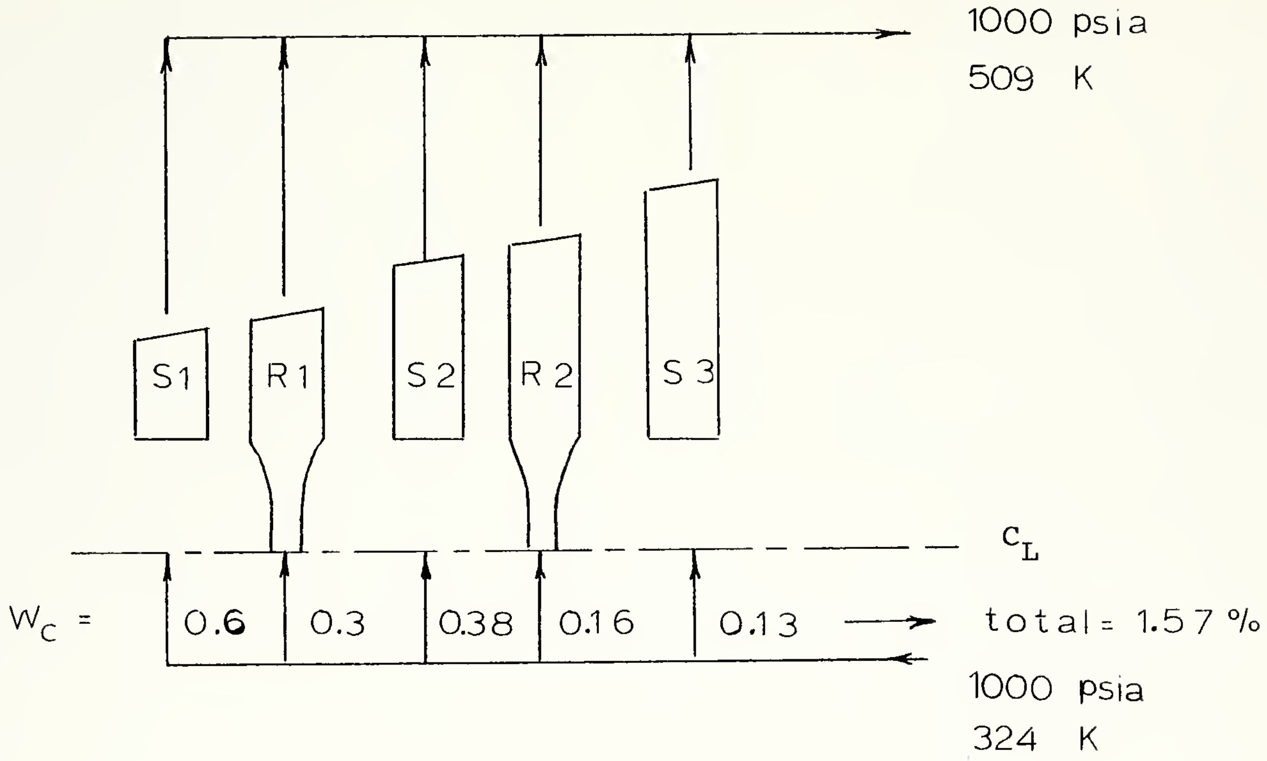
1000 psia
509 K
S1
R 1
S 2
R 2
S 3
C_L
W_c =
0.6
0.3
0.38
0.16
0.13
total = 1.57 %
1000 psia
324 K

W_c = coolant flow (% compressor inlet flow)

FIGURE 6.7 Combined Cycle Coolant Distribution Map

7. IMPLICATIONS FOR MARINE UTILIZATION

7.1 METHOD OF COMPARISON

To properly determine an optimum power plant for a ship requires a comprehensive cost estimate (total monetary and non-monetary, i.e. weight or volume) based on detailed knowledge of the individual proposed installation. Since all of the advanced cooling methods considered thus far are still under development, most costing data are either unknown or proprietary and therefore unavailable. A simple partial method of comparing the various turbine cooling methods can be accomplished, however, by analyzing the savings in fuel weight and improvement in endurance - two key parameters of concern to ship machinery plant designers.

Gas turbine installations for naval ships of displacement greater than 1000 tons are typically in "cruise-boost" configuration, with a low power gas turbine supplemented by a larger turbine for short periods of full speed. High specific power is desirable at all power levels to minimize ducting and machinery size and weight, but high efficiency and low SFC are becoming as important to naval ships as they have always been to merchant vessels that spend most of their

operating time at a single speed. The most probable naval gas turbine configurations in the future then will consist of a highly cooled turbine for cruising plus a "boost" turbine with the possible addition of a bottoming cycle to the cruising turbine.

An arbitrary naval vessel of 80,000 SHP with a maximum speed of 36 kts shall be considered, with an assumed propulsion fuel weight of 850 tons (284,200 gal). The machinery arrangement consists of two shafts with two identical gas turbines providing power to each shaft. The part-load fuel consumption curve of Figure 7.1 (derived from data for the LM 2500 marine gas turbine) and an endurance speed of 18 kts are assumed. (See Appendix II for sample calculation).

7.2 COMPARISON RESULTS

For the plant configuration described, the improvements in range or potential weight savings are negligible to small for simple cycle, advanced air cooling methods (film and transpiration); much greater potential performance is evidence by the application of a steam bottoming cycle to a state-of-the art cooled turbine. Employing transpiration cooling in a combined cycle results in a greater percentage increase in fuel economy

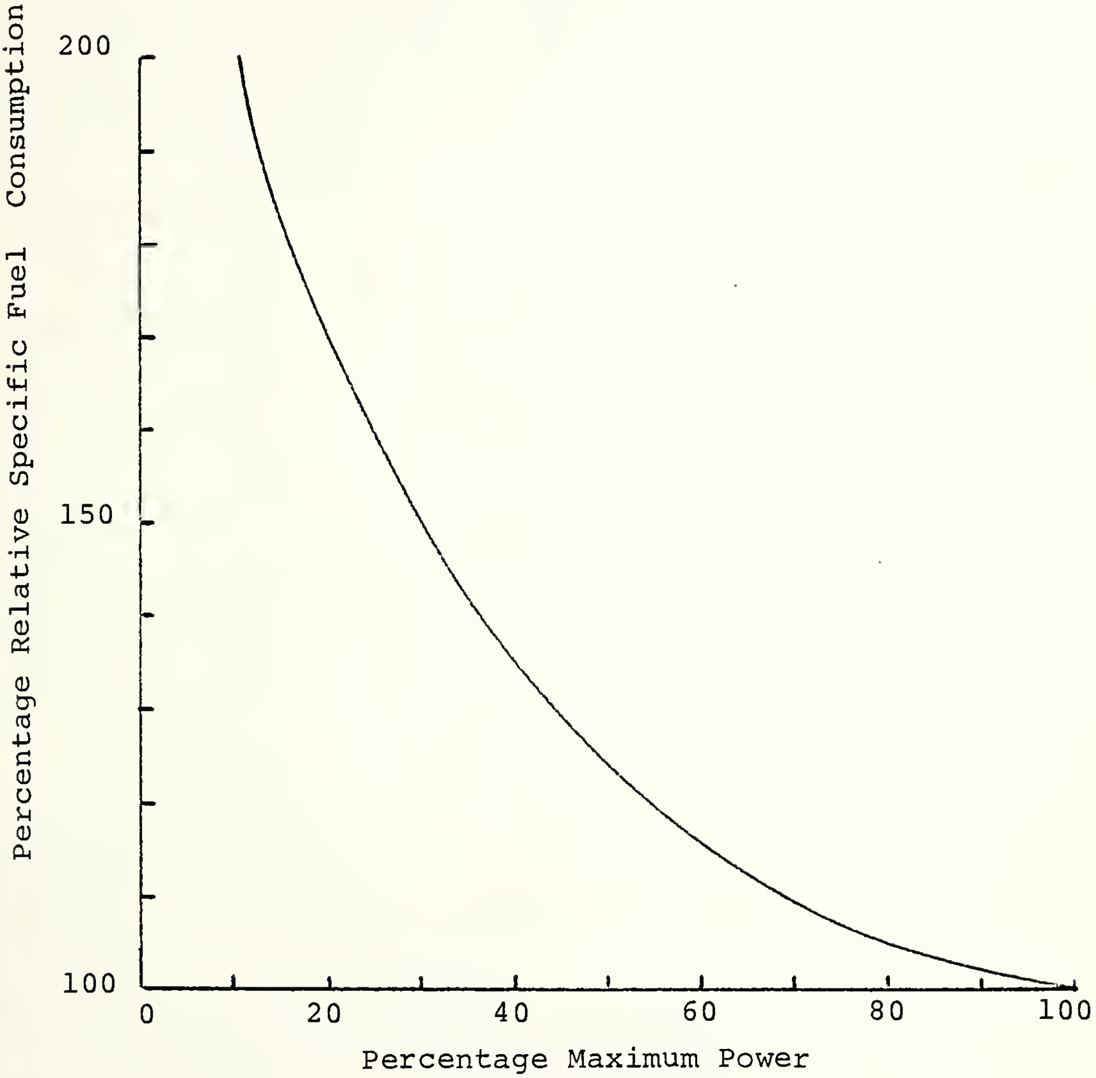

FIGURE 7.1 Typical Part Load Specific Fuel Consumption for Simple Cycle Gas Turbine.

than from a transpiration cooled simple cycle (10% vs. 3.7%) Table 7.1 summarizes the results.

The remarkable savings and economy observed with the water-cooled model are mitigated somewhat by the troublesome history of mechanical problems associated with water-cooled systems. In addition, this model has assumed a closed, convective cooling system and the pumping work required at the high system pressure (although thermosyphon techniques can reduce) is certain to deduct some performance penalty, of the order 3 to 5 percent in turbine efficiency [3]. It is also reasonable to expect that losses would exist in an actual feed system. The heat rejected to the coolant may be profitably employed in auxiliary use and it is useful to examine the potential of the rejected heat to contribute to the anticipated make-up feed required.

Figure 7.2 is a schematic of a typical shipboard distillation system employing a single flash evaporator operating at 27 inches Hg vacuum; the heated turbine cooling water is employed tube-side in a counter flow shell-and-tube heat exchanger to preheat the seawater feed (assumed inlet 300 DEG K) to the evaporator flash temperature (at 27 in Hg vacuum) of 319 DEG K. To return the turbine cooling water to 324 DEG K (ignoring

TABLE 7.1 Improvements in Performance of Projected Shipboard Gas Turbine Propulsion Plants Relative to a Standard (Composite) Cooled Simple Cycle[1]

Cycle	Gas Turbine Cooling Method	Maximum Cycle Temperature (DEG K)	SFC/% Change in SFC (lbm/HP-HR)	Specific Power/ % Change Specific Power (HP/lbm-sec)	Endurance Range (n.m.)	Fuel Weight Savings 3 (Tons)
Simple	Standard	1480	.388/0	186/0	5520	0 (REF)
	Film	1550	.387/0.3	204/9.7	5534	3.2
	Transpiration	1660	.374/3.7	304/63.4	5726	19.1
	Water	1350	.300/29.3	220/18.3	7139	120.5
Combined[2]	Standard	1380	.310/25.2	223/19.9	6909	106.8
	Transpiration	1540	.286/35.7	309/66.1	7489	139.6
	Water	1500	.255/51.4	330/77.4	8355	179.3

[1] All comparisons at pressure ratio 16; metal limiting temperature 1090 K; other conditions as listed in Table 5.1.

[2] WHRU pressure 400 psia; single-stage feedheating (no reheat); other conditions as listed in Table 5.4.

[3] For constant endurance range of 5520 n.m.

for the moment heat exchanger size requirements), the seawater feed flow rate W_{sw} may be determined (assuming some losses) by

$$W_{sw} \, c_{p\ sw} \, (319-300) = 0.9 \times W_{cw} \, c_{p\ cw} (509-324) \tag{7.1}$$

Assuming equal specific heats,

$$W_{sw} = 8.76 \, W_{cw} \tag{7.2}$$

If the fresh-to-brine ratio is assumed 0.02 (for every unit mass of feedwater flashed, 98 percent returns to brine, producing only 2 percent fresh per unit mass in), then the fresh distillate W_{fw} produced for cooling system augmentation is

$$W_{fw} = 0.175 \, W_{cw} \qquad 7.3)$$

In the open cycle considered with W_{cw} = 81 lbm/min (approximately 565 gallons per hour) the estimated distillate produced is about 99 gallons per hour (0.175 x 565 gal/Hr). The heat available from the turbine coolant then can (under nearly ideal conditions) contribute sufficient energy to enable the cooling system to sustain water losses of over 17 percent. Multi-flash units could increase both the amount and quality of the distillate.

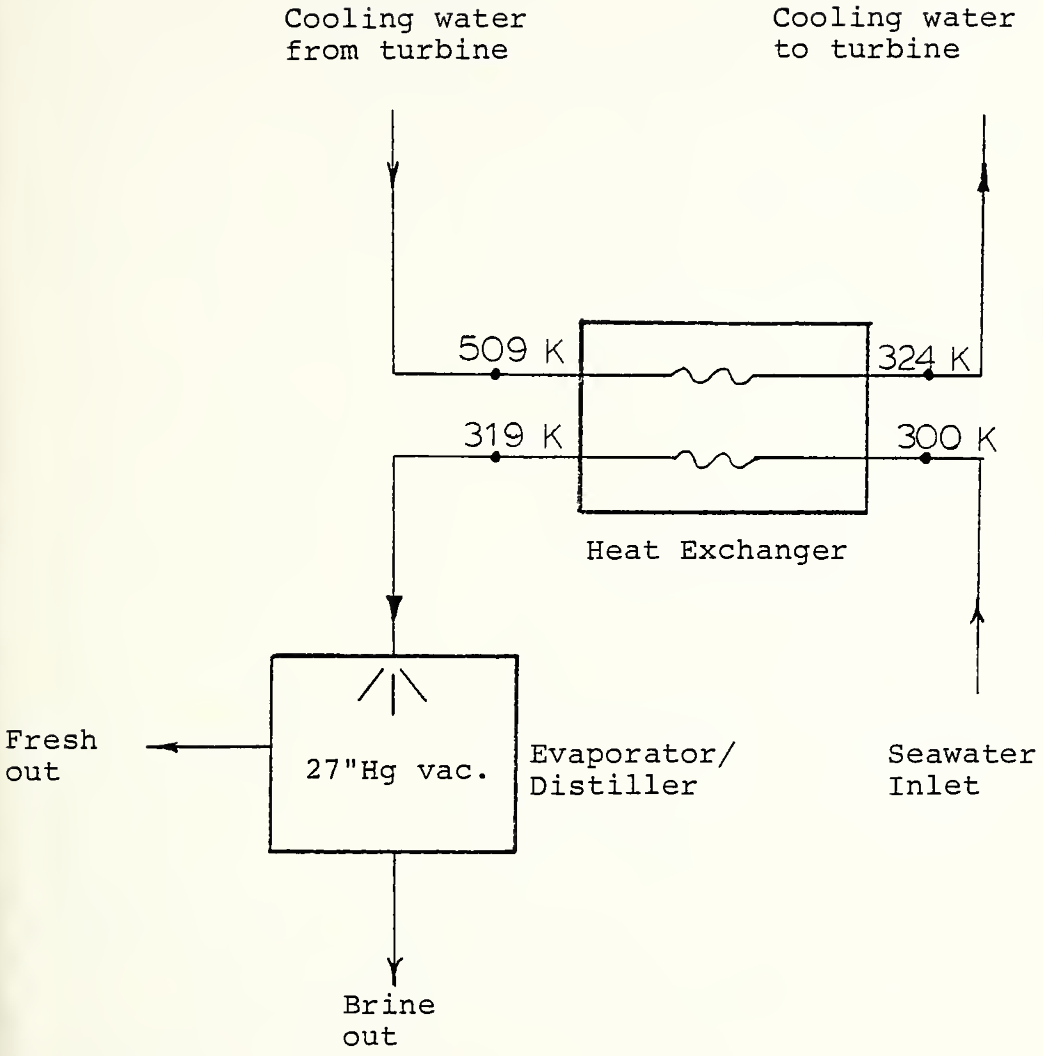
Cooling water from turbine
Cooling water to turbine
509 K
324 K
319 K
300 K
Heat Exchanger
Fresh out
27"Hg vac.
Evaporator/ Distiller
Seawater Inlet
Brine out

FIGURE 7.2 Schematic of Single-Stage Flash Evaporator for Water-cooled Gas Turbine.

The water produced in this manner is ready for immediate use in the cooling system without additional treatment. The question of water purification requirements and treatment in turbine cooling systems is currently not well-defined; reference [37] reports experimental evidence that indicates the scrubbing action of the coolant within the blade passage is sufficient to prevent the formation of deposits. The use of high pressures to suppress ebullition results in low coolant temperatures and reduces the chemical treatment requirements familiar to operators of high pressure (1200 psi or greater) steam plants. The mechanical difficulties in coolant metering of a pressurized system such as this involve blade strengthening to withstand high tip pre-sures and careful cooling passage design to eliminate throttling obstructions that could cause internal pressure drops and induce flashing in the hot (509 DEG K) coolant.

The required area (and therefore size) of the heat exchanger required for the above process is not excessive, estimated at 28 square feet for an overall heat transfer coefficient of 400 BTU/HR FT^2 F (Appendix I).

Without attempting detailed blade design, one possible check on the realism of the coolant flow rate (1081 Gal/HR for the combined cycle) is a comparison

with the detailed design of reference [15]. Table 7.2 summarizes the key parameters for that design; the ratio of total coolant flows on the basis of gallons/HR/HP is about 6.88. If for system 2 (the model developed here) the error in required coolant flow were 100% (3.14 percent compre-sor flow required as coolant) the ratio gallons (collant/HP/HR drops to 3.57. The water flow requirements predicted by the model are then considerably less (one-third to one-sixth) that those of an actual design. This fact indicates that the model is conservative in estimating heat losses (and therefore cooling water requirements) but also that the flows demanded by the model should be easily accommodated by reasonable blade design. The distribution of the coolant in each system compares reasonably well, with 29 percent going to rotors in system 2 and 19.2 percent in system 1. As noted in Chapter 6 there exists a significant discrepancy in the expected total water flow rates between the detailed design and the model predictions. The simplified assumptions concerning coolant side behavior are possible factors contributing to this variation.

An interesting result of the optimization analysis is the relatively significant impact that the type of turbine cooling system has on the maximum cycle

TABLE 7.2 Comparison of Actual to Proposed Water-Cooled Gas Turbine Design

System	1	2
Design Power (HP)	131278	20000
Compressor air flow (lbm/sec)	700	60.6
Specific power (HP/lbm-sec)	187.5	330
# Cooled stages	3	2.5
Coolant conditions (water)		
Pressure, stator/rotor (PSI)	1250/250	1000/1000
Temperature (F)	250	125
Coolant flow required		
GAL/HR	48817	1081
Percent compressor gas flow	16.7	1.57
Stator	13.5	1.11
Rotor	3.2	0.46
GAL/HR/HP	0.372	0.054
Makeup (% air flow)	2.8	17(available)
Combined cycle efficiency	.476	.565

System 1 - Combined cycle power plant, water-cooled turbine [15].[1]

System 2 - Combined cycle power plant with water-cooled Gas Turbine (Chapter 6).

---

[1] This design is evaporative, permitting 67% of rotor coolant flow to exhaust to gas steam; for the comparison it was assumed fully collected.

temperature in the simple cycle, as opposed to minor effects with a combined cycle. The peak temperature "inversion" between simple and combined cycles contrasted to air cooled turbines was noted in Chapter 5.

Finally, the potential increases in specific power achievable with water and transpiration cooling in simple cycle arrangements indicate that further peaking or "boost" power units may be able to achieve significant reductions in size, weight and cost of the turbine plus ducting, as stage loading can be increased (fewer stages in the high pressure turbine) or air flow required for a desired power level reduced. This is particularly important to naval ships as the advent of increased weapons payloads has increased the demand for space and power, simultaneously reducing the space available for machinery while demanding additional output - hence a trend to greater specific power machinery [14].

8. CONCLUSIONS

A study of the potential of several advanced gas turbine cooling methods has been made to assess the impact on performance in simple and combined cycles. It is concluded that:

1. Continued increases in efficiency and specific power for simple cycle gas turbines require the attainment of turbine inlet temperatures between 1300 and 1600 DEG K at current pressure ratios. As these temperatures exceed the current metal limiting temperatures (about 1090 DEG K), some manner of turbine cooling is required;

2. Air cooled designs are the most developed; this is partially a result of the compatibility of the cooling medium with the turbine working fluid; liquid-cooled designs have been the subject of much research but the mechanical problems associated with liquid systems have prevented the achievement of a production design;

3. The anticipated reduced coolant flows and forecast ability provide more uniform and effective cooling with transpiration and film cooling methods should offer significant improvements in efficiency and specific power; the overall performance gains from film cooling as observed in this analysis were very small. Transpiration

cooling achieves moderate improvements in the simple cycle configuration. These modest differences from composite, state-of-the-art cooling may result from:

(a) An oversimplification of the cooling effectiveness correlation; while the composite correlation is effective in predicting actual turbine performance, contrasting elements of the film and transpiration cooling processes are not made significant enough through this method;

(b) The scarcity of data points (12) in developing the film correlation;

(c) The inability to adequately isolate a full-coverage film case from other methods;

(d) Differing conditions affecting data; although the data utilized were collected at approximately equal Reynolds numbers, additional similarity conditions (primarily Biot number) are required for heat transfer (hence coolant flow) predictions;

(e) Poor modelling of the film cooling mechanism with this generalized approach;

4. The film cooling data employed indicate significant improvement over earlier analytical predictions;

5. The levels of effectiveness obtained with standard (composite) cooling are high, exceeding the previously accepted threshold of 50 percent maximum effectiveness and attaining levels of 60 to 70 percent effectiveness. These improvements in the "baseline" cooling system diminish the differences among the advanced air cooling methods in this study;

6. Transpiration cooling results in higher exhaust temperatures, indicating greater combined cycle performance benefits. Transpiration cooling also permits an increase in maximum cycle temperature at a fixed pressure ratio; the development of high pressure-ratio enignes for shaft power will result in simple cycle efficiencies exceeding 41 percent;

7. Progress in materials development could achieve much greater improvements in efficiency than through sophisticated air cooling techniques by achieving greater reductions in required coolant flow;

8. Precooling can achieve moderate increases in efficiency with any air cooling system but at added complexity and design cost. Precooling with current cooling systems can improve cycle efficiencies by 50 percent of the potential gains with transpiration cooling;

9. Combined cycle efficiencies exceeding 50 percent are attainable with transpiration and water-cooled gas turbines; the employment of standard cooling practices in a combined cycle delivers greater performance than with transpiration or water-cooled turbines in a simple cycle;

10. The water-cooled model developed in this study adequately predicts gas side heat transfer (Figure 6.6) but the cooling water flow requirements are based on overly simplified assumptions and could be in excess of 100 percent too low. In addition, the fact that a water-cooled combined cycle achieves peak efficiencies at higher turbine inlet temperatures than in simple cycle use is a major difference from current air-cooled trends and indicates a possible discrepancy in the water-cooled model.

11. Predicted simple cycle efficiencies with water cooling exceed 46 percent while combined cycle efficiency approaches 60 percent; allowance for losses and pumping work could reduce these figures by about 3 to 5 points. Cooling water requirements at 1000 psi and 324 DEG K are estimated at 565 and 1081 GAL/HR for simple and combined cycles, respectively, at a nominal 20,000 HP. Preliminary calculations indicate that in a typical shipboard installation, the heat rejected by the gas to the coolant could be recovered to enable the

system to sustain losses of 17 percent. This would improve cycle thermal efficiency although some additional pumping power is required;

12. The performance improvements of transpiration and water-cooled turbines in typical shipboard configurations demonstrates that increases in maximum cruising range or equivalent fuel weight reductions for a fixed range are significant, especially in a combined cycle.

REFERENCES

1. Hare, A. and H. H. Malley, "Cooling Modern Aero Engine Turbine Blades and Vanes", Society of Automotive Engineers (SAE), Paper 660053; January 1966.

2. Goodyer, M. J. and R. M. Waterston, "Mist Cooled Turbines", Conference on Heat and Fluid Flow in Steam and Gas Turbine Plants, Paper C60/73 Institute of Mechanical Engineers, London; 1973.

3. Stuart-Mitchell, R. W. and V. A. Ogale, "Gas Turbine Blade Cooling-Retrospect and Prospect", American Society of Mechanical Engineers (ASME), Paper 67-WA/GT-9; 1967.

4. Shepherd, D. G., Introduction to the Gas Turbine, McMillan Company, New York; 1965.

5. Coates, R., "Efficient Application of Marine Gas Turbines", Proceedings, Symposium on Marine Propulsion Systems; Marine Media Management Limited; 1974.

6. Bayley, F. J. and A. B. Turner, "Transpiration Cooled Turbines", Proceedings, Institution of Mechanical Engineers, Vol. 185, Paper 69/71.

7. Esgar, J. B., J. N. B. Livingood and R. D. Hickel, "Research on the Application of Cooling to Gas Turbines", Transactions, ASME, Vol. 79, NR 3; April 1957.

8. Lombardo, S., Advanced Component Developments for Industrial Gas Turbines, Curtiss-Wright Corporation; 1974.

9. Alpert, S., R. E. Grey and W. O. Flaschat, "Development of a Three-State Liquid Cooled Gas Turbine", Transactions, ASME, Journal of Engineering for Power, Vol. 82A, 1961.

10. Japikse, Dave., "Advances in Thermosyphon Technology", Advances in Heat Transfer, Vol. 9, 1974.

11. Kreith, Frank, Principles of Heat Transfer, International Textbook Company; 1969.

12. Gabel, R. M., "High Inlet Temperature Doubles Turbine Engine Power - But Blade Cooling is a Must", SAE Engineering Journal, Vol. 77, NR 5, 1969.

13. Smith, A. G., "Heat Flow in the Gas Turbine", Proceedings, Institution of Mechanical Engineers, Vol. 159; 1948.

14. Baham, Gary J. and Hugh D. Marron, "Efficiency Considerations for Future Marine Gas Turbines", Paper Tl-3, Society of Naval Architects and Marine Engineers, STAR Symposium; May 1977.

15. General Electric Company, High Temperature Turbine Technology Program, Topical Report, Reference Turbine Subsystem Designs; July 1977.

16. Cohen, H., G. F. C. Rogers, and H. I. H. Saravanamuttoo, Gas Turbine Theory, Second Ed., Longman Group Ltd., 1972.

17. Halls, G. A., "Air Cooling of Turbine Blades and Vanes", AGARDograph 120, Supersonic Turbojet Propulsion Systems and Components, Ed., J. Chauvin, 1967.

18. Sawyer, John W., Sawyer's Gas Turbine Engineering Handbook, Second Edition, Vol. I; Gas Turbine Publications, Inc., Stamford, Connecticut; 1972.

19. Lebrocq, P. V., Launder, B. E., Pridden, C. H., "Experiments on Transpiration Cooling", Paper 1, Proceedings, Institution of Mechanical Engineers, Vol. 187, No. 17; 1973.

20. National Advisory Committee on Aeronautics, Conference on Turbine Cooling, Collected Papers; 1949.

21. Brown, T. W. F., "Some Factors in the Use of High Temperatures in Gas Turbines", Proceedings, Institution of Mechanical Engineers, Vol. 162; 1951.

22. Hawthorne, W. R., "The Thermodynamics of Cooled Turbines, Part I: The Turbine Stage", ASME Paper 55-A-186.

23. Horlock, J. H., Axial Flow Turbines, Butterworths, London; 1966.

24. May. H., "Investigations of Forced Convection Liquid-Cooled Gas Turbine Blades", ASME Journal of Engineering for Power; January 1965.

25. Johnson, B. V., Giramonti, A. J., and S. J. Lehman, "Effect of Water Cooling Turbine Blades on Advanced Gas Turbine Power Systems", ASME Paper 77-GT-80; 1977.

26. "ERDA Backing 2500 DEG F 10-MW Desing for 1982", Gas Turbine World; May 1977.

27. Kerrebrock, Jack, Aircraft Engines and Gas Turbines, MIT Press, Cambridge, Massachusetts; 1977.

28. Louis, Jean F., "Systematic Studies of Heat Transfer and Film Cooling Effectiveness", Unpublished Paper, Massachusetts Institute of Technology; 1977.

29. Gladden, H and J. Gauntner, "An Adverse Effect of Film Cooling on the Suction Surface of a Turbine Vane", NASA Technical Note TN D-7618; June 1974.

30. Smith, I. E. and M. J. Watts, "Radiation Heat Transfer to a Porous Surface Cooled by a Transpiring Flow", Combustion and Heat Transfer in Gas Turbine Systems, E. R. Norster (ed.), Pergamon Press, 1971.

31. Yeh, F *et al*, "Comparison of Cooling Effectiveness of Turbine Vanes with an Without Film Cooling", NASA Technical Memorandum TM-X-3022; June 1976.

32. Hiroki, T. and I. Katsumata, "Design and Experimental Studies of Turbine Cooling", ASME Paper 74-GT-30; 1974.

33. Eckert, E. R. G. and J. P. Esgar, "Survey of Advantages and Problems Associated with Transpiration Cooling and Film Cooling of Gas Turbine Blades", NACA Research Memorandum RM E50K15, 1951.

34. Keenan, J. H. *et al*, Steam Tables, John Wiley and Sons, Inc., New York; 1969.

35. Rohsenow, W. M., "The Effect of Turbine Blade Cooling on Efficiency of a Simple Gas Turbine Power Plant", ASME Paper 55-A-120, 1955.

36. Walz, Alfred, Boundary Layers of Flow and Temperature, MIT Press, Cambridge, Massachusetts, 1969.

37. Kydd, P. H. and W. H. Day, "An Ultra High Temperature Turbine for Maximum Performance and Fuels Flexibility", ASME Paper 75-CT-81; 1975.

APPENDIX I-A

COMPUTER MODEL VECTOR DIAGRAMS

ASSUMPTIONS:	HUB Reaction	0.0
	α_1(HUB) (DEG)	70.0
	$v_{\theta 2}$ (m/s)	0.0
	Reaction at $r/r_H = 1.054$	0.1
	Stage work (kcal/kg)	31.0
	α_1 (DEG)	69.0
	Free vortex	
	v_x (m/s)	constant
	rv_θ	constant
CALCULATE:	$v_{\theta 1}$ (m/s)	481.9
	u_1 (m/s)	267.6
	$w_{\theta 1}$ (m/s)	214.3
	v_1 (m/s)	516.0
	v_x (m/s)	185.0
	w_1 (m/s)	283.1
	$v_{\theta 2}$ (m/s)	0.0
	u_2 (m/s)	267.6
	$w_{\theta 2}$ (m/s)	267.6
	α_2 (DEG)	0.0
	β_2 (DEG)	-55.3
	v_2 (m/s)	185.0
	w_2 (m/s)	325.0

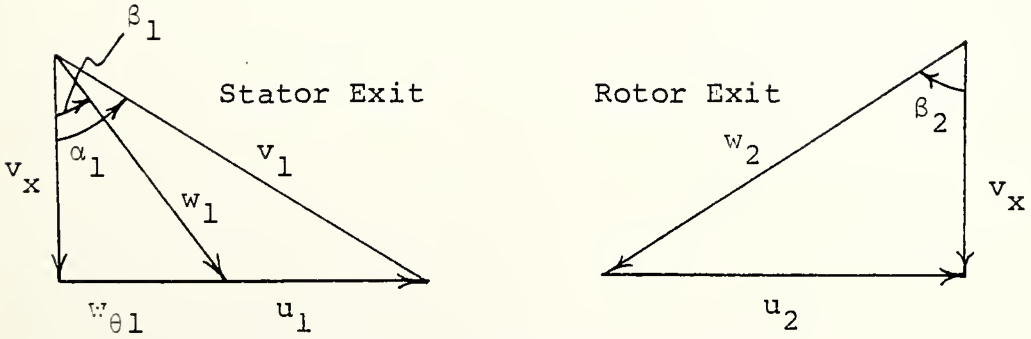
β_1
Stator Exit
v_x
α_1
v_1
w_1
$w_{\theta 1}$
u_1
Rotor Exit
β_2
w_2
v_x
u_2

FIGURE I-1 Velocity Triangles

APPENDIX I-B

WATER COOLED TURBINE MODEL (GTTR)
VARIABLE LISTING

Rankine and GTUR/GTTR employ SI units as listed with appropriate variable names below:

CP	Specific heat	kcal/kg-K
CONB	Gas conductivity at rotor	kcal/s-m-K
CONS	Gas conductivity at stator	kcal/s-m-K
ENTH	Enthalpy	kcal/kg
ENTR	Entropy	kcal/kg-K
MHUB	Gas dynamic viscosity at rotor	$N-s/m^2$
MHUS	Gas dynamic viscosity at stator	$N-s/m^2$
QBLA	Heat loss due to blade cooling	kcal/kg
QSTA	heat loss due to stator cooling	kcal/kg
QTOT	Total heat loss	kcal/kg
RCW	Rotor cooling water	kg water/s/kg air/s
SCW	Stator cooling water	kg water/s/kg air/s
REYB	Blade Reynolds number	
REYS	Stator Reynolds number	
RHOB	Relative gas density	kg/m^3
RHOS	Gas density	kg/m^3
TCWS	Total stage cooling water	kg water/s/kg air/s

```
C SUBROUTINE GTTR IS EMPLOYED WITH THE COMBINED CYCLE PROGRAM ''RANKINE''
C OF THE DEPARTMENT OF OCEAN ENGINEERING, MASSACHUSETTS INSTITUTE OF TECH-
C NOLOGY, TO SIMULATE A GAS TURBINE
C THIS  LISTING DESCRIBES A PRELIMINARY WATER-COOLED TURBINE MODEL FOR USE
C WITH ''RANKINE.''


      SUBROUTINE GTTR (P3G,P4G,T2G,T3G,T4G,TBL,XMC,XMT,EPC,EPT,DHT,WHOT)
      DIMENSION XMC(5), XMT(5)
      REAL MHUS,MHUB
      TGAS=T3G
      P=P3G
      DHT=0.0
      TCW=0.0
      QTOT=0.0
      PRT=1.0
      N=1
      IF(TGAS.GT.TBL) GO TO 1
      GO TO 2
C CALCULATE HEAT LOSS DUE TO STATOR COOLING
    1 MHUS=1.486E-6*(TGAS**1.5)/(110.6+TGAS)
      P=P3G*PRT
      G=GAMA(XMT,TGAS,TGAS)
      WRITE(5,110)N
      RHOS=(P/(CP(XMT,TGAS)*((G-1.)/G)*TGAS))/4186.
      REYS=(RHOS*26.21)/MHUS
      IF(TGAS.LT.811.) CONS=1.4056E-5
      CONS=1.4056E-5+1.3159E-8*(TGAS-811.)
      QSTA=(0.1212*REYS**0.68*CONS*3.155*(TGAS-TBL))/(RHOS*185.*.0508)
      WRITE(5,100)QSTA
      SCW=QSTA/185.
      WRITE(5,700) SCW
      C=CP(XMT,TGAS)
      TREL=TGAS-22.3/C
      IF(TREL.LE.TBL) GO TO 2
```

```
C CALCULATE HEAT LOSS DUE ROTOR COOLING
      MHUB=1.486E-6*(TREL**1.5)/(110.6+TREL)
      RHOB=P/(((TGAS/TREL)**(G/(G-1.)))*CP(XMT,TGAS)*((G-1.)/G)*TREL*418
     16.)
      REYB=RHOB*16.51/MHUB
      IF(TREL.LT.811.) CONB=1.4056E-5
      CONB=1.4056E-5+1.3159E-8*(TREL-811.)
      QBLA=(0.1212*REYB**0.68*CONB*3.303*(TREL-TBL))/(RHOB*185.*.0508)
      WRITE(5,200)QBLA
      QTOT=QTOT+QSTA+QBLA
      RCW=QBLA/185.
      WRITE(5,800) RCW
      TCWS=SCW+RCW
      WRITE(5,900) TCWS
      T=TGAS-31./C
      G=GAMA(XMT,TGAS,TGAS)
      SPR=(T/TGAS)**(G/(G-1.)/EPT)
      IF(SPR.LE.P4G/P) GO TO 2
      PRT=PRT*SPR
      DHT=DHT+WHOT*(ENTH(XMT,TGAS)-ENTH(XMT,T)-QSTA-QBLA)
      TGAS=T
      WRITE(5,910) TGAS
      N=N+1
      IF(TGAS.GT.TBL) GO TO 1
    2 S1=ENTR(XMT,TGAS,P)
      PRS=(P4G/P)**EPT
      T=TGAS*PRS**((G-1.0)/G)
      P=P*PRS
    3 S=ENTR(XMT,T,P)
      X=(S1-S)/CP(XMT,T)
      IF(ABS(X).LT.0.0001) GO TO 4
      T=T*EXP(X)
      GO TO 3
    4 T4G=T*EXP(X)
      WRITE(5,910) T4G
      DHT=DHT+WHOT*(ENTH(XMT,TGAS)-ENTH(XMT,T4G))
```

```
      WRITE(5,960) QTOT
      RETURN
  110 FORMAT(1H0,'STAGE',T11,I2)
  100 FORMAT(1H0,10X,'HEAT LOSS IN STATOR (KCAL./KG.)', T76,E11.5)
  200 FORMAT(1H0,10X,'HEAT LOSS IN ROTOR(KCAL./KG.)',T76,F11.5)
  700 FORMAT(1H0,10X,'STATOR COOLING WATER(KG.WATER/S/KG.AIR/S)',T76,E11
     1.5)
  800 FORMAT(1H0,10X,'ROTOR COOLING WATER(KG.WATER/S/KG.AIR/S)',T76,E11.
     15)
  900 FORMAT(1H0,10X,'STAGE COOLING WATER(KG.WATER/S/KG.AIR/S)',T76,E11.
     15)
  910 FORMAT(1H0,10X,'TEMPERATURE OF GAS LEAVING TURBINE(DEG.K)',T76,F7.
     12)
  960 FORMAT(1H0,10X,'TOTAL HEAT LOSS(KCAL/KG.AIR)',T76,E11.5)
      END


C NOTE

C THE TOTAL COOLING WATER FLOW IS DETERMINED PER UNIT MASS OF MIXTURE IN THE
C TURBINE ASSUMING UNIT MASS INTAKE AT THE COMPRESSOR.  IT IS NECESSARY TO
C NORMALIZE BY THE RATIO OF MASS FLOW OF MIXTURE TO MASS FLOW OF AIR,  WHICH
C IS DETERMINED IN "RANKINE."
```

APPENDIX I-C

CONTINUITY ACROSS ROTOR

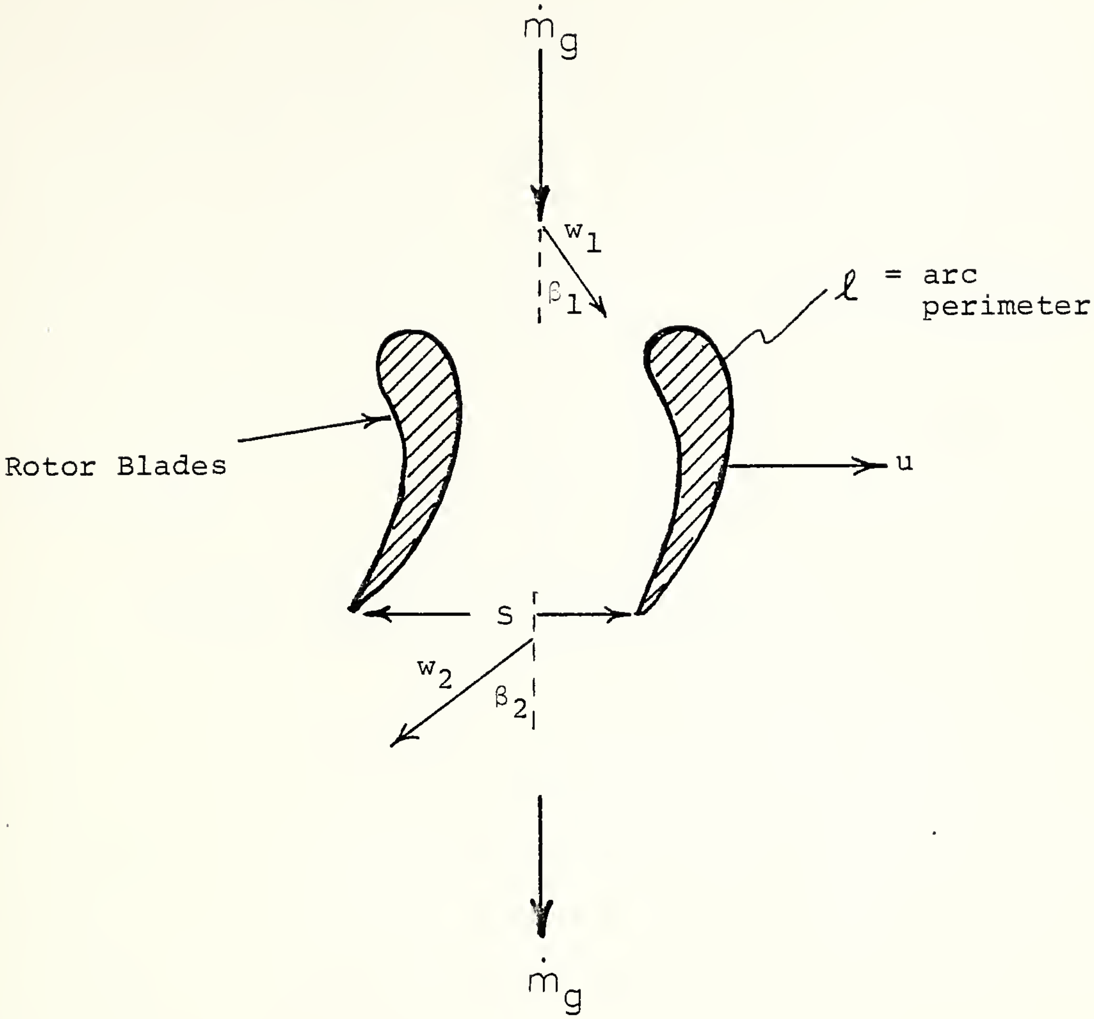
$\dot{m}_g$
w_1
β_1
ℓ = arc perimeter
Rotor Blades
u
s
w_2
β_2
$\dot{m}_g$

FIGURE I-2 Continuity Through a Pair of Rotor Blades

APPENDIX I-D

PRELIMINARY HEAT EXCHANGER SIZING

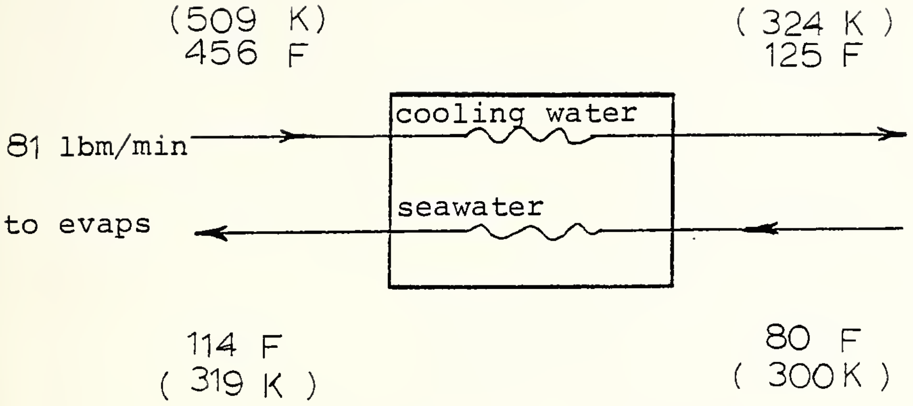
(509 K)
456 F
(324 K)
125 F
81 lbm/min
cooling water
seawater
to evaps
114 F
(319 K)
80 F
(300 K)

FIGURE I-3 Heat Exchanger Schematic

Assume $U = 400 \dfrac{\text{BTU}}{\text{HR FT}^2 \text{ F}}$, seawater feed temperature 80 F, others temperatures ($^\circ$F) and flow rates as in Figure I-1 (open cycle).

$$\Delta T_{Lm} = \frac{(456 - 114) - (125 - 80)}{\ell_n \left(\frac{342}{45}\right)} = 146$$

$$Q = W_{cw}\ c_{p\ cw}\ \Delta T_{cw} = U A\ \Delta T_{Lm}$$

$$= 81 \frac{\text{lbm}}{\text{min}} \times 1 \frac{\text{BTU}}{\text{lbm F}} \times 331 \text{ F} \times \frac{60 \text{ min}}{\text{HR}} = 1.60866 \times 10^6 \text{ BTU/HR}$$

$$A = \frac{1.60866 \times 10^6}{400 \times 146} = 27.55 \text{ FT}^2 \text{ (minimum with counter flow)}$$

APPENDIX II

SAMPLE CALCULATIONS FOR TABLE 7.1

The standard (composite) cooled, simple cycle gas turbine (Table 5.2) at a rated power of 2000 SHP has SFC = 0.388 and is established as the reference plant. From the propeller law, power varies as the cube of speed, hence for endurance power at 18 kts,

$$P_E = \frac{1}{8} P_{max} = 10{,}000 \text{ SHP}$$

or 5000 SHP per shaft. The plant configuration shall be to operate one turbine per shaft at 5000/20000 SHP = 25% full power. From Figure 7.1,

$$SFC_E = 1.6 \text{ SFC Full Power}$$

$$\text{Fuel Rate} = (1.6)\left(0.388\frac{\text{lbm fuel}}{\text{HP-HR}}\right)(5000 \text{ HP}) =$$

$$3104 \frac{\text{lbm fuel}}{\text{HR}} \text{ per shaft}$$

$$\text{Range} = 850\frac{\text{tons fuel}}{\text{2 shafts}} \times 2240\frac{\text{lbm fuel}}{\text{tons}} \div 3140\frac{\text{lbm fuel}}{\text{HR}} \times$$

$$18 \text{ kts} = 5520 \text{ n.m.}$$

To compare a simple cycle, transpiration cooled gas turbine to the baseline, the ratio of SFCs is inversely related to the endurance ratio, hence

$$\frac{\text{Range Transpiration}}{\text{Range Reference}} = \frac{\text{SFC REF}}{\text{SFC TRANS}} \times \text{Range REF}$$

$$= \frac{0.388}{0.374} \times 5520 \text{ n.m.} = 5726 \text{ n.m.}$$

To determine the fuel weight savings for a constant endurance range of 5520 n.m.,

$$\frac{(5726 - 5520)\text{n.m.}}{18 \text{ kts}} \times 0.374\frac{\text{lbm fuel}}{\text{HP-HR}} \times 2 \text{ shafts} \times$$

$$5000\frac{\text{SHP}}{\text{shaft}} = 42802 \text{ lbm fuel} \times \frac{\text{ton}}{2240 \text{ lbm}} =$$

19.1 tons fuel

Thesis
S7895
c.2

Strawbridge 184497
Advanced cooling
methods for marine gas
turbines.

7 MAR 84

30099

Thesis
S7895
c.2

Strawbridge 184497
Advanced cooling
methods for marine gas
turbines.

thesS7895
Advanced cooling methods for marine gas
3 2768 002 02071 1
DUDLEY KNOX LIBRARY